Arju Shekh

Development of Friction Flash to Tube (F2T) and Application to S355 Grade Steel

School of Engineering

Thesis submitted as a partial fulfilment of the requirements for the degree of Master of Science in Technology

Espoo 26.05.2017

Thesis Supervisor: Prof. Pedro Miguel dos Santos Vilaça da Silva

Aalto University
School of Engineering

Author Arju Shekh

Title of thesis Development of Friction Flash to Tube (F2T) and Application to S355 Grade Steel

Degree programme Mechanical Engineering

Major/minor Mechanical Engineering **Code** IA3027

Thesis supervisor Professor Pedro Vilaça

Thesis advisor(s) Professor Pedro Vilaça

Date 26.05.2017 **Number of pages** 103+4 **Language** English

Abstract

Friction Flash to Tube (F2T) is an innovative friction based manufacturing technique to produce seamless tubes based on open die forging, invented at Aalto University. These tubes can be produced economically in small sizes and batches, envisaging applications of high value materials that are not available in the market. The objective of this Master thesis was to develop the experimental condition of F2T as well as the proper parameters in F2T by approaching Taguchi method. The pre-defined parameters to investigate in Taguchi method were established as forging force, tool rotation and initial transient plunging depth and the investigating of geometrical and metallurgical characteristics were done. Cold rolled high strength and low alloy structural steel S355 is the material used in this research work. The parameters of the F2T process were developed based on design of experiments, with geometrical and hardness properties as performance parameters. The optimized conditions and parameters were applied to produce tubes for extensive evaluation of the mechanical and metallurgical material properties.

The F2T process has specific components and control demands that cannot be met by the existing manufacturing systems. This challenge was overcome by developing one first version of a dedicated system based on an existent Friction Stir Welding equipment. One additional challenge was to produce tubes longer than 40 mm because of buckling. The buckling was prevented by implementing a lateral support system constraining the consumable rod during the initial transient plunging period. The test specimens for extensive mechanical test and metallurgical analysis were extracted from tubes produced with 80 mm in length. These longer tubes were manufactured using the support system to prevent buckling. The results on tensile test, flattening test and flare test of F2T tube reveal that the mechanical properties of produced tubes are as good as tube of similar material produced by another manufacturing technique.

The temperature during the application of the F2T process was monitored with thermo-couples. The mechanical properties of produced tubes were evaluated by hardness measurement of cross and longitudinal sections. Tensile test were applied to sub-sections of wall of the tubes, and flare and flattening test to the whole tubes. The metallurgical analysis encompasses optical microscopic analysis, and SEM/EBSD with grain size evaluation. The research work demonstrate the feasibility of producing seamless tubes by F2T in structural steel. A correct design of a dedicated system to prevent the buckling, enables to produce long tubes.

Keywords Friction Flash to Tube (F2T), Structural Steel, Viscoplastic, Design of Experiment (DOE), Taguchi.

Acknowledgements

First and foremost, a big applause to a man behind the invention of novel process of seamless tube manufacturing process called friction flash to tube (F2T), Prof. Pedro Vilaça. I acknowledge the funding from Aalto University and Tekes programme via TUTL project "Friction Flash to Tube - F2T". Aalto's Project Number 211629.

I would like to express my deepest gratitude to my supervisor and advisor, Prof. Pedro Vilaça, for an opportunity to become a part in F2T project. I am sincerely grateful for the inspiration and support provided by him. I am thankful to my friend Avinash Dhital for notifying me about this opportunity. My sincere thanks to Prof. Sérgio Duarte Brandi, visiting professor from University of São Paulo, for sharing his knowledge on design of experiments part of this thesis. The project won´t be successful without enormous helps from the staff in material engineering department therefore, thanks to all the staff and special thanks to Seppo Nurmi. I really appreciate the support that I have got from my colleagues during the work. I am thankful to the tremendous support shown by Gonçalo Sorger which makes easy in completion of this thesis. Also, my thank goes to Prabilson Khadka and Janak Aryal for their support. I´m grateful to Pauli Lehto, Jaime Casanova, Tuomas Pihlajamäki and Roman Mouginot for their assistance in different stages of the research work. Of course, I would like to thank all co-worker for all kind of support given by them and making great atmosphere at the work and I will always remember the time spent in coffee break with KAKE members.

Finally, I would like to thank all my family members for their support. I am highly grateful to the love shown by them. Thank you for the motivation and thank you for believing on me.

Espoo, 26.05.2017

Arju Shekh

CONTENTS

Appendices

Symbols and Abbreviations

Symbols

A	Nominal cross-section area
C	Materials conductivity
D	Diameter
d_{max}	Maximum outer diameter measured in tubular shape
d_{min}	Minimum outer diameter measured in tubular shape
D_u	Expanded diameter of tube in flare test
E	Young´s modulus
F	Force
f_o	Test frequency
F_z	Plunge force
H	Hardness
HV_{av}	Average of measured Vickers hardness in tubular shape
HV_{bm}	Vickers hardness measured in base material
HV_{σ}	Standard deviation of measured Vickers hardness in tubular shape
I	Current in amperes
K	Total amount of heat losses through radiation and conduction
L	Final gauge length
L_0	Original gauge length
n	Total number of experiments performed
R	Resistance of the materials in ohms
SS_T	Total sum of square deviation
SS_P	Total sum of square deviation due to process parameters
SS_e	Total sum of square error
T	Time of current flows in seconds
t	Thickness of tube
t_{av}	Average of measured thickness in tubular shape
t_{max}	Maximum thickness measured in tubular shape
t_{min}	Minimum thickness measured in tubular shape
t.s.	Thickness stability

Y_i	Experimental results for i number of test
Y_m	Total Mean S/N ratio
Ve	Mean of squares deviations
V_p	Mean of squares error
V_z	Plunge speed
β	Angle of conical mandrel
ε	Strain
Ω	Rotation Speed
μ_o	Relative permeability
σ	Stress
σ_{02}	Yield Strength at 0.2 offset
$\bar{x}$	Mean

Abbreviations

AFM	Atomic-Force Microscopy
ANOVA	Analysis of Variance
BCC	Body-centered Cubic
CCD	Charge Coupled Device
DIC	Digital Image Correlation
DOE	Design of Experiment
DoF	Degree of Freedom
EBSD	Electron Backscatter Diffraction
ECD	Equivalent Circle Diameter
EDM	Electric Discharge Machine
ERW	Electric Resistance Welding
F2T	Friction Surfacing to Tube
FPRO	Finnish Patent and Registration Office
FS	Friction Surfacing
FSW	Friction Stir Welding
GMAW	Gas Metal Arc Welding
ID	Inner Diameter
IR	Infra-red
MHT	Microindentation Tester
MST	Micro Scratch Tester
NDT	Non-Destructive Testing
OA	Orthogonal Array
OD	Outer Diameter
PMI	Positive Material Identification
SMAW	Submerged Arc Welding
S/N	Signal to Noise ratio
TRS	Transverse rupture strength
UTS	Ultimate Tensile Strength
WC	Wolfram carbide

1 INTRODUCTION

1.1 Scope of Study

According to the report [1], by the year 2022, the global market of seamless tubes alone is projected to reach 65 million tons. The main reasons identified are the high demand of high strength tubes in infrastructure, growing use of seamless tubes in industrial and utility boilers, growing demand for premium pipes capable of operating in tough environments. There is a rise in demand for high performance pipes and tubing in energy and manufacturing sector. Examples of high performance applications are engine parts where especially tubes that withstand high temperature and pressure are needed and medical equipment where corrosion resistance and high strength is more important. To fulfill the demand of high performance tubes, there are various researches going on either in special materials or in different techniques of manufacturing of tubes. Titanium alloy, nickel alloy, stainless steel, duplex steel tubes are the demanding materials in high performances tube.

Figure 1: Application of high performance tubes. a) Rocket nozzle used in defense industry, b) Titanium tube adapter with pyramid receiver, prosthetic component, c) Water or Foam nozzles for fire extinguishing systems [2]

The Figure 1 shows some examples of high performance tubes. Manufacturing of those tubes acquiring the properties according to the application has high demand in the market. It is not easy to manufacture those tubes using the common manufacturing technique of tube which exist as a common process today. Current manufacturing process of seamless tubes are especially suitable only for mass production. The other techniques of manufacturing, such as, machining and casting are also somehow expensive and difficult to achieve the required material´s properties, such as, strength, toughness and high temperature resistance. There is the perceived need to develop an alternative way of manufacturing tubes focusing on high-value applications. Friction Flash to Tube (F2T) was invented and is being developed towards becoming one feasible alternative technique to

fulfill such demand of producing seamless tubes for high value application. The F2T enables tailor made solutions in a shape and materials not commercially available in the market [2].

1.2 Friction Flash to Tube

The Friction Flash to Tube (F2T) is a new friction based manufacturing technique, operating in solid-state phase, able to transform a rod into a seamless tubes under open die forging. The concept of F2T arose from friction surfacing tests at the welding laboratory of Aalto University. The tube manufactured by F2T method is able to produce continuous tubular shapes or tubes with continuous variable diameter and thickness. The process do not require any outer power source as the heat dissipated during the material deformation is the heat power source. Since it is based on solid state thermomechanical processing of materials, the same kind of processing applied to get the best material properties in most of the engineering materials, it is expectable that the tube final mechanical properties will be distinctly good [2]. To evaluate some of these properties is the objective of the present work.

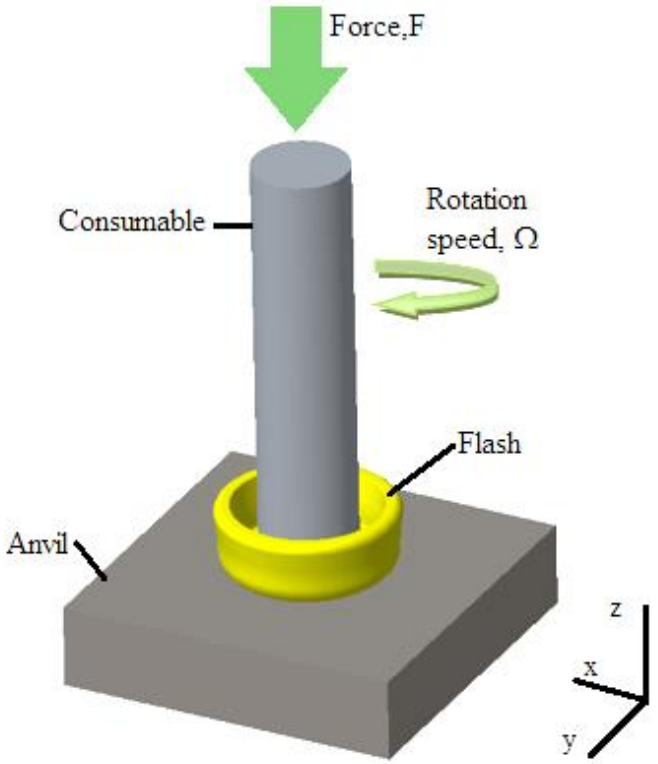

Figure 2: Principles of Friction Flash to Tube (F2T) process

In F2T process, the consumable cylindrical shaft (rod) is plunged against non-consumable anvil as shown in Figure 2, and through a process of solid state deformation, the visco-plasticized material flows radially outwards until it inverts the flow into axial direction, parallel and opposite from the initial plunging, forming a cylindrical flash, growing stationary around the tube. The non-consumable anvil is rigid compared to the consumable

rod, at the operation temperature. The F2T process is based on the `on demand lean production´, no setup cost and no batch production is necessary which makes it more economy method for tube production. The technique is able to fulfill the demand of high temperature tube application. Also, it is possible to manufacture tubes of material which is not yet available in the market. It is able to address the demand of customer needing the special materials even in small quantity. F2T has possibility to innovate tube design based in continuously varying section configurations, as in pottery.

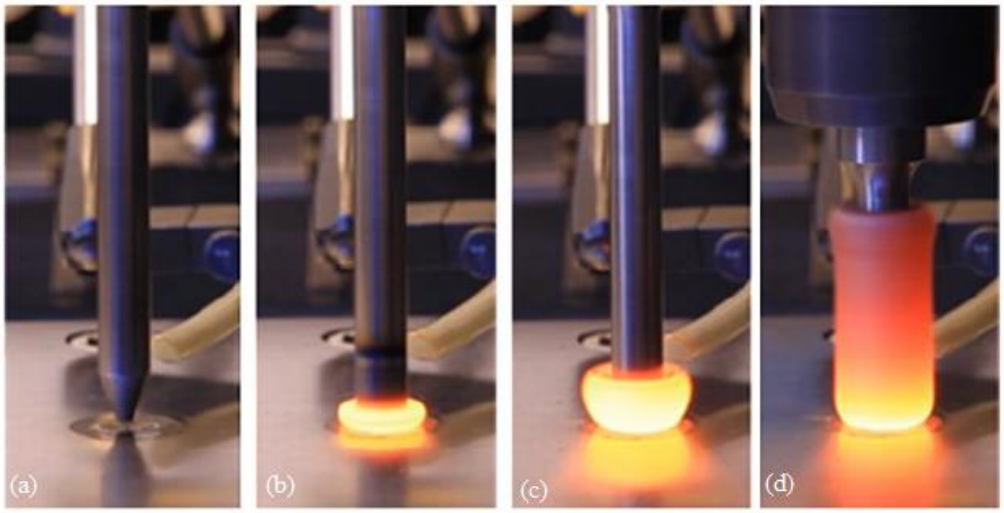

Figure 3: Stages in F2T. (a) Consumable rod approaching to anvil, (b) Starting of a plunging process, (c) Starting of a tube formation and (d) Tube formation

The Figure 3 shows the important four stages during the F2T process. At the beginning, the consumable rod approaches to the non-consumable and rigid anvil. In this stage, the spindle of machine started to rotate and no force was applied here since there is yet no contact between consumable rod and anvil. In second stage, the initial plunging of consumable rod begun. The process is typically speed controlled in this stage and continued till the temperature reaches the operational conditions. As the operational temperature is reached and the proper flash is created, the plunging of consumable rod is transferred into force control. Finally, the process stops when the tubular object of required length was formed. The produced object exists in the form of a canister, and need post-processing of both ends to form a tube, see Figure 4.

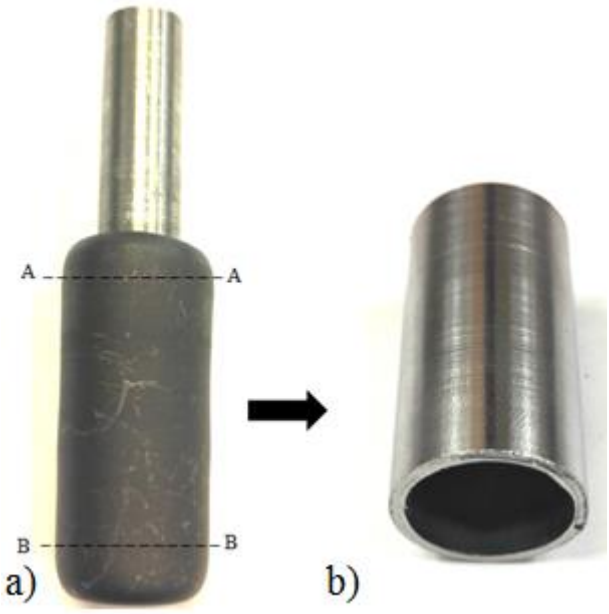

Figure 4: F2T tube a) Tubular product as produced by F2T process. b) The resulting tube, upon machining of both ends.

1.3 **Objectives and Methodology**

The F2T is a disruptive new technique invented in Aalto University and the present research is funded by Aalto pre-seed funding and Tekes TUTL programme. The overall objective of the present research is to discover the feasibility of tube production, in a common structural steel, using F2T technology so that the technology can be transferred with trust into a very competitive market. In more detail, the objectives of present F2T research works can be described in the following points:

- To develop one first version of the experimental setup for F2T process, enabling the establishment of a foundation for future research in F2T domain:
    - To design and select the proper materials for anvil. The designing of anvil is also important to prevent deformation of it when high pressure and temperature was applied on it during the process;
    - To produce the anvil including cooling system. Cooling system helps to reduce the wear and the sticking effect of the base material during F2T process;
    - To design the buckling preventive system or a guide in the F2T process which will be able to produce longer tubes. Before this thesis, the technology is only able to produce tubes of 30-40 mm length.
- To produce tubes by F2T, of structural steel S355, in a preliminary approach using wide range of parameters to set the more focused window of operation;
- To apply Taguchi method (Design of Experiments) selecting for performance parameters important geometrical features, addressing the shape stability, and hardness;

- To produce samples for extraction specimens for evaluation of mechanical properties and microstructure;
- To perform mechanical test on F2T tubes to obtain mechanical properties. The mechanical test are tensile test, flattening test, flare test and hardness test;
- To characterize the metallurgical properties of F2T tubes by performing optical microscopy analysis and Electronic Backscatter Diffraction (EBSD) test.

1.4 Structure of Thesis

There are five chapters in this thesis. It starts with the present introduction including the fundaments of the innovative friction flash to tube (F2T) technology.

The literature review is presented in chapter two. As a background knowledge, it is also important to know the concurrent tube manufacturing processes thus, manufacturing techniques of seamless tubes and welded tubes has been presented in same chapter. Furthermore, study on application of tubes is also presented to illustrate the commercialization scope of F2T. The thesis includes the design of experiment (DoE) using Taguchi method to discover the best performance parameters so literature review on DOE is essential and has been included. The standard test methods of tubes are also presented in same chapter.

Third chapter in this thesis is fully concerned with the application and development of F2T. This chapter focus on the design and development of experimental conditions for F2T, and testing methods and conditions.

Chapter four addresses the implementation of the Taguchi analysis. The optimization of parameters is presented here where with analysis of variance and algebraic model. Moreover, the monitoring of the thermal cycle and and mechanical parameters of F2T process is presented in this chapter.

The materials engineering analysis is presented in chapter five. This includes all mechanical tests and metallographic analysis of F2T tube specimens.

The chapter six encompasses the conclusions from the thesis work and the future developments of research on F2T technique.

2 LITERATURE REVIEW

2.1 Introduction

The theoretical and methodological contributions in a F2T technique were presented in this chapter. Tube is a hollow cylinder which is used to move liquids and gases. Tube has higher engineering requirement than a pipe however, both of them are al-most interchangeable. The difference between tube and pipe is seen in their standard pipe designation. For example, pipe is specified by nominal outer diameter (OD) whereas tube is specified by nominal inner diameter (ID) and thickness. The application of tube can be found in various areas such as construction, aeronautics, marine, chemical industries, petroleum industries and many more. [3]

The chapter has described on fundamental of F2T in section 2.2 where concept of viscoplasticity and friction surfacing which is a base for F2T were discussed. Since there is already patent application applied in F2T by Aalto University, the brief discussion on patent concept was also made under the same section.

Section 2.3 is about the current tube manufacturing method available in market. Here, different type of tube manufacturing technique such as seamless tubes, welding tubes and extruded tubes are described. The section 2.3.1 described about the various types of seamless tube manufacturing method including the description on continuous casting of round. Continuous casting of round is a base to produce seamless tube. Section 2.3.2 explained about the welded tubes. Also, the forming process required in welded tubes are presented in section 2.3.3.

The application of tubes is extensive. In section 2.4, the tube´s application areas were presented which helps to know about the potentiality of F2T technique.

Similarly, about the standard test analysis used in tube manufacturing were presented in next section 2.5. Explanation on some of the standard test are presented in this section.

Another major section in this chapter is design of experiments which was presented in section 2.6. The Taguchi approach was applied in this study therefore; Taguchi process was discussed briefly in this section. Summary of chapter is presented in section 2.7.

2.2 Fundamental of F2T

2.2.1 Concept of Viscoplasticity

In continuum mechanics, it was said that viscoplasticity is the rate-dependent or time dependent inelastic behaviour of solids. Rate-dependence in this context means that the deformation of the material depends on the rate at which loads are applied. [4] In contrast to fluids viscoplastic materials can sustain a shear stress even at rest which begin to slow with viscous stresses after a yield condition has been satisfies which is the reason that

viscoplastic materials are called solid [5]. The most striking feature of plastic behaviour is yielding. The presence of yield stress is an exception. That is why mild steel belongs to this exceptional class. And hence it is the most commonly used metal. Many attempts had been made for theoretical description for its behaviour for other metals. Those results have incorporated an essential feature to be added what come to be called as plasticity theory. Later this theory is called as Viscoplasticity. It is sensitive to rate. In solid mechanics, it is widely used. Viscoplasticity denotes the rate dependent behaviour with a well-defined yield criterion. [6]

Viscoplasticity is an extension of the plasticity study. The difference is that plasticity is rate independent, whereas viscoplasticity deals with the plastic deformation of materials depending on the rate at which the loads are applied. A more notable difference is that viscoplastic model continues to undergo a creep flow as a function of time under the influence of the applied load. In other words, a material will deform permanently under as a result of long-term exposure to high levels of stress that are still below the yield strength of the material. It is an irreversible behavior that materials experience at high temperatures due to an applied load. Similar to viscoelasticity, viscoplasticity is also time-dependent, but permanent deformation remains following it.

Typically, viscoplasticity is modelled in three-dimension using overstress models of the Perzyna or Duvaut-Lions types [4]. Hookean spring elements which are in one dimension are the best representation of the elastic response of the viscoplastic materials. And dashpot elements which are non-linear in nature are the perfect representation of the rate dependency in viscoplastic materials. Three-dimensional modelling is adopted for viscoplasticity, in which over stress models describes the stress increment beyond the yield surface which is rate independent and which is then permitted to get back to the yield surface in amount of time. In these models the yield surface is generally taken as rate dependent. [6] Another method is by adding rate dependence of strain to yield stress. This technique is useful in calculating the response given by the material. Many researches had been carried out on Viscoplasticity, one of which was given by Prandtl which stated the application of Viscoplasticity. In his research, he described the concept of normality of flow to the yield surface and rules for plastic flow were derived. In some case Viscoplasticity has different role. In case of metals it is the macroscopic nature which is the result of the grain dislocation while movement. In addition of gliding criterion, this creates superposed effects. [7]

Viscoplastic material when analyzed qualitatively three tests are uncovered which are: at constant stress or strain rate hardening test, at constant force creep test, and at constant elongation stress relaxation test [5]. In strain hardening test an increment in stress is initiated to generate additional stress. In hardening test one important point is proved that is the viscoplastic has same hardening curves are observed as of the rate dependent plastic. For viscoplastic material the elastic strain is not negligible. And the plastic strain's rate is function of yield stress obtained initially. Hardening does not affect, and yielding stress is represented by the sliding element this is happens when elastic limit is exceeded. Sim-

ilarly, deformation of a solid materials under the constant stress is called creep and measurement of the strain responses due to that constant stress was done in creep test. And relaxation test shows the stress relaxation in uniaxial loading at constant strain.

2.2.2 **Concept of Friction Surfacing**

The F2T technique is developed in lab of Aalto University while doing friction sur-facing. The unwanted excessive amount of flash produced in friction surfacing led to the innovation of F2T. Friction surfacing (FS) is a solid-state process that is used to produce metallic coatings of hot forged microstructures. By using friction surfacing, it is possible to produce a continuous deposit from the wear of the consumable rod. Friction welding is an effective surfacing method which has a lot of prospects. [8]

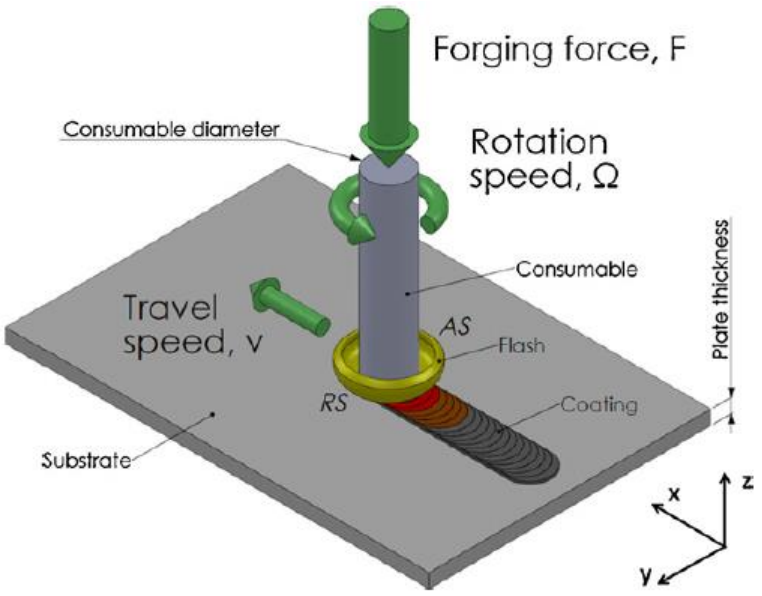

Figure 5: Principle of Friction Surfacing (FS) [9]

The process includes the deposition of a consumable materials under the application of friction that ultimately produces enough heat for plastic deformation. Further plastic deformation produces more heat to deposit or coat the materials on the surface of substrate. As shown in Figure 5, the rotating consumable feeds to the substrate in z-axis with simultaneous move in x- or y-axis. The axial load applied in the process depends upon the materials and desired properties of deposition.

The initial phase of surfacing is to create proper flash. Figure 6 shows the creation of flash along with the thermo-mechanics of friction surfacing. As the consumable rod feed to the substrate, flash create. The material deposited at the tip of consumable rod and revolve with it. The material was blocked by the highly plasticized material in beneath thus, goes to the edges of consumable. The produce flash grow and harden which increases the necessary forging pressure into the viscoplastic layer closing the viscoplasticity of rod. Whenever, the excessive mechanical force is produce, then only size of flash grows. The

growing of excessive flash is unwanted in friction surfacing however, it is a core achievement in case of F2T. The consumable rod was plunges and let to move only in z-axis to grow flash around the circumference of consumable rod which was later machined to produce seamless tubes.

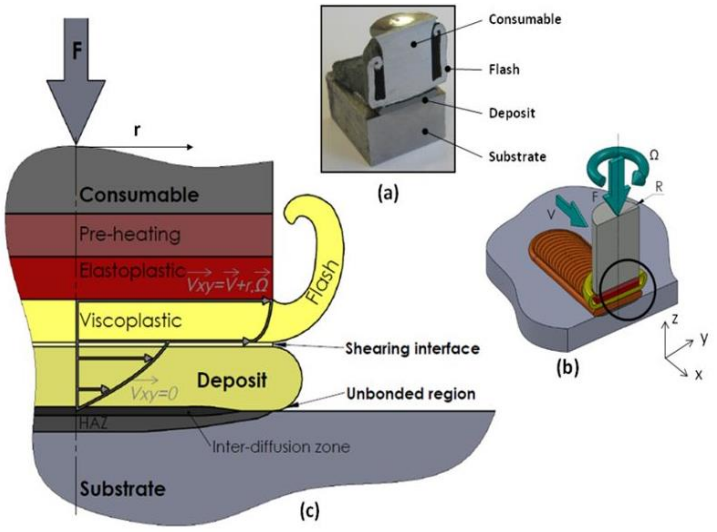

Figure 6: Thermo-mechanics of Friction Surfacing a) Sectioned consumable; b) Process parameters and c) Thermo-mechanical transformation and speed profile. Nomenclature: F – Forging force; Ω - rotation speed; v- travel speed; Vxy – rod tangential speed in plane xy given by composition of rotation and travel movements. [8]

In friction surfacing, the amount of deposit material is depended on parameters such as forging force, feed rate, travel speed and etc. Similarly, the characteristics of produced tube in F2T is also depend on same parameters. However, initial diameter of consumable rod has huge effect on geometry of produced tube that define diameter and thickness of tubes.

2.2.3 **Review on Patented Concept**

Friction Flash to Tube is an innovative technique to produce seamless tubes which was developed in Aalto University. The technique has been filed as an application in Finnish Patent and Registration Office (FPRO) on February 20, 2017 under the name of "Method and tools for manufacturing of seamless tubular shapes, especially tubes". The application number is PCT/FI2017/050109 and the applicant institution is Aalto University Foundation (IPID 1776). F2T is a novel process invented by Pedro Vilaça. [10] The survey by Finnish patent and registration office (FPRO) concluded that no documents with significant relevance have been retrieved.

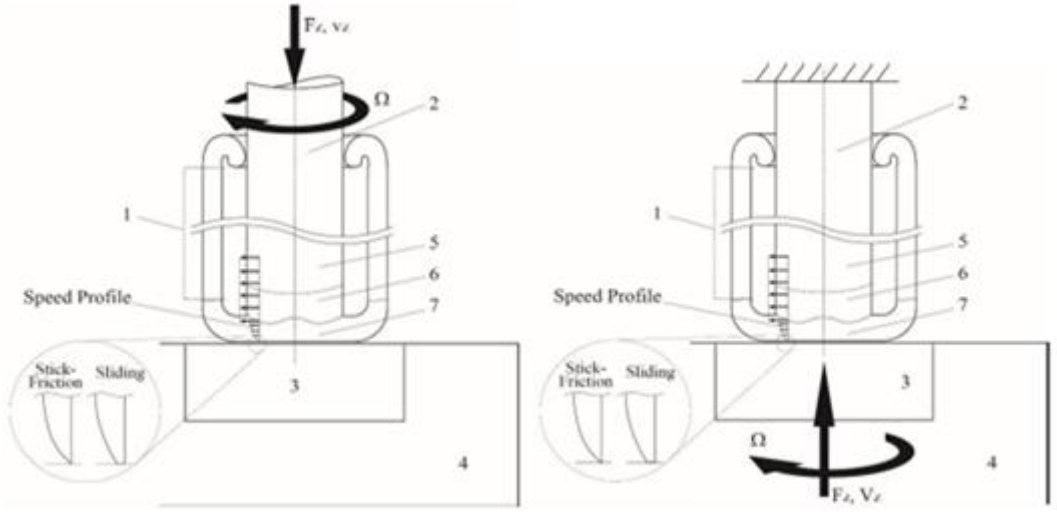

Figure 7: Process fundaments during stationary of plunge period (i.e. tube formation) of F2T, with representation of the alternative control of the plunge force (F_z) or plunge speed (V_z). [10]

According to the patent application [2], the F2T process is a process to produce seamless tubes, extracted from the flash (1) continuously produced during the plunging of a consumable rod (2) against a non-consumable rigid anvil (3) as shown in Figure 7. Between the rod and the anvil there is a relative rotational speed. The flash (1) is cylindrical with stable and controllable geometry. The axis of symmetry of the flash is coincident with the axis of the consumable rod and the axis of rotation during the plunging period. The geometry of the flash has an outer diameter and thickness (which can be seen in Figure 8) that are set via controlling of the following parameters:

- Plunge force (F_z) or plunge speed (V_z).
- Relative rotation between consumable rod and the non-consumable rigid anvil.
- Diameter of the consumable rod.
- Thermo-physical properties of the consumable rod materials

Boundary conditions such as mechanical, thermal and geometrical conditions applied to the flash.

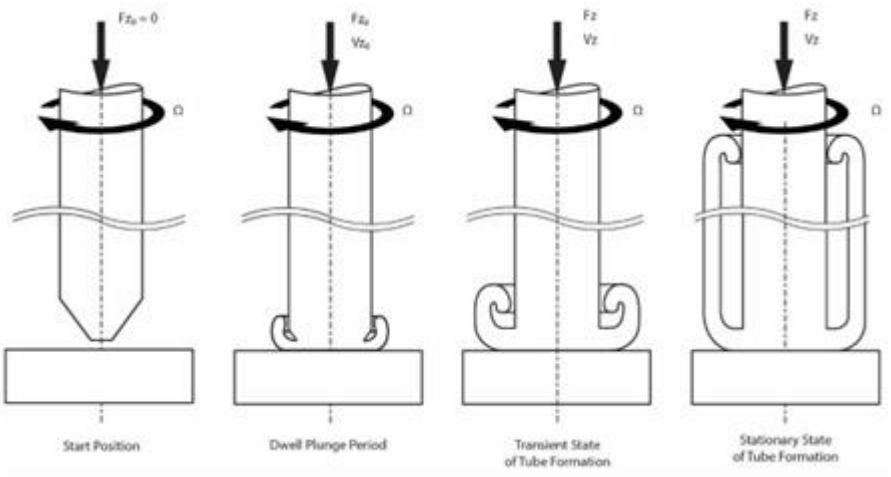

Figure 8: Sequence of the main periods of F2T: a) Start positon; b) Dwell plunge period; c) Transient plunge period; d) Stationary plunge period: the tube formation by F2T [4]

Patent has introduced the range of possible tip geometry of consumable rod. Also, there were alternative clamping method for consumable rod and longer consumable rod, sample of possible boundary conditions and alternative shapes for the non-consumable insert. In the sample of possible boundary condition, externally cutting tool device and mould device has introduced which helps to get good outer surface finishing and produce variable tube dimension respectively. Clamping system introduced for longer tube has addressed the buckling problem that arise in production of longer tube.

It was expected that, the F2T technique solves customer demands of producing tubes in small series, tailored made tubes, side range of dimensions in tubes and tube of different engineering materials including tube of those materials which are not available yet in market.

2.3 Tube Manufacturing Methods

In general, there are two ways of manufacturing tubes; Welded tube and Seamless tube. Welded tubes are manufactured mostly for the bigger diameter tube and used in mostly construction. Submerged arc welding, electric resistance welding, pressure welding etc. are the welding process used in manufacturing of welded tubes. Seamless tubes are manufactured either by extrusion or by rotary piercing processes. Extrusion is widely used in aluminium tube manufacturing process whereas rolling process can be used in manufacturing of steel tubes. Seamless tubes are considered more beneficial in sensitive engineering application because of their increased pressure rating, uniformity in shape and strength under loads. However, seamless tubes are more expensive than welded tubes and comparatively hard to manufacture in bigger diameter.

2.3.1 Seamless Tubes

Seamless tubes are extruded and drawn from round billet which are manufactured by continuous casting. There are various steps involved in manufacturing of seamless tube depending upon their types such as heating of a billet, piercing, rolling, straightening, and cooling and so on. Both seamless tube and welded tube has good scope depending upon their application. The main advantages of seamless tube over welded tube is that, they don´t have a weld seam which means they withstand more pressure inside than welded tubes. However, there have been massive improvise in the manufacturing process for a welded tube recently, which have definitely increase the strength and performance of the welded seam. Seamless pipes have better roundness than welded pipes. The more description of the preparation of billets and different types of seamless tubes are below: [11]

a. Continuous Casting of Round Billets

Round billets are important raw materials to produce seamless pipe. These billets are produce by continuous casting process which is the process of solidifying a molten steel into a semi-finish billets, bloom or slab. The finish is done by rolling it in the finishing

mill. The circular arc continuous caster is most common process used in continuous casting to produce round billets. Also with high productivity, several benefits can be achieved in this process such as reduced segregation and porosity. It also reduces the cracking in the center of the round and provide more uniform properties in a given heat. [12]

At the top of the caster, clean and micro alloyed steel passes to the ladles at the temperature of 1700^{o}C. The process was shown in Figure 9. Typically, ladle is 225 tons from which liquid steel pours into tundish. Typically, tundish has a rectangular shape but the most common shapes are delta and T which has capacity of 25 tons. Tundish distribute liquid to the mold via nozzle which is located at the bottom. At a same time, it also acts as a buffer and remixing vessels and inclusion float in the top therefore clean liquid for the further process. Other function of tundish is to provide a continuous flow of liquid to the mold during ladle exchanges and maintain steady metal height above the nozzle to the molds, thereby keeping steel flow and casting speed constant. Simultaneous flow of liquid steel to several strands in a caster via tundish prevent oxidation too because of the presence of argon sealing between ladles to tundish. Also, the nozzle through which liquid transfers to the mold is submerged. The mold is an open ended rectangular structure, containing a water cooling in inner lining made up of copper alloy. 18mm thick and 700mm long mold is placed concentrically to the pressurized cooling water and as a result solidification begin at the top of mold and continuously move throughout the mold. The shell in exist of the mold contains liquid core of strand. This is tapered internally, preventing separation of the solidify shell from the mold. Also, it improves the heat flow and reduce porosity. To prevent steel from sticking to the copper (mold), the round shaped mold is lubricated and also the whole assembly vibrated during the process. In next step, strand exists from the mold and it has solid shell outer layer which 11-19 mm depending upon the caster speed. Casting speed can be achieved up to 3.5m/min but the common on is 2-2.5 m/min. The strand gradually moves downward and is supported by V shaped grooved roller where also cooling is provided by water spray. The roller helps to maintain the circular shape of strand. The radius of caster is depending upon the diameter of strand. There are larger casters of radii 10.5, 13.5, 18, 30.5m which can produce strands of 117, 220, 270, 310 and 340mm respectively. The metallurgical length is 36.5 m. Then the strand passes to the pair of powered three-point bender where straightening process occurs and continue to solidify too. And in the end of the process strands were flam cut to the required length and cooled. Typically, the round billets have length of 9-14m which is further process to produce seamless tube. [11]

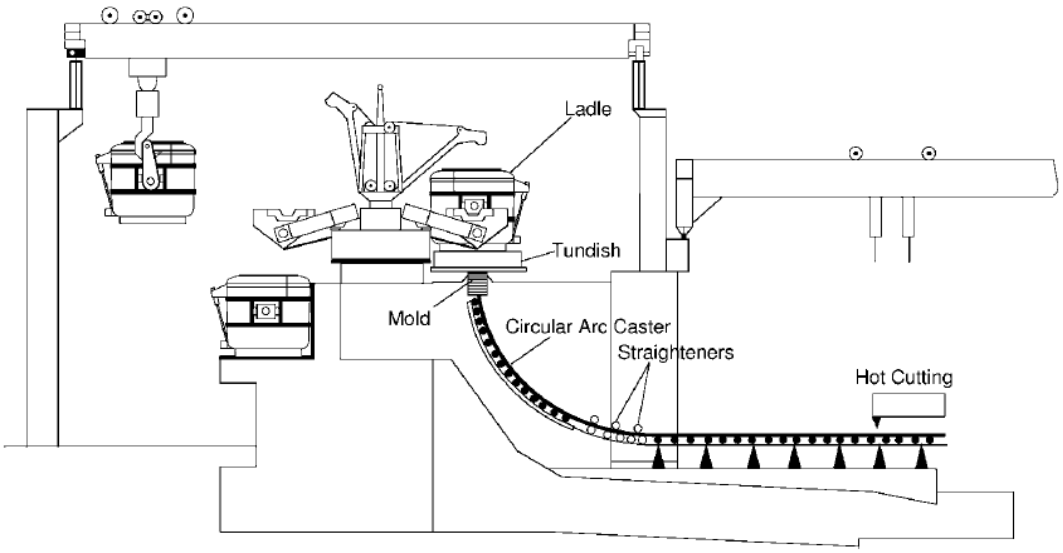

Figure 9: Circular arch continuous caster for round.

b. Pilger Rolling Process

A Pilger, name itself means the unique forming step which was invented by Mannesmann brother. The process is generally used to produce seamless tubes having thicker wall. The thickness could be 25mm to 60mm and the diameter of tubes are generally 9.625 inch to 26 inch. The benefits of the process are that; it can manufacture specified IDs. The typical applications of a tubes manufactured by this process are oil field tubulars, boiler´s tubing etc.

The process starts with the typically casted round ingots which are relatively short and thick. The ingots could weight up to 7 tons. As shown in the Figure 10, the first step is to heat the ingots in rotary-hearth furnace up to the temperature of 1280^{o}C. Then, the ingots are center pierced by the application of high load capacitive press and followed by plug piercing. This may bring some eccentricity on the specimen which will remain to some ex-tent in a final product. The plug remained at the bottom of specimen is removed in next step; by piercing. The pierce rolling step is the first step of reducing diameter and wall thickness in the process. A long mandrel is inserted in the annulus in the pilger mill step which is the main forming step of the process. When the whole length is formed, the mandrel is transported to water bath for fooling and a new mandrel is used for the next part. The back end of the tube in pilger mill is removed by hot sawing and the tube next goes to the cooling bed. This cooling is necessary to obtained desire microstructure and then process followed by the reheating of tubes in furnace up to the temperature of 1200^{o}C. The final reduction of OD is done in sizing steps. The roller sets in this step are arranged to increasingly smaller diameters, which reduces the OD up to the required final dimension. The tubes do not rotate in sizing instead the roller provide rotary action and moves tube forward to the cooling bed. The cooling of tubes is done to achieve required microstructures and straightening of tubes are done next. Tube straightening is the final step in plug rolling process however, quality inspection and tests are done before shipping

of the tubes. The ultrasonic test, magnetic particle tests are done to find the defect on produced tubes. [11]

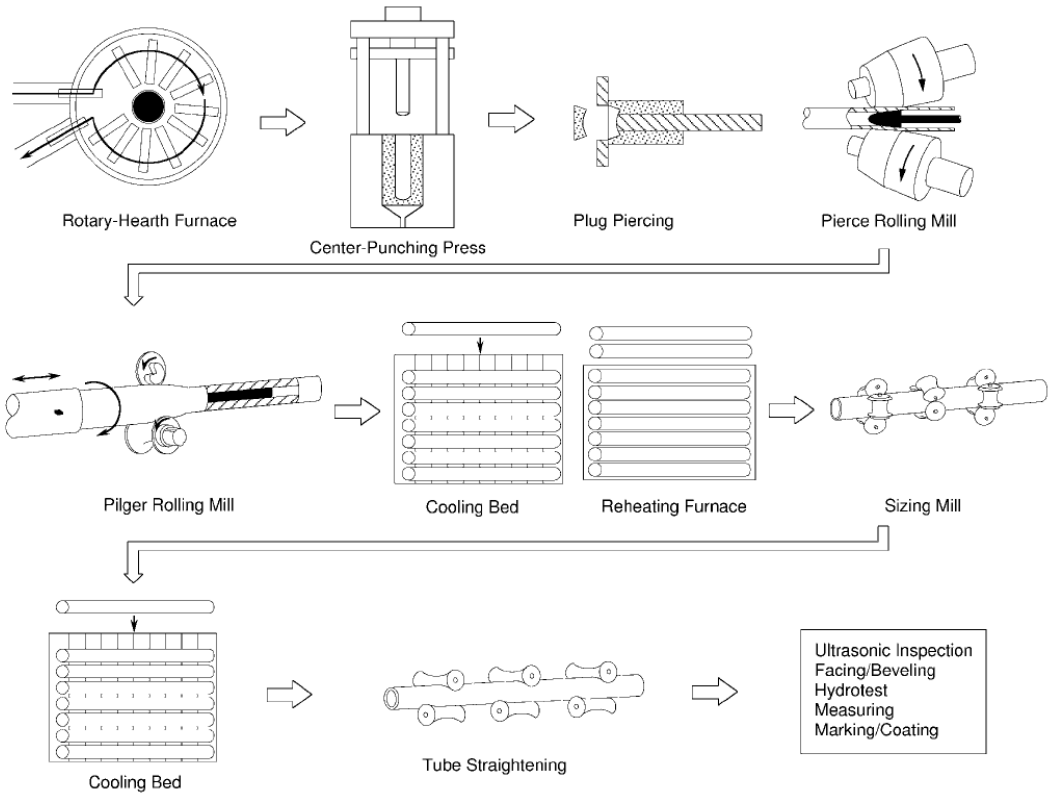

Figure 10: Steps involved in seamless tube manufacturing method by Pilger Rolling Process.

c. Plug Rolling Process

The main forming step in the plug rolling process is, pierced hot round is rolled over a plug inserted in the annulus with a long rod which is the reason of naming this process a plug rolling. The typical diameter of a tube which can be manufactured from this process is 7 inch to 16 inch and tube of bigger diameter is produced via continuously vast round. The diameter of tube has influence on the thick-ness of tube itself. For example, wall thickness of 5.6 - 25mm can be found in tube of 7-inch diameter and wall thickness of 11 - 36 mm in 16 inch.

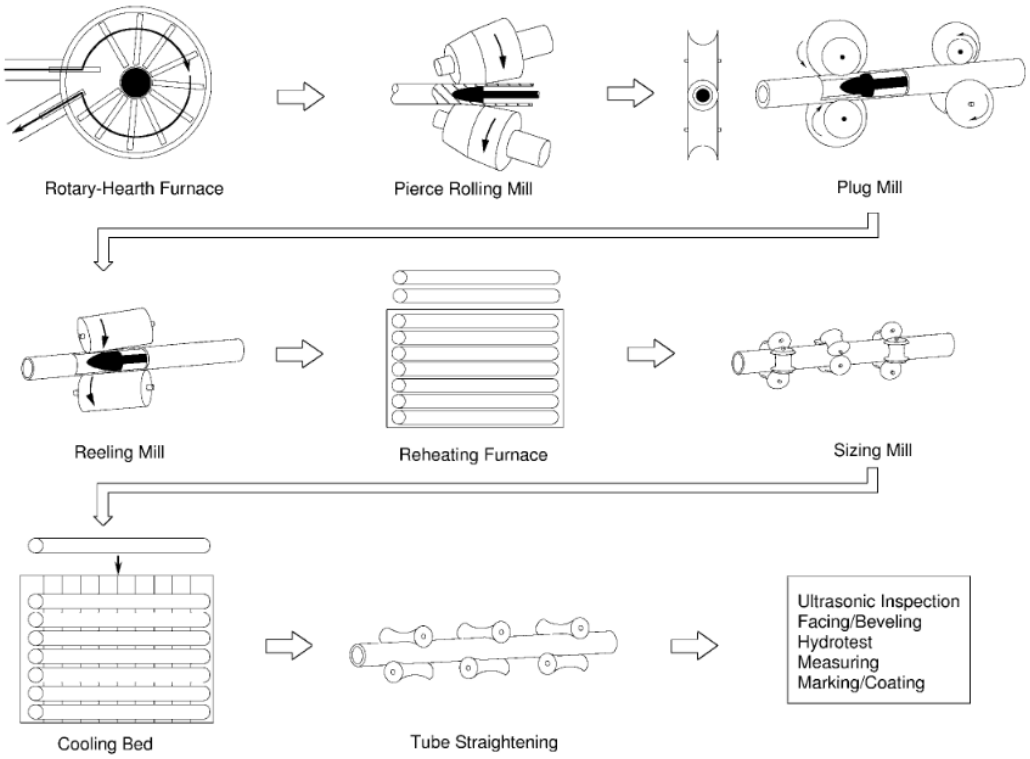

Figure 11: Steps involved in seamless tube manufacturing method by Plug Rolling Process.

As in Pilger rolling process, the plug rolling process is also starts with continuously cast round of specific diameter. There is some mill specific diameter of a cast round such as 180, 220, 270 and 310mm. Depending upon the dimension of a final tube, one specific diameter of cast wound was selected and further processes were done. As shown in Figure 11, the rounds are preheated to the forming temperature of 1280^0C at gas rotary-hearth furnace. The process followed by pierce rolling mill which is a modern version of Mannesmann piercing process. In this step, two large double-conical work rollers roll the round and simultaneously force forwarded to the plug mill process. The large double conical work rollers are connected to large electric motors via shaft. During the piercing, some eccentricity may occur and to some extent, it will remain in final product too. The main forming step of the process is done in plug mill. This reduces the diameter of tube and wall thickness as well. The process followed by reeling mill where diameter of tubes is smoothened. During the smoothening of the specimen, it gets cool down therefore, tubes are reheated in furnace at temperature about 1200^oC. As in Pilger process, the final reduction of OD is done in sizing steps. The roller sets in this step are arranged to increasingly smaller diameters, which reduces the OD up to the required final dimension. The tubes do not rotate in sizing instead the roller provide rotary action and moves tube forward to the cooling bed. The cooling of tubes is done to achieve required microstructures and straightening of tubes are done next. Tube straightening is the final step in the process and forwarded to the quality inspections. [11]

d. Continuous Mandrel Rolling Process

In continuous mandrel rolling process, mandrel mill is a main forming step that involves rolling over a solid mandrel insert. However, combination of 4 different forming steps is involved in the process. This is the process of continues manufacturing of a tube mainly of diameters 1 to 7 inches and a wall thickness of 2-32 mm. As in other processes, the casted round steel ingots are used in this process which may have dimension of 5 m length and 180 mm diameter.

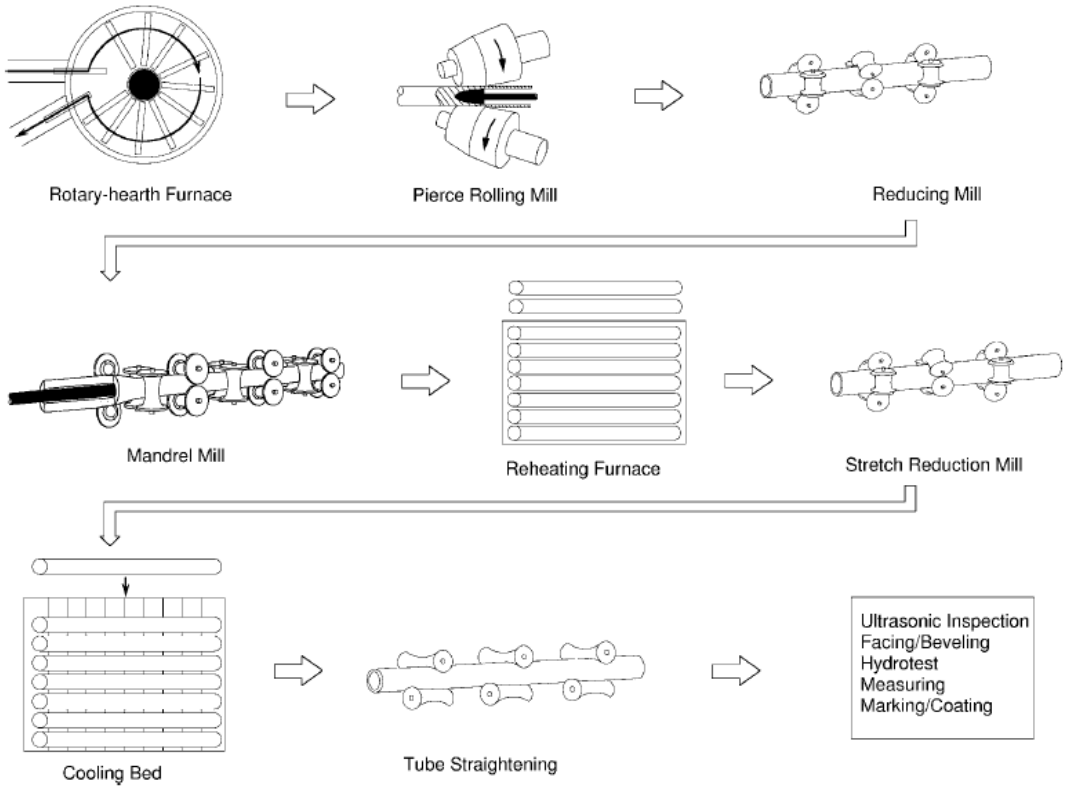

Figure 12: Steps involved in seamless tube manufacturing method by Continuous Mandrel Rolling Process.

Similar to other process, this process also starts with heating of ingots in gas rotary-hearth furnace. The temperature of a round goes up to 1280^{o}Cfollwed by a piercing of a rounds using a Mannesmann piercer similar to the pilger and plug mill processes. The pierced tube blank passes through the six three- rollers which contains the reducing mill. The reducing mill helps to get a tube of desired dimension by reducing it in step-by-step manners. The diameter of different tubes can be achieved by using a sing diameter ingots in this process because of the step-by-step manners in reducing mill. The wall thickness of tubes measured by ultrasonically while exist from reducing mill to the mandrel mill which is the main forming step in this process. In mandrel mill, the solid mandrel inserted into the annulus as of a specimen as shown in the Figure 12. The mandrel mill contains 8 pair of stands located at 90-degree angle of each stands which helps to reduced OD. It is necessary to have a speed in mandrel mill step in order to keep specimen hot enough to achieve the step´s objective. While existing from the mandrel mill the tube may have

diameters of 119, 152 or 189 mm and length could have maximum 30 m. The temperature may drop to 700ºC that´s why it is reheated to 1000ºC and passes to the stretch reduction mill to reduce the diameter and wall thickness of tubes. In stretch reduction mill, 28 three-rollers are placed at 60-degree angle of each roller stand which results star-shaped ID. The combination of different four forming step in this process has a scope of producing tube up to 160 meters in length using the ingots of only 5 meters. The next step in to go through cooling bed to obtain desired microstructures and followed by a final step of straightening of a tube. As in other processes, final inspection and quality inspection is performed then. [11]

e. Tube Extrusion Process

When a material is pushed through a die of the desired cross section to create an object of certain cross-sectional profile, the process is called extrusion. And manufacturing of a tube using a process of extrusion is called tube extrusion. Tube extrusion process is very common process of manufacturing seamless tube especially in non-ferrous steels like aluminum, copper etc. Also, it is very popular to manufacture polymer tubes and pipes for example poly-propene tubes can be manufactured up to 1600 mm in diameter. Today because of the development of the manufacturing technique, extrusion process is popular to manufacture stainless-steel variety as well. [13]

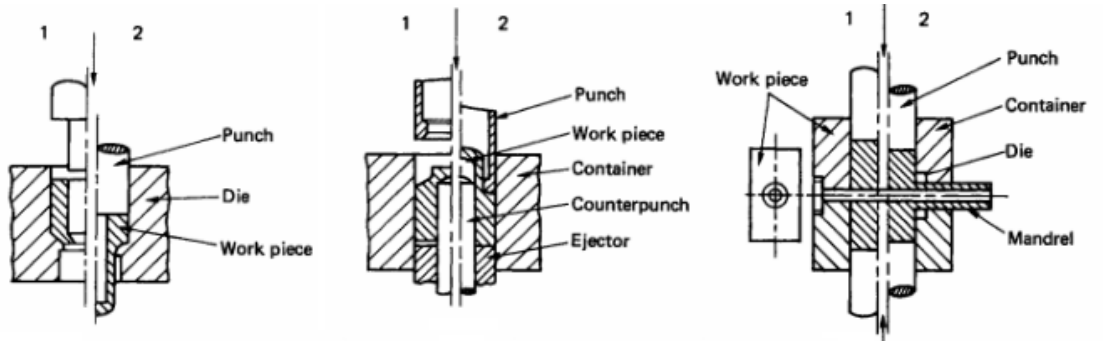

Figure 13: Forward extrusion of tube, Backward (reverse) extrusion of tube and Side extrusion of tube [13].

There are 3 basic types of extrusion process: forward, backward and side flow as shown in Figure 13. In forward extrusion process, previously prepared billets are placed in the container and extruded. It is directly extruded threaded onto a cylindrical mandrel if it is pre-pierced and then extruded. This results thinning of a wall of tubes and elongation of tube. Similarly, in case of backward extrusion, the billet is placed at the bottom of container and a hollow punch, of bore diameter corresponding to the outer diameter of the tube to be extruded, is forced into the material, causing it to flow upwards. The ejector is used in both forward and backward extrusion to remove the product. In case of side extrusion, the die is placed in the side of the container and billets positioned at right angles to it with the support at its lower end. The axial forced movement of a punch towards downward results the flow of a materials through the die. The billets are pierced at the beginning, inserted into the container and mandrel threaded through it in all three types of extrusion process to produce a tube.

There are various steps involved in commercial production of tubes using extrusion technique. For example, in manufacturing or a stainless-steel´s tube, the steps involved are: preparation of billets, heating, lubricating, providing a pilot hole, reheating and re-lubricating, extruding, removing the lubricants and finally straightening if needed.

Table 1: Materials and die geometries in simple conventional hot extrusion [13].

Metal extruded	*Billet temperature* (°C)	*Extrusion ratio*	*Comments*
Aluminium (soft architectural alloys)	400–500	10–400 (630 for indirect extrusion)	Flat dies, hollows using bridge, spider, porthole types. Highly complex shapes
Brass	650–750	10–400 (600 for indirect rod extrusion)	Flat dies, hollows using mandrels. Complex shapes
Copper	750–950	10–250	Flat dies, hollows using mandrels. Simpler shapes
Steels	1000–1300	10–25	Extrusion ratios apply to sections, not tubes. Profiled or bell-mouthed dies are essential for the Ugine–Sejournet process. Hollows using mandrels. Simple shapes
Nickel alloys	1050–1200	7–50	
Titanium alloys	850–1150	9–100	

The first step of extrusion of tube process is preparation of billets. The billets are faced at least in one side and the surface quality of billets has effect on the surface quality of hollow. The prepared billets then heated in the induction furnace up to 1200 degree Celsius in case of steel or heating using salt bath heating technique. The general practice in induction heating technique is to preheat to the certain temperature for example 1080^{o}C in case of steel and final heating to reach the extrusion temperature i.e. 1200^{o}C for further process. In case of salt bath heating technique, preheating is done in gas-fired furnace which also helps to prevent scaling and followed by heating in a salt bath to extrusion temperature. The use of induction furnace made easy to regulate and ensures the correct rate of heating in a given material. The heating temperature of billets depend upon the used base materials. Table 1 shows the required temperature of billets during the heating of different materials. Lubrication is next key technique in the extrusion process and is essential to deal with the high temperature and applied heavy loading during the process. The Lubrication process is followed by extrusion. As described in Figure 13 there are three different type of extrusion process and as per the requirement certain process is used. The next step is removal of lubricants and then followed by cutting a tube in required dimension and final surface treatment. [13]

2.3.2 **Welded Tubes**

Welded tubes are produced by forming a metal sheets into a cylindrical form over a mandrel to produce open pipe, and then followed by welding. According to the forming and welding process, the welded tube method has been distinguished. Continuous rolling and single forming operations are a forming processes involved in welded tube production whereas electric resistance welding and electric arc welding (fusion welding) are the most

common welding processes used in welded tube production. In electric resistance welding tube, only continuous forming process is used and welded longitudinally whereas, in case of fusion welded tubes, both continuous and single forming processes are used. Figure 14 shows the forming process and different welding process used in welded tube along with the size ranges. Welded steel tubes are produced either by longitudinal or spiral seam. In both cases, the metal sheets rolled flat which may take hot or cold rolled steel strip form depending upon the manufacturing process, dimension and the applications of tube.

Compare to seamless tube, welding tubes are less expensive and available in longer continuous length. However, the working pressure in seamless tube is higher than that of welding tube therefore, it is good idea to not choose welded tube where working pressure is critical. Welded tubes are available more readily than seamless and also wall thickness of welded pipes are more consistent. The inner surface quality of welded pipe can be checked beforehand to maintain the quality level as need-ed. The application of welded tubes are food & beverage industries, biopharmaceutical market, air heater, air cooler etc. [14]

Forming process	Welding process	Nomenclature	Weld	Size range (OD)
Continuous	Hot pressure welding	Fretz-Moon	longitudinal	13 ... 114
	Electric resistance welding (ERW)	Direct current Low-frequency High-frequency (e.g. HFI)	longitudinal	10 ... 20 (30) 10 ... 114 20 ... 600
	Electric arc welding (Fusion welding)	Submerged-arc (SAW) Gas metal arc (MAG) (tack welding only) Gas metal arc (TIG, MIG, ERW)*	spiral spiral/ longitudinal	168 ... 2500 406 ... 2032 30 ... 500/10 ...420
Single forming operation 3-roll bending machine C-ing press		Submerged-arc (SAW) Gas metal arc (TIG, MIG, ERW)*	longitudinal	≥ 500 200 ... 600
Single forming operation U/O-ing press		Submerged-arc (SAW) Gas metal arc (MAG) (tack welding only)	longitudinal	457 ... 1626

Figure 14: Welded tube and pipe production processes [15].

The further discussion on the welding process used in welded tubes production and forming process will discuss below:

a. Electric Resistance Welding Processes

Electric Resistance Welding (ERW) is a welding process that produces coalescence of the faying surfaces with the heat obtained from resistance of the work-pieces to the flow of the welding current in circuit of which the work-pieces are a part, and by the application of pressure. [16] The differences between resistance welding and arc welding is that, there is no need of filler materials and flux in resistance welding. There are 4 factors involved in the resistance welding; the amount of current, the pressure used by electrode, the time of the current flow and the area of electrode which has contact with the work-pieces. When current passes through a resistance circuit, heat generated. When there is maximum resistance, the amount of heat is also maxi-mum, which is the exact part being joined. The pressure is needed throughout the process to ensure closed circuit. The amount of current up to 100,000 A at low voltage could generate enough amount of heat to change

the work-pieces' contact area to molten state which eventually get joined. The total heat energy generated in this welding method can be expresses as follow [16]:

$$H = I^2RTk \qquad \text{Equation 1}$$

Where H = Heat energy in Joule

I= Current in amperes

R= Resistance of the materials in ohms

T = Time of current flows in seconds

K = Total amount of heat losses through radiation and conduction

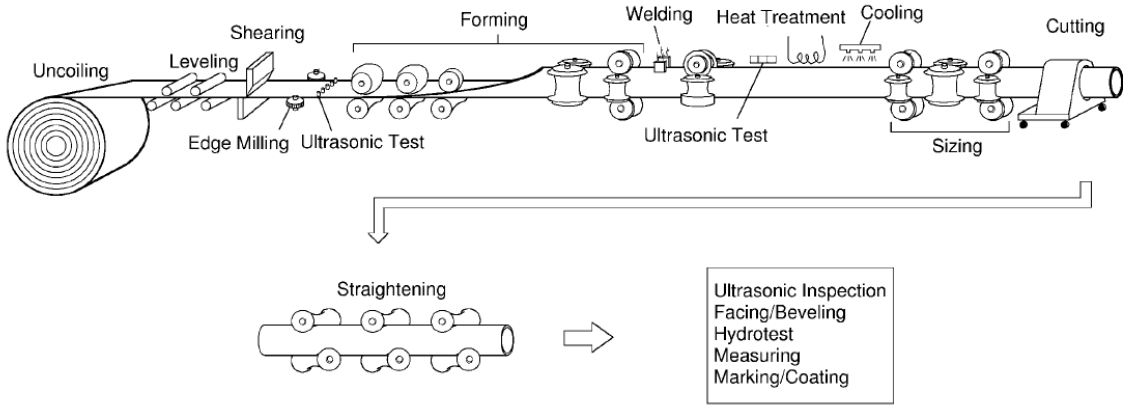

Figure 15: Schematic representation of major manufacturing steps if an ERW pipe mill [11].

There are various types of resistance welding such as Flash welding, Percussion Welding, Resistance spot welding, Upset welding and Resistance seam welding (RSEW) and so on. Resistance seam welding is the on which is used to manufacture a tube. The resistance welding is used when there is continuous forming of a rolled strip of plate which is available from 2.375 to 24 inches [11]. Without any filler materials and flux, the strip edges of the open-seam tube are joined by applying pressure and heat simultaneously. The introduced welding current in open seam could be conductive means using sliding contact and inductive means by using single or multi-wind coils [15]. The schematic representation of steps involved in ERW was shown in Figure 15. And as shown in Figure 16 the electrode is in wheel shape which rotate continuously to ensure the pressure at the edges of open seam. There is no internal water cooling system developed thus, the weld area is flooded to keep electrode wheel cool. As joining done, the tube can either be left as it is or heat treated as per application. The finishing of tube includes straightening step, trimming if needed and test and quality inspections.

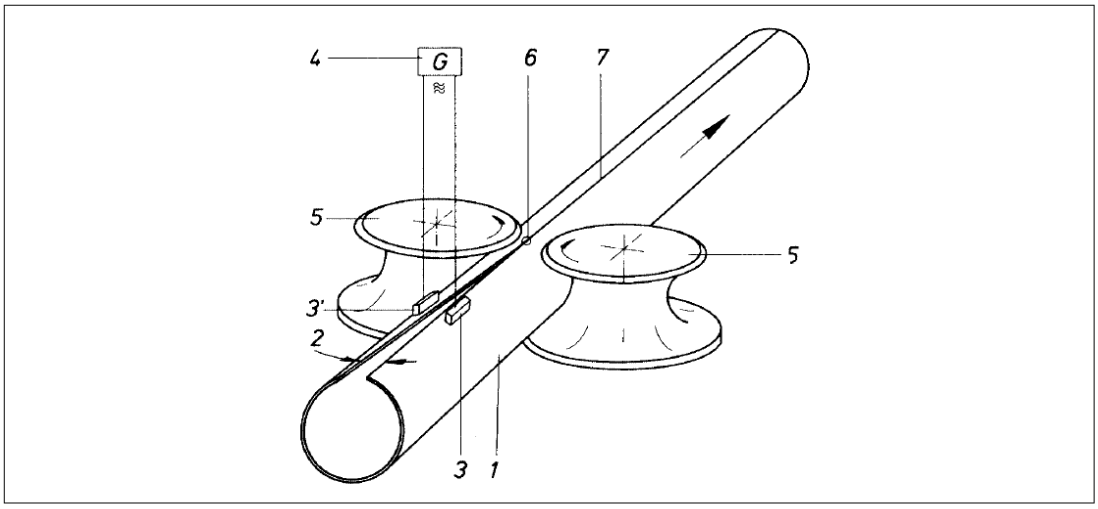

Figure 16: Electric Resistance Welding: 1) Open-seam tube; 2) Welding gap entry angle; 3) and 3´) Sliding contacts; 4) Welding generator; 5) Squeeze rolls; 6) Welding point; 7) Weld [15

b. Fusion Welding Process

The fusion welding process is excessively used in manufacture a pipe of more than 457 mm pipe. The forming used in this process are: three-roll bending process, C-ing press process, U-ing press process and spiral tube forming process. The three-roll bending process was used as cold or hot forming processes whereas, others are as cold forming only. *Submerged-arc welding* and *gas-shielded arc welding* are the fusion welding processes to produce fusion welding pipes. The applications fusion welding process are manufacturing of a high alloy stainless steel and non-ferrous metals such as titanium, aluminum and copper. [16]

- ***Submerged arc welding process (SMAW):***

Submerged arc welding process is an arc welding process in which electric fusion welding performed with a concealed arc where arc produces during the weld is hidden under the blanked of slag and flux. This slag also helps to prevent oxidation of the surface. The SMAW has high deposition rate and also high operating factors in mechanized application resulting increase of the speed of tube manufacturing. The weld has good quality and because of the flux, the fume produces or an arc emitted during the welding is minimal. The process is limited to ferrous materials. [16]

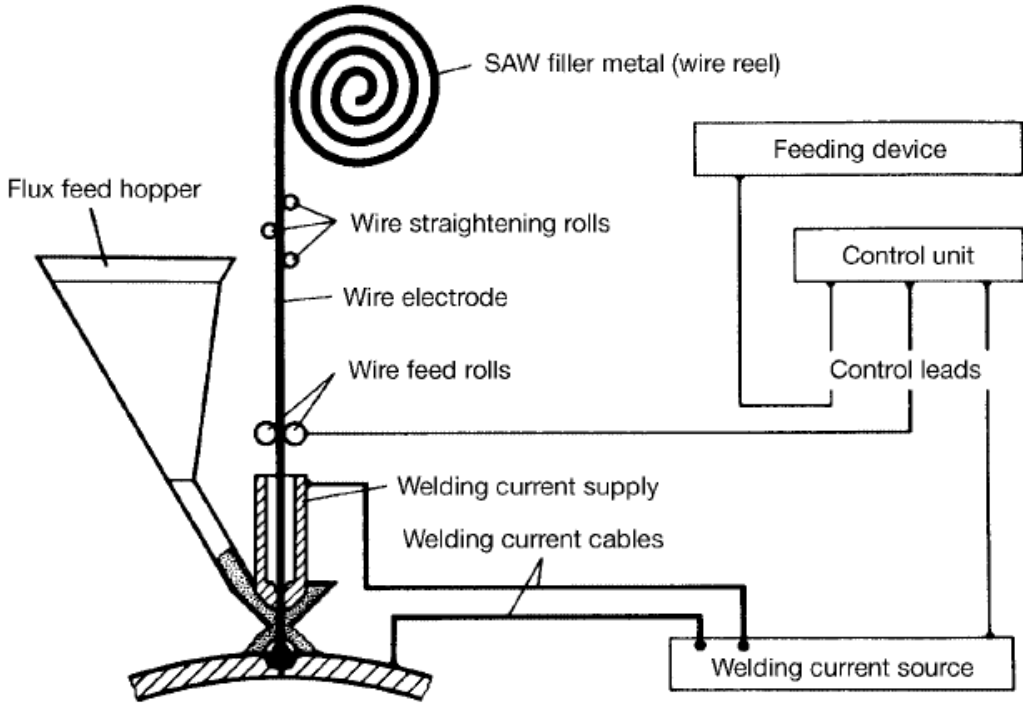

Figure 17: Submerged-arc welding process [15].

As shown in Figure 17 the filler materials are in the form of coil which is continuously fed to the molten metal pool via wire straightening rolls and wire feed rolls. The speed of feeding depends upon the desired deposition rate. And the welding current con-ducted into the electrode which has sliding contact there and returned back through the ground lead connected to the tube. The produced arc results the melting of open edges of tube and filler materials and eventually joined. Additionally, welding flux helps to form weld bead by preventing melting losses and oxidation. The slag is also used to alloy weld metal to enhance mechanical and chemical properties. The slag can be easily removed once it solidifies and can be reuse or recycle from 50% to maximum 90%. The chemical composition of flux and wire electrode must be matched to the tube´s materials. The process of manufacturing of tubes using sub-merged arc welding usually applied two-pass method which can be seen in Figure 18. The internal pass was made first and outside pass as second which ensures sufficient overlap of the passes.

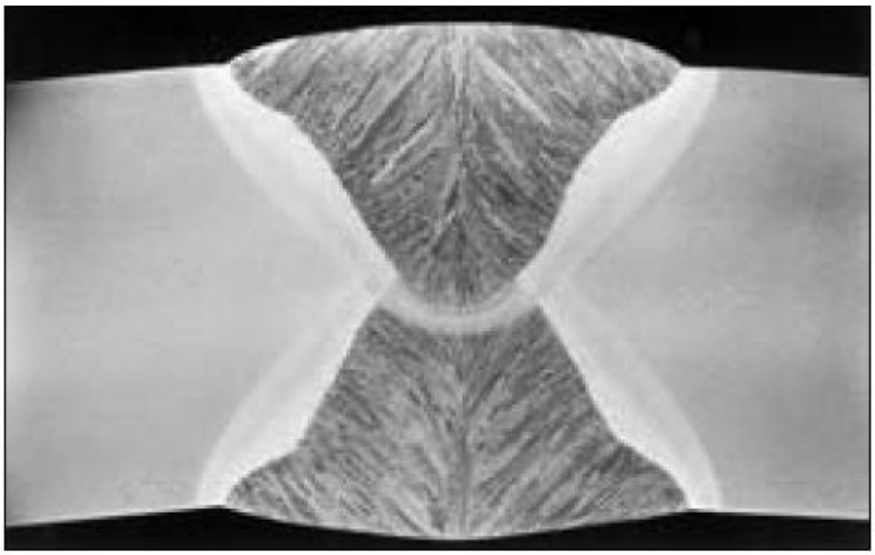

Figure 18: Submerged-arc weld [15].

- ***Gas Metal Arc Welding (GMAW):***

Gas metal arc welding is also called as metal inert gas (MIG) welding process where an arc is used between continuous filler metal electrode and weld pool. The shielding of the welding is done by using inert gas around it without pressure. The type of shielding gas is also depending upon the type of metal transfer and base metal to be welded. [16]

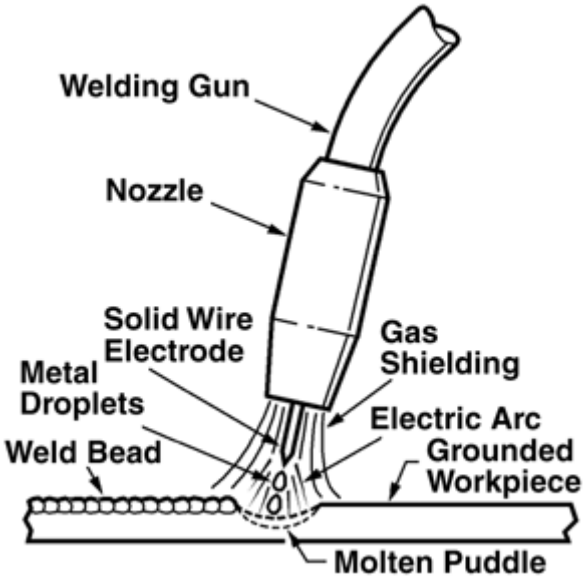

Figure 19: A typical GMAW torch [17].

Figure 19 shows that the arc is created between the continuously fed consumable electrode and the materials to be joined produced the needed heat energy to perform the welding. The heat melts the edges of tube and electrode resulting flow of electrode´s materials to the molten pool at the base materials and eventually get joined. There are many factors to control the penetration of welding and width of molten pool. But the primary one factor is a welding current which controls the penetration and the travel speed to control the width of molten pool. To get a good quality of welding there are many things to consider

such as right depth of penetration, good width of molten metal, electrode size, the mode of metal transfer etc. Especially in pipe production if the molten pool is too large, the molten metal will run out and could create a big welding problem. It is necessary to shield the welding pool, the arc and the surrounding area to save it from contamination. The continuous flow of shielding gas from nozzle during the welding solve the problem of contamination. The shielding gas could be inert gas, active gas or mixtures depending upon the materials. The major ad-vantages of GMAW are high operator factor, high deposition factor etc. [16]

2.3.3 **Tube Forming Processes**

The tube forming processes are important initial step in welded tubes. The major four processes are described below:

a. UOE Forming Processes

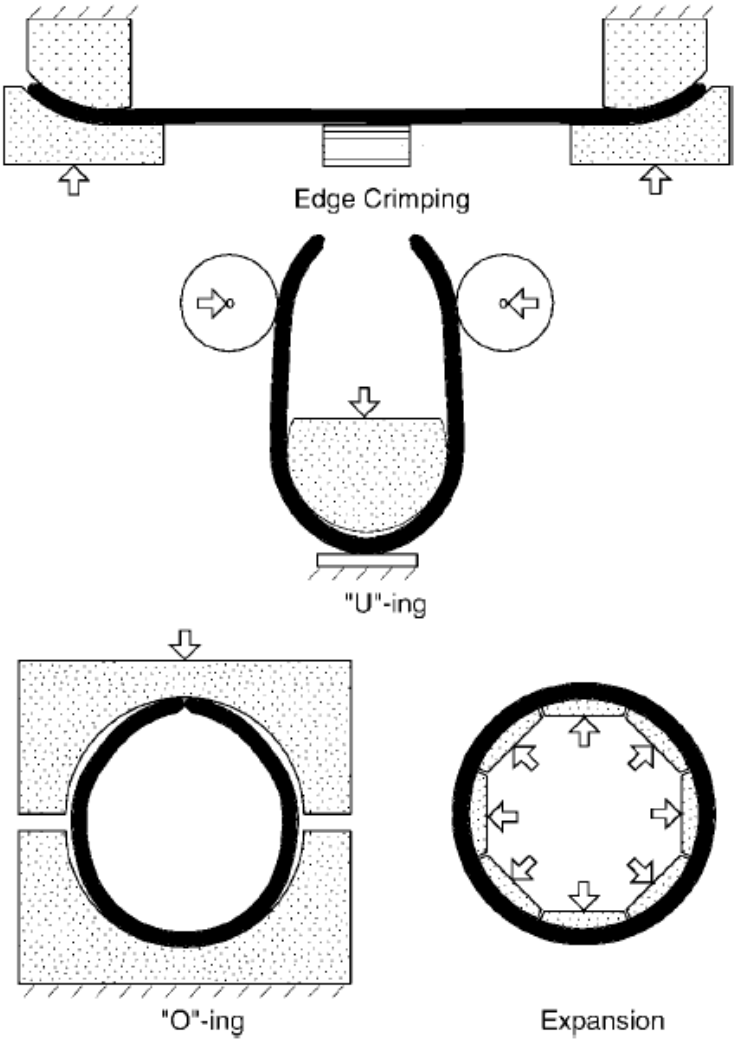

Figure 20: Schematics of the four cold forming steps of the UOE process [11].

UOE forming process is very common to produce welded pipe larger than 16 inches. The maximum diameter it can produce is 64 inches and has standard length of 12m or 18 m.

The capacity of wall thickness of pipe varies with the steel grade and diameter of pipe itself. It can be found up to 45 mm wall thickness for some steel grade industry-wide. There are mainly four mechanical steps involved in UOE forming process; Edge crimping, ``U´´-ing, ``O´´-ing and Expansion as shown in Figure 20. As plate is ready, the edges of plate are crimped into a circular arc. The second step is to U-press in a U-shape followed by pressing in O-shape which is achieved by pressing the ends between two-shaped dies. Then the pipe goes for submerged arc welding process in this case and the seam of the pipe get welded. As a final step, mechanical expansion of welded pipe is done to improve the roundness and straightness and al-so helps to bring pipe in its final dimension. The typical expansion rate is 0.8-1.3% from its diameter to achieve low ovality. From these three important steps of U-ing, O-ing and Expansion, the name of process UOE stands. UOE manufactured pipes have nearly uniform shape; ovality and straightness typically have range of 0.1-0.3 percent. [11]

b. JCO Forming Processes

JCO forming process is an alternate way of forming to UOE. The step of U-press and O-press involved in UOE is replaced by JCO here. The initial step of plate preparation and edge crimping is same and then process followed by feeding a crimped plate to a press. The press shaped simultaneously the whole length by local pressing of part of the circumference. The process was shown in Figure 21.

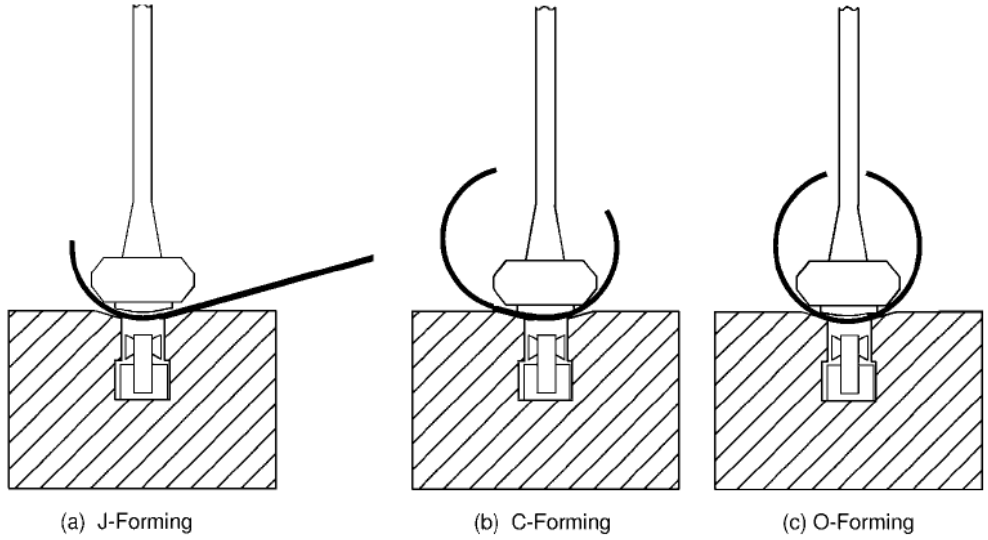

Figure 21: Forming of plate in JCO process [11].

The pressing start at the on edge of the plate and progressed to other edge and finally to the mid width of circumference. The first stroke formed J-shaped cross section and second stroke is applied to other edge which results C shaped cross section. Then the final stroke is applied just in the mid width of it to make O-shaped cross section. This completes the forming process so, pipe further processed to welding step. The tack welding is done initially before submerged arc welding here. The welding is done in both inside (first) and outside of the seam. The final step in JCO forming process is expansion. The expansion through the circumference is done to improve the circularity and straightness of pipe. The

expansion at level 1% is needed in this case to obtain good circularity. Overall, JCO process is similar to UOE in both shape and mechanical properties. The difference of this process compared to UOE is that, it is more convenient to make pipe with thicker wall because of the forming of its circumference in step-by-step which means less force is enough during O-forming. [11]

c. Spiral Tube Forming Processes

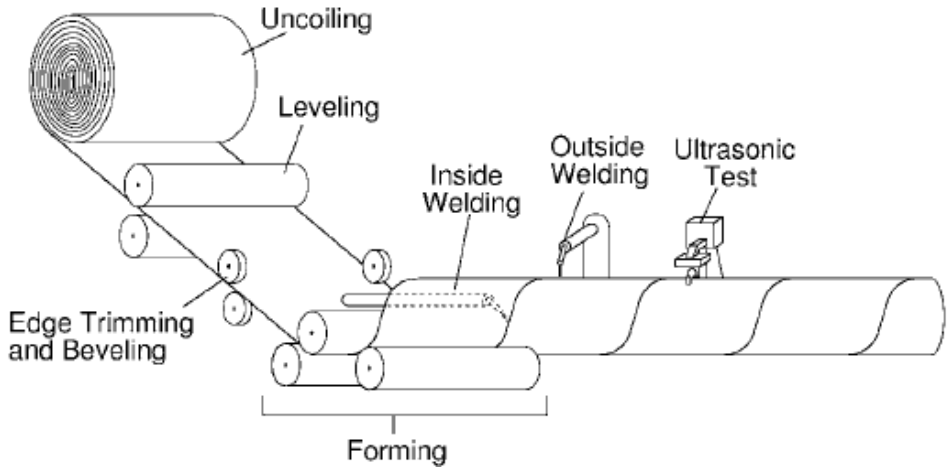

Figure 22: Schematic representation of a spiral weld pipe mill [11].

Spiral tube forming is a continuous forming process in a pipe production of a larger diameter: typically, 20-100 inches. As shown in Figure 22 there is a continuous hot rolling of plate stripe from a huge coil having desired thickness and width. The leveling of a stripe is done and followed by trimming of the edge and beveling. Finally, the forming is done with appropriate spiral angle by rolling it into a circular share as in Figure 22. The diameter of pipe depends upon the angle of spiral and the width of plate. The further process of welding is done in next step to produce a pipe. Since it is a continuous process, resistance welding is most common welding process which is done in inside and outside of the tubes. The pipe produced by spiral forming can be made larger diameter than the standard diameter of pipes made by other forming process. Also, longer pipe than the standard length of pipe made by other forming process (12m or 18 m) is also possible. The wall thickness, uniformity and tolerances are very good here, because the pipe is rolled from plate and the continuous process made it the most efficient process in terms of prices. Because of the long spiral weld length and the out-of-roundness, it is less common to use in off-shore application which involves high internal or external pressure. It is mainly used in low pressure application, tunnel liners, and power plants and so on.

2.4 Application of Tubes

By the year 2022, the global market of seamless tubes alone is projected to reach to 65 million tons according to a [1]. The data shows that, there is huge demand of tubes and area of its application. According to the type of tubes such as different materials and

different dimensions, the application area may vary. Some example of tube application areas are oil and gas industries, nuclear industries, heat exchangers and condensers, power plants, chemicals and petrochemicals industries, boilers, automobiles, medical industries etc. Figure 23 shows the different application of steel and copper tube. There are various type of tubes based on the materials such as ferrous, non-ferrous, plastic, wood and so on. Here, the applications of metallic (Ferrous or steel tubes and non-ferrous tubes) tube were presented which are relevant to F2T process.

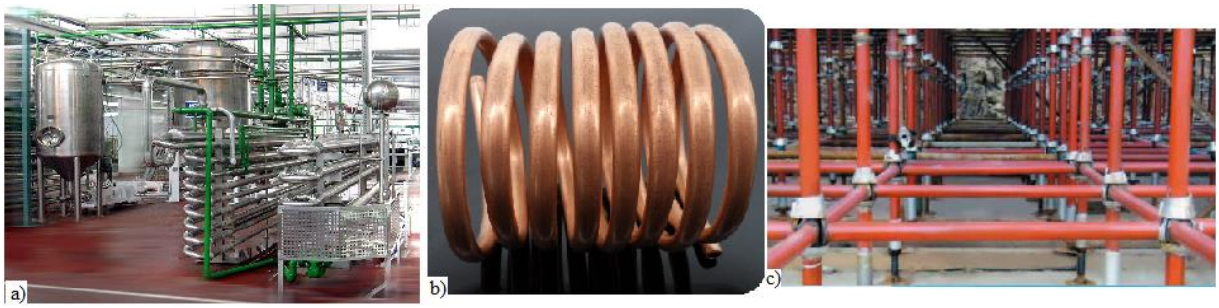

Figure 23: Application of Pipes/tubes: a) Stainless steel tubes in food industry, b) Cupper coiled tube coil heat exchanger, c) Structural steel pipes used in scaffolding.

2.4.1 **Steel Tubes**

The most common materials used in manufacturing of tubes which are highly applicable in any industries is steel. It can be used in many applications such as water pipes, sewage pipes, scaffolding pipes, oil and gas pipes and so on. The properties of steels are altered as per the application. Cast iron, stainless steel, structural steel etc. are the different types of steel used in tubes. The application of steel tubes in industries are described below:

- **Cast iron tubes** are primarily used for designing of soil and rain water disposal systems (drainage or sewer system). It is widely used in building and construction area. Generally, they are made by sand cast process and heavier than other pipes.
- **Galvanized tubes** were common to convey drinking water in residential areas several years ago because of corrosion resistance which is not always true if the pipes are old. Copper tubes and PVC tubes have replaced galvanized tubes by the time however galvanized tubes are still common in many industrial areas to convey pressurized water.
- **Steel casing tubes** are used in casing of oils and gases. The objective of casing tubes is to protect the main tube which convey oils and gases. In many countries, it is also used as a casing in drinking water supply.
- **Alloyed steel tubes** are those which has one or more alloying elements other than carbon and generally more responsive to heat and mechanical treatment than carbon steel tubes. Therefore, these types of tubes can be used in industrial areas where temperature and strength are critical such as engine parts. Structural steels, stainless steels etc. are also called alloyed steels.

- **Structural steel tubes** are primarily a construction material. Many types of tubes such as steel pole, steel fencing, steel exhaust pipes, steel handrails and steel columns are called as structural steel tubes.
- **Steel scaffolding tubes** are used temporary framework to support construction activities. The desired properties of scaffolding tubes are light weight and strength.
- **Stainless steel**: Stainless steel tubes are used in variety of industries because of their properties. They are corrosion resistance, cryogenic resistance, ductile, high strength etc. The minimum chromium content in stainless steel in 10.5% and other alloys can be added according to the application [19]. The use of stainless steel tubes is popular in oil and gas industries, automobiles, shipping industries, medical industries, food and beverages and so on. In the industrial use of tubes there was transportation of different type of fluids or gases in different pressure. Stainless steel tubes are very popular tubes used in industries to fulfil such demands. More examples of stainless steel tubes applications are engine parts, prosthetics in medical areas, supply of food and drinks etc.
- **Duplex stainless steels** are almost twice strong compared to other stainless steels (austenitic) [20] and improved resistance to corrosion cracking. This types of tubes are used in heat exchanger tubes, pulp and paper making equipment etc. Because of improved corrosion resistance, they are also used in seawater handling systems.

2.4.2 **Non-ferrous Metal Tubes**

Tubes of aluminium, copper, titanium, nickel, lead etc. are categorized under non-ferrous metal tubes. Because of their properties such as higher corrosion resistance, higher conductivity, higher weight to strength ratio, non-magnetic property etc. they are widely used in industries. However, non-ferrous metal tubes are expensive than steel tubes. The selection of materials was done according to the application.

- **Copper tubes:** Copper tubes are typically used for conveying hot and cold water in residential area and in industries. Copper tubes along with PVC tubes has replaced the use of galvanized tubes in water supply system. Though copper tubes are expensive, they are used because of their highly corrosion resistance property. Other application of copper tubes is as refrigerant line in HVAC, cooling purposes in radiators etc.
- **Aluminium tubes:** Aluminium is mostly known for the light weight. Aluminium tubes are commonly used in such application where weight issue is critical for e.g. aeronautics, racing cars and space rockets. Aluminium tubes are also corrosion resistance and non-magnetic therefore, they can be used in conveying of chemical in chemical industries. The aluminium alloys could get as higher strength as steel while their density is one-third of steels. This is the reason that aluminium tubes are also used as structural steels in construction industries. Scaffolding is a good example of it where light weight and strength in mainly demanded.

- **Titanium alloys:** Titanium alloys tube are made up of titanium and other chemical elements and they have very high tensile strength and toughness compare to steels. Even at extreme temperature titanium are firm to their properties. Titanium alloys tubes are used in aircraft hydraulic system, medical implants, offshore drilling rig components, subsea equipment, marine and chemical processing plants. [21]
- **Nickel alloys:** Nickel is alloyed with different other elements such as aluminium, chromium, titanium etc. They are highly resistant to corrosion, heat and stress. There is increasing demand of nickel alloy tubes in the application of chemical and petro-chemical, aerospace, medical technology food processing, fertilizer production, coal and gas processing, environmental-waste treatment, etc. Heat exchangers in chemical processing and nuclear power industry are made up of nickel alloys. It is used in aerospace parts and components. Also in oil and gas extraction programme where corrosion, pressure and temperature resistance tubing is required, nickel alloys tubes are used.

2.5 Standard Test Analysis of Tubes

The quality control of a raw materials in a tube production is a primary factor to achieve high quality tube. And control of the quality of the pipe production process is another essential condition. There are different ways of quality inspection of a tube which includes visual inspections and mechanical inspections. The details on mechanical inspection will be discussed in this section. Conventionally, pipe producers relied on eddy current and ultrasonic testing for detecting the failure of welded pipe [21]. But today there is a practice of many other testing equipment along with the conventional one. Some of the standard testing methods are presented as follows:

2.5.1 Tensile Test

One way of destructive test, where application of tensile force applied into a test specimen until the failure. The test related to the mechanical testing of steel products subjects a machined or full-section specimen of the material under examination to a measured load sufficient to rupture to find the properties of materials such as ultimate tensile strength, maximum elongation, Young´s modulus ratio, Poisson's ratio etc. [23]. These factors were defined by stress-strain curve which are important factors to choose a right material depending upon the application.

To perform the tensile test, test specimen is prepared following certain standard. The test specimen prepared in F2T was presented in section 5.2. In tensile test, the relation shown by stress and strain which is present as stress-strain curve is unique for each material. Strain-stress curve is derived by measuring the deformation at distinct intervals of tensile or compressive loading (stress). Figure 24 shows the typical strain-stress diagram for a ductile metallic material. The engineering strain ($\mathcal{E}$) or nominal strain in the test is calculated by measuring the elongation of the gauge section against the applied force which is also shown in equation 2. [24]

$$\varepsilon = \frac{L-L_o}{L_o}$$ Equation 2

Where L is a final gauge length and Lo is original gauge length.

Similarly, another factor in stress-strain curve, engineering stress or nominal stress (σ) is calculated using equation 2.

$$\sigma = F/A$$ Equation 3

And here, F is the applied tensile force and A is the nominal cross-section area of the test specimen.

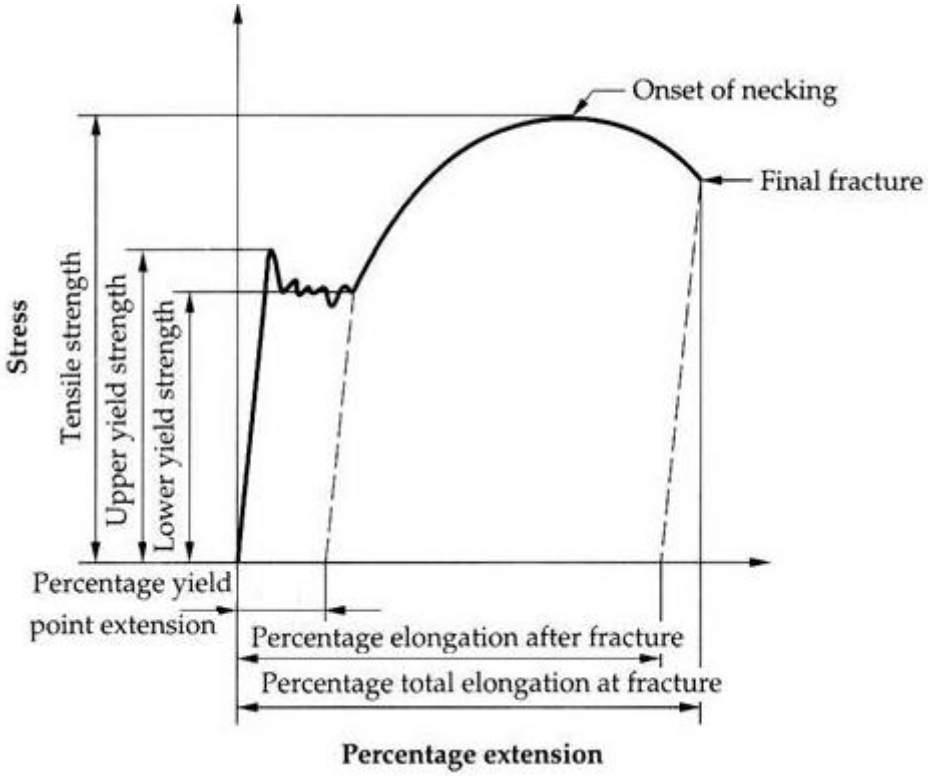

Figure 24: Typical stress-strain diagram for a ductile metallic material exhibiting yield phenomenon [25]

The ultimate tensile strength (UTS) or simply known as tensile strength is the maximum stress level reached in tensile test as shown in Figure 24. When a solid material is subjected to small stresses, the bonds between the atoms are stretched. When the stress is removed, the bonds relax and the material returns to its original shape and the phenomena is called elastic deformation. Whereas as at higher stresses, planes of atoms slide over one another and in this case, the deformation is not recovered when the stress is removed and the phenomena is called plastic deformation. The stress required to produce a small-specified amount of plastic deformation is called yield strength.

2.5.2 **Hardness Test**

The property of a material that enables it to resist plastic deformation, usually by penetration is called hardness. However, the term hardness may also refer to resistance to bending, scratching, abrasion or cutting [26]. Hardness test is a mechanical testing method to measure the mechanical resistivity of a material to the mechanical penetration of another harder body. Materials such as metals, concrete, ceramics are known as a harder material. Diamond is the hardest materials known by the date therefore, industrial diamond is used as an indenter in hardness testing procedure. There are several methods of hardness measurement such as Rockwell hardness test, Brinell hardness test, Vickers hardness test, Micro-hardness test etc. The Vickers hardness test is the one which was carried out during this thesis work.

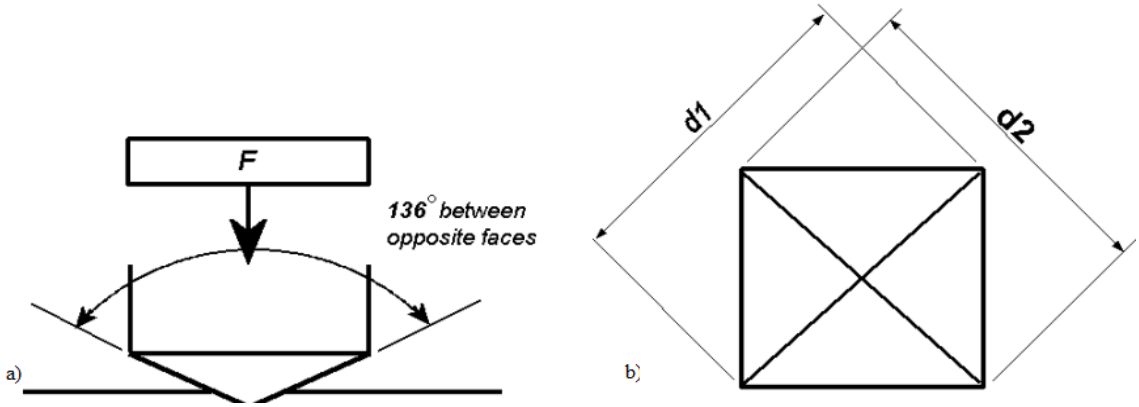

Figure 25: Principle of Vickers hardness test measurement. a) Force (F) applied to indent by diamond indentation b) Square base indentation and measurement of diagonal d1 and d2. [26]

The Vickers hardness test method has an indenter of a diamond in the form of right pyramid. The indentation has square base in an angle of 136 degree. As shown in Figure 25, the load of 1 kg to 100 kg force was applied in the test specimen too get the square base indentation. The principle is to indent in a specimen with the diamond indenter and measure both diagonal of the square base which later on interpret as hardness value. The interpretation depends upon the Vickers equation 4. [26]

$$HV = \frac{2Fsin\left(\frac{136}{2}\right)}{d^2} = 1{,}854\frac{F}{d^2} \qquad \text{Equation 4}$$

Where,

HV = Vickers hardness

F = load in kgf

d= Arithmetic mean of diagonals, d1 and d2.

2.5.3 **Flattening Test**

The flattening test is a method of checking ductility in a metallic circular cross-section tubes. The test is performed to evaluate the ability of tubes to undergo plastic deformation

and may be the defect on it. [27] The specimen for the test is cut from the tube in a direction perpendicular to the longitudinal axis. Flattening of the specimen may be done either after separating it from the tube or before separating and may be done hot or cold [28]. Generally, the cold flattening is performed in a tube of diameter less than 60mm by placing it between two flat surfaces to a distance of (H) as shown in Figure 26. The value of H is calculated using the equation 5.

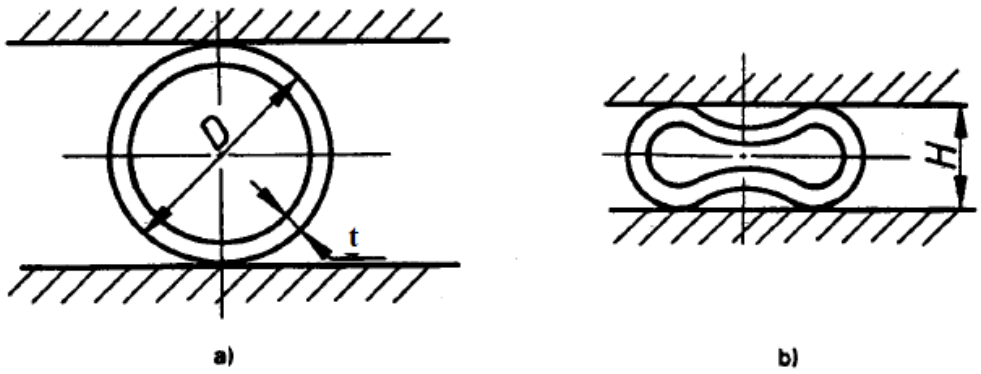

Figure 26: Flattening test of circular cross-section tube of diameter D and wall thickness t. a) Before flattening b) Flattened specimen [27]

The visual inspection is enough in flattening test. As the specimen get flattened, the visual inspection was observed to see the cracks on it.

$$H = \frac{(1+e)t}{e+\frac{t}{D}}$$ Equation 5

Where,

t = Tube thickness

D = Outer diameter of tube

e = constant (0,07 for carbon steel having carbon content 0,19% or more; 0,09 for carbon content less than 0,19%)

H = Distance between plates measured under load

2.5.4 **Flare Test**

The Flare test is a test conducted in a metallic circular cross section tube to determine the ability of it to undergo plastic deformation in drift expansion [29]. The objective of flare and flattening test is similar in the view that, both tests were done to know the ductility and may be the defect on tube too. In test, expansion of the end of the tube was done symmetrically by pressing the hardened conical steel called mandrel. The preferable angle of conical mandrel is 30, 45 and 60 degree. The mandrel is pressed into the specimen until the percentage increase in the outer diameter at one end of the tube reach to the certain value as provided in specification requirement. [30].

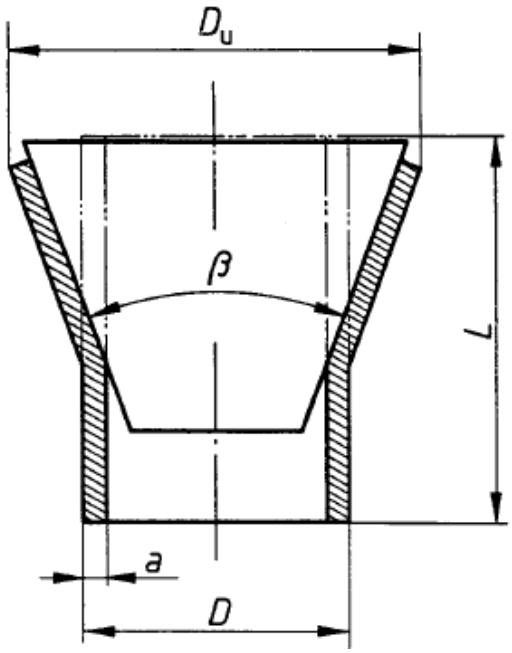

Figure 27: Drift-expansion of the specimen of length (L), thickness (a) and Outer diameter (D) to expanded diameter (D_u) by conical mandrel with an angle (β) [29]

The Figure 27 shows the expansion of one end of the tube when it is pressed by the mandrel. As per [29] The length of the specimen need to be approximately two times of the outer diameter of it when the angle in conical mandrel is 30 degree or less but when angle is more than 30-degree, length need to be approximately one and half times the outer diameter. The both end of the specimen should be plane perpendicular to the axis of tube. The test is performed in room temperature and force is applied to specimen without any shock. The speed of should not exceed 50mm/min. The mandrel may be lubricated and it should not rotate while performing the test.

2.6 **Design of Experiments: Taguchi Method**

2.6.1 **Introduction**

The set of methodologies developed by Dr. Genichi Taguchi by which the inherent variability of materials and manufacturing processes has been taken into account at the design stage [38]. The method has improved the desire characteristics and simultaneously reduced the number of defects by studying the key variables controlling the process and optimizing the procedures or design to yield the best results [41]. Just after the Second World War, Taguchi started to develop new methods to optimize the process of engineering experiment and come up with the techniques which are now known as Taguchi method and today, the method is widely used industries. [39]. With some similarity with Design of Experiments (DOE), the method only conducts the balanced (orthogonal) experimental combinations, which makes Taguchi design even more effective than a fractional factorial design. Thanks to the Taguchi method that, today industries are able to have massive deduction in product development cycle time for both design and production, therefore reducing cost and increasing profit. [38]. Taguchi method also known as

the Robust design method focuses on improving the fundamental function of the product or process.

Taguchi method did also recognize controllable and non-controllable variables that exist in DOE. The variables which can be controlled are called control factors and which cannot be controlled are called noise factors. Noise factors are further distinguished in three types; External noise, internal noise and noise drive unit. The environmental factors like temperature, humidity etc. comes under external noise whereas changes that occur when a product is damaged during storage, wear and tear etc. are under internal noise factor. And in Noise drive unit there's the effect due to the imperfections in manufacturing process which could cause by machine set up`. The noise factors may have negative impact on system performance or the final product quality. [40].

The key contributions of Taguchi methods are: 1) Quality Engineering philosophy 2) Methodology 3) Experimental design 4) Analysis.

An excellent philosophy for quality control in manufacturing industries exposed by Taguchi basically arise from three concepts which are [39]:

- Quality should be designed into the product and not inspected into it.
- Quality is best achieved by minimizing the deviation from a target. The product should be so designed that it is immune to uncontrollable environmental factors.
- The cost of quality should be measured as a function of deviation from the standard and the losses should be measured system-wide.

2.6.2 **Loss Function Concept**

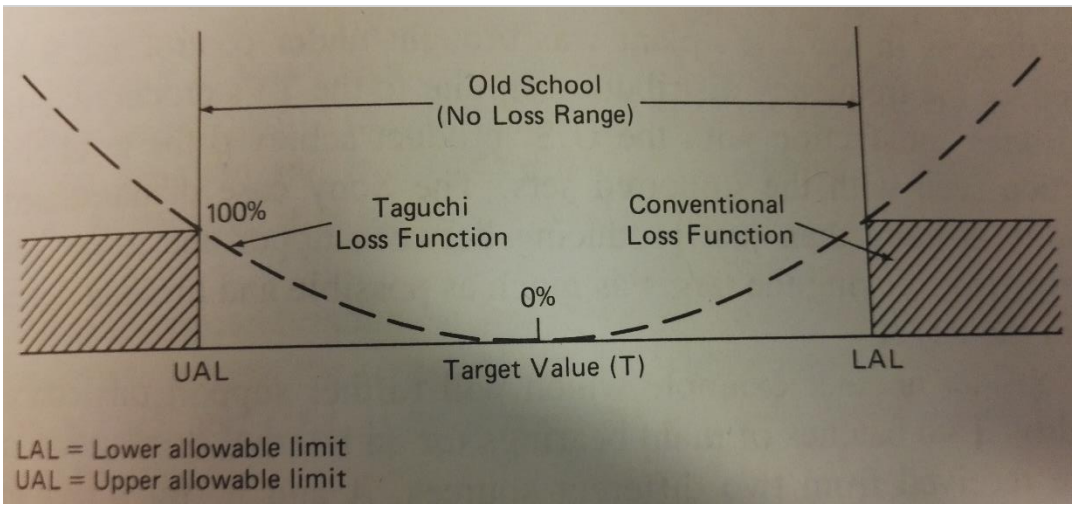

Figure 28: Taguchi and conventional loss function [41]

As shown in Figure 28, Taguchi has developed a graphical depiction of loss which shows the phenomenon affecting the value of products. Comparing to the conventional concept of quality, which says the product is termed as low quality and rejected if it doesn´t meet the design specification. But Taguchi has change whole concept stating that, quality does

not suddenly plummet if it doesn´t meet the target. Instead it follows certain function called loss function in parabolic curve as in Figure 28. Mathematically, it expressed as:

$$L= k(y-m)^2 \quad \text{Equation 6}$$

Where,

L= loss

K = constant

Y = actual size of the product

M= theoretical target value of mean value

2.6.3 **Methodology**

Taguchi method´s procedure can be listed in eight different steps which are as follows [41]:

1. Identify the main function, side effects, and failure mode
2. Identify the objective function to be optimized
3. Identify the noise factors, testing conditions, and quality characteristics
4. Identify the control factors and their levels
5. Select the orthogonal array matrix experiment
6. Conduct the matric experiment
7. Analyze the data, predict the optimum levels and performance
8. Perform the verification experiment and plan the future action

Defining the purpose of study to be performed, the Taguchi process starts. One should be clear about the objective of work and process to do further steps. As objective is clear, it is important to identify the response to be optimized. These responses have critical effect on the quality of final product which could be machine parameters such as rpm, feed etc. The quality features are of three types, they are: the higher the better (e.g. tensile strength), the smaller the better (e.g. cost) and rated the best (e.g. dimension) [40]. The next step in Taguchi method is to identifying the noise factors which may have negative impact on system performance. These noise factors could be effect of temperature or humidity. The details on noise factor has been explained in section 2.6.1.

Knowing the right parameters or control factors for the process is another important step in Taguchi method. The proper knowledge of parameters is intensely important in Taguchi method. It is not possible to do a process without prior knowledge of parameters. Before starting the Taguchi method, one should decide about the minimum and maximum

value so called level of parameters. For example, the parameters can be machine parameters such as rpm, feed etc. Depending upon the control factors and their levels selection of a proper orthogonal array matrix is another step which is also known as Taguchi Orthogonal Array (OA). The selected matrix should satisfy the number of degree of freedom. Taguchi Orthogonal array is a highly fraction orthogonal design that allows to consider a selected subset of combinations of multiple factors at multiple levels. The next step to be follow is conducting the different set of matrix experiment. It is recommended to follow the random order during the experiment to avoid the influence of the set conditions. The experiment could be done in different two ways: Replication and Repetition. In Replication, one set of test is done randomly and another set of test is done only after new setup of experiment condition. This could increase the cost of the experiment. Another way of Repetition is a way where experiments are done randomly but in same experimental run avoiding the re-setup cost of experimental conditions.

As all sets of experiments are performed, the next step is to analyze the data received from the experiments to find the optimum or best condition by studying the main effects of each factors. The arithmetic manipulation of numerical results are done in this step. It is important to know the contribution of each factors which helps to find out the way to control those factors in a view to improve performance. The analysis of variance (ANOVA) is commonly used to calculate the percentage contribution of each factors. This is standard approach of analysis however, there is another approach of signal to noise ratio *(S/N)* too where signal to noise ratio is used in analyses. *S/N* analysis is especially recommended for multiple runs and it determines the most robust set of operating conditions from variations within the results [39]. It is always a good idea to perform the verification experiments after all the results are obtained. This step ensures the things are going on right track and also helps to plan future action

2.7 **Summary**

The chapter covered literature review on different manufacturing technique of seamless and welded pipes. In the beginning of chapter, the review on patent concept of F2T, viscoplasticity and friction surfacing were presented. The F2T was invented in Aalto University while doing friction surfacing therefore, it is important to understand friction surfacing too before going to the F2T process. The chapter also emphasis in application of tubes and different test analysis method of tube. Test includes destructive and non-destructive testing methods. They are tensile test, hardness test, flare test and flattening test in destructive testing method. Similarly, eddy-current test, PMI, ultrasonic test etc. were explained in non-destructive testing section. More importantly, the design of experiment was done using applying Taguchi method to find the optimal parameters of F2T in this study. Therefore, the literature review on Taguchi method was also presented.

3 MATERIALS AND EXPERIMENTAL CONDITIONS

3.1 Introduction

This chapter explain about the reason of selecting of S355 grade steel as a base materials and equipment used in F2T and test analysis. In section 3.2, selection of base material for this thesis work was presented.

In section 3.3, equipment and accessories used in F2T were explained.

In section 3.4, description of various testing equipment are presented. Microhardness, tensile test, flare test, flattening test etc. are the test conducted in this thesis work.

3.2 Selection of Base Materials

Structural Steel S355 is the material selected for thesis work which is a high strength and low alloy steel. The standard of a material is EN 10277-2. According to EN 10025 [42], the material is cold rolled steel and has yield strength of minimum 355 MPa. Similarly, has longitudinal charpy v-notch of 27 Joules at -20^{o}C. The S355 is very common structural steel and can be used in almost every application. The typical application of S355 includes structural steel works such as bridges, components for offshore structures etc. Other application includes power plants, mining equipment, wind tower components etc. [43].

The main alloying elements of this structural steel is manganese. The chemical composition of S355 is presented in Table 2.

Table 2: Chemical composition (wt.-%) of S355J2C-h9. [43]

Composition	C	Si	Mn	P	S	Cu
Max (%)	0,2	0,55	1,6	0,03	0,03	0,55

According to material standard the mechanical properties of S355 such as yield strength, tensile strength etc. are presented is Table 3. The mechanical properties were also measured in laboratory conducting tensile test and Vickers hardness test to compare. Table 4 shows the achieved value of a base material. The standard tensile specimen was prepared and conducted a test in a laboratory. The gauge diameter of specimen was 10 mm and gauge length of 50 mm. The speed used in test was 0,025m/s. Similarly, the hardness test was conducted using Vickers method where load of 1 kg was applied and loading time was 10 s.

Table 3: Standard mechanical properties of S355J2C-h9. [44]

Dimension	Yield Strength $R_{p0,2}$ (Mpa)	Tensile Strength Rm (Mpa)	Young´s modulus E (Gpa)	Brinell hardness (HB)
∅ 15	min. 355	min. 580	min. 190	min. 146

Table 4: Measured mechanical properties of S355J2C-h9

Dimension	Yield Strength $R_{p0,2}$ (Mpa)	Tensile Strength Rm (Mpa)	Young´s modulus E (Gpa)	Brinell hardness (HB)
∅ 15	579	639	199	202

The stress-strain curve was plotted from the data obtained from tensile test of base materials. This is presented in Figure 29. The curve shows the ultimate tensile strength of 639 MPa and the yield strength of 579 MPa. Because of the cold rolled steel it shows better ductility.

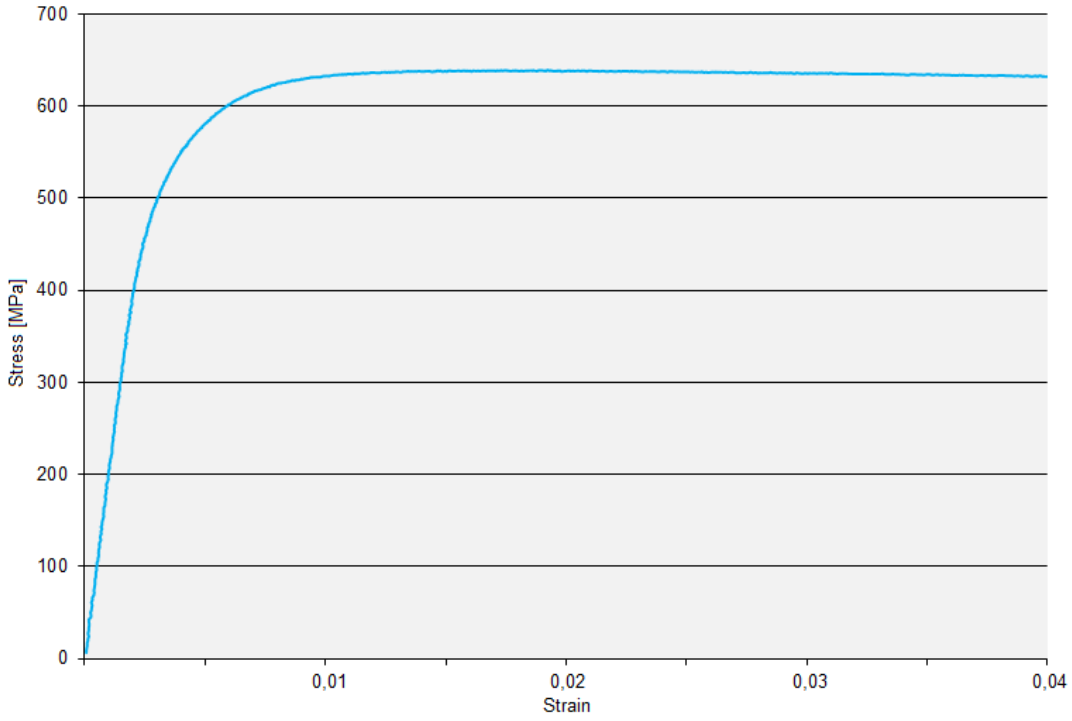

Figure 29: Stress- strain curve of base material: cold rolled structural steel S355

The F2T was conducted in structural steel S355 because of its good mechanical properties and easily availability. Materials has good weldability and machinability too.

3.3 Equipment for F2T

Since the F2T technique is utterly a new invention in tubular product technology, there is no dedicated production unit developed yet. The Friction stir welding (FSW) machine at the lab of mechanical research group, Aalto University was a good choice to fulfill the

requirement of technology. However, machine has a limitation of vertical stroke which resist the production of longer tube.

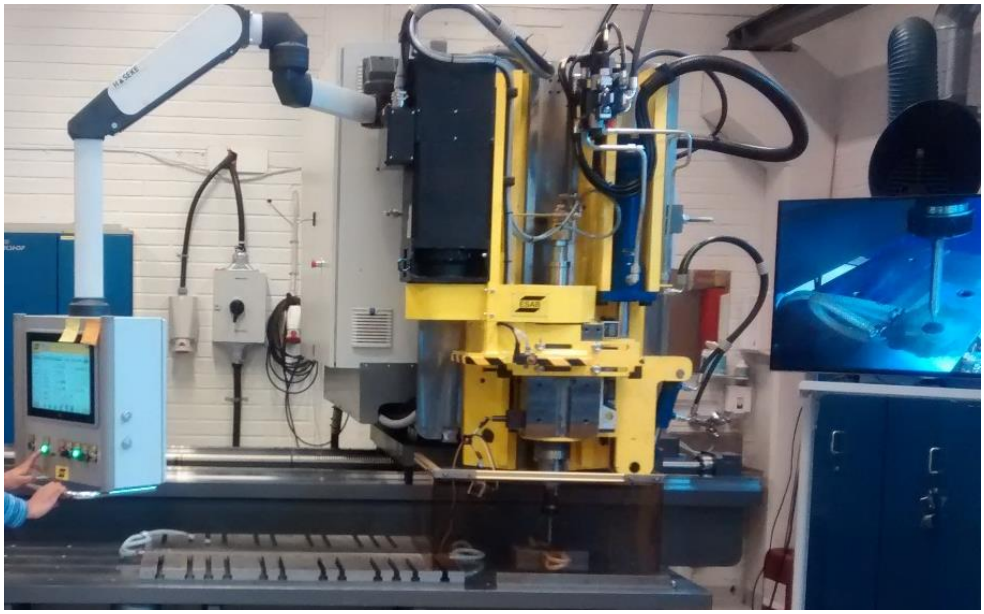

Figure 30: ESAB *LEGIO*™ *FSW 5U* Friction Stir Welding machine

According to [45] The ESAB LEGIOTM FSW 5U Friction Stir Welding equipment, shown in Figure 30 has following main specifications:

- Maximum Torque: 200 [Nm]
- Maximum Forging Force: 100 [kN]
- Maximum Rotational Speed: 3000 [rpm]
- Maximum Welding Travel Speed: 4 [m/min]
- Work Envelope Dimensions: 2000 x 400 x 300 (XX,YY, ZZ) [mm]
- Welding Control (Z-axis):
  - Force
  - Position
  - Speed
- Welding angle: 0o to +5o
- Monitoring parameters
  - Position, speed and force in XX, YY and ZZ axes
  - Spindle speed and torque,

The FSW machine has user interface at left side where, parameters for the process were set initially and run the process. It is possible to access log file of process and can be saved in external memory for future reference.

Though machine used in F2T is FSW, the tool was different. Collect chuck holder was put in the spindle of FSW for F2T purpose. The benefit of using collet in tool holder is that, it is possible to make a tubular product of different diameter just by changing collet.

Figure 31: Tool holder for F2T test. a) Collet holder b) Collet for 15-16 mm diameter c) steel round bar

The collet was placed in tool holder which was shown in Figure 31. The size of collets depends upon the size on consumable rod used. In this case, collet of 15-16 was used for 15 mm consumable rod. The clamping of consumable rod consumes about 60 mm of consumable rod. To save some materials, permanent steel round bar of 15 mm diameter was made as shown in Figure 31c and placed at the end of collet which goes inside a collet holder. This round bar helps to save 30mm of materials in a single test. There is cooling system in FSW machine which passes inside the collet holder. Therefore, to prevent leakage of cooling liquid collet was assembled using O-ring inside it and thread seal tape in screws.

3.4 **Testing Equipment**

3.4.1 **Microhardness**

The Vickers hardness measurement was done using two equipment: CSM Micro combi tester platform and Buehler tester. The principle of Vickers hardness was presented in section 2.5.2. Figure 32 shows the microhardness testing devices available at Aalto´s laboratory and used in this thesis works.

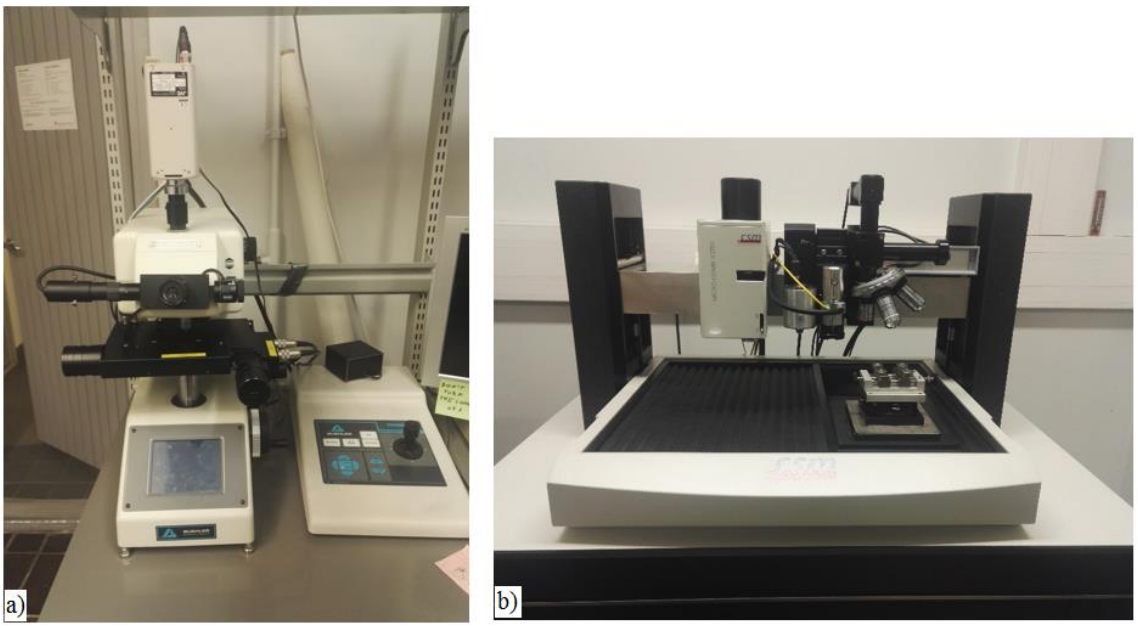

Figure 32: Hardness testing equipment: a) Buehler tester b) CMS Micro combi tester platform

❖ **Buehler Tester**

The Buehler microhardness tester 1600 series (Figure 32. a) was used in hardness testing of specimen. The hardness measurement on all samples to perform Taguchi analysis as well as sample produce in optimal parameters were measured using this tester. According to [46], Buelhler tester is a Japanese manufactured precision measuring instrument for the study of material hardness. The digital micro hardness tester is suitable for micro Vickers and Knoop indentations, the turret is equipped with high magnification for measurement and low magnification for setting up of the indenter position on the samples. The tester has a camera port to allow for the addition of a hardness measurement system on the computer to improve accuracy of measurement and offering reporting functions with the help of software called Enterprise. More technical specification of tester is given below [46]:

- Model number: 1600-6400
- Two objective lenses
- Variable weight range: Max. 1000 (g)
- Variable dwell time
- Adjustable stage with micrometers
- Variable light intensity
- RS232C and printer port

❖ **CSM Micro Combi Tester**

The Micro Combi Tester (Figure 32.b) is a combination of a Micro Scratch Tester (MST), Microindentation Tester (MHT), Nanoindenter and Atomic-Force Microscopy (AFM).

The microindentation tester is ideally suited to the measurement of mechanical properties such as the hardness and elastic modulus of thin hard coatings, thick soft coatings and bulk materials such as PVD and CVD hard coatings and ceramic surface layers. The microhardness in the samples which are made using optimal parameters are measured using this tester. The microhardness data are analyzed and extracted using software Indentation 5.21. The technical specifications of micro combi tester are: [47]

- Combines the capabilities of Micro Indentation Tester and Micro Scratch Tester
- Maximum applied load is 30N with resolution of 0.1mN
- Speed range is 0.1mm/min to 600mm/min
- Maximum depth is 1000µm

3.4.2 **Tensile, Flattening and Flare Test**

The MTS Landmark 810 material testing system was used in 3 mechanical test: Tensile, Flattening and Flare. MTS 810 is a versatile, multipurpose servo-hydraulic testing system for static and dynamic test [48]. The tension force was used in tensile whereas compression force was used in flattening and flare test. Figure 33.a shows the MTS 810. According to [48], some features of MTS 810 are as follows:

- Force ranges from 25 kN to 500 kN
- A wide performance range
- The ability to test materials ranging in strength from plastics to aluminum, composites and steel
- A large test space to accommodate standard, medium and large size specimens, grips, fixtures and environmental subsystem
- The capability to perform a wide variety of test types from tensile to high cycle fatigue, fracture mechanics, and durability of components

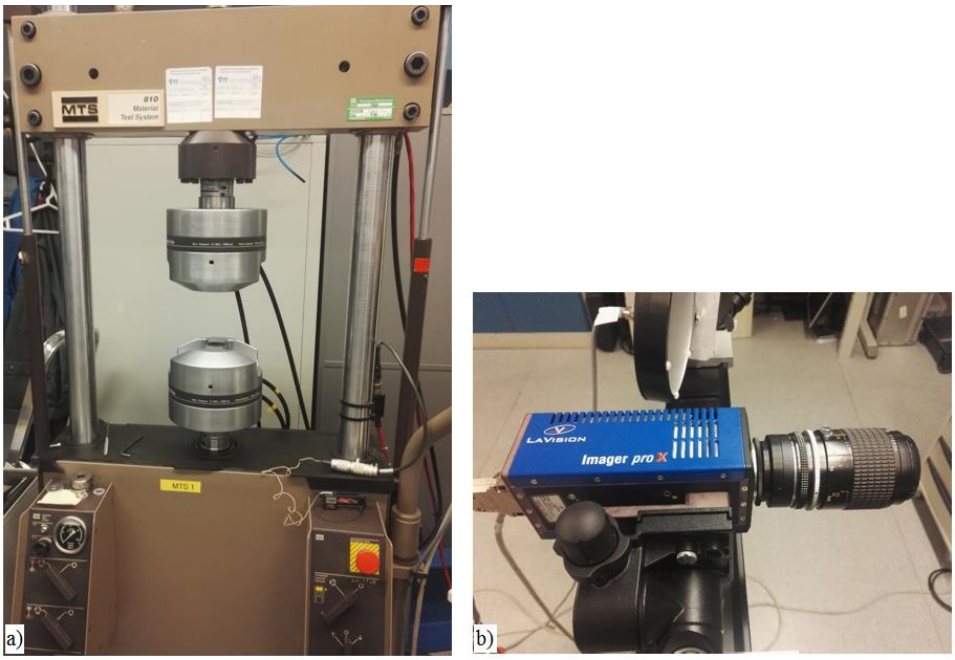

Figure 33: MTS and maybe DAVIS camera

❖ **Digital Image Correlation (DIC)**

Exceptionally in tensile test, digital image correlation was used to analyze the localization of strain of tubes. The Lavision imager proX camera was used (Figure 33.b) in the process and analyzed using the software called DAVIS. Imager pro X is advanced, high resolution, progressive scan, and fully programmable 14 bit CCD cameras ideally for large field area. The camera delivers up to 14 bit digital images and gives unsurpassed resolution from 8 million pixels to 29 million pixels combined with a short interframe time down to 0.3 µs and modern CamLink interface for fast storage to PC RAM. It has a double exposure feature with an interframe time down to 100 ns. [49]

3.4.3 **Optical Microscopy**

For microscopic observation of samples, optical microscope available in laboratory was used which was Nikon Epiphot 200 (Figure 34). The Nikon Epiphot 200 inverted metallurgical microscope is a compact and highly upgradeable package. The projection of the results was done in computer with the help of software called NIS-Elements F 2.30.

Figure 34: Nikon Epiphot 200 inverted metallurgical microscope

This is a versatile instrument which features the CF infinity corrected optical system, which combines Nikon's CF optics with infinity corrected design for greater system flexibility. It has also lowered stage design and ergonomic controls. There were five objectives used in a microscope, they are 5x, 10x, 20x, 50x and 100x. [50]

3.4.4 **EBSD**

Electron Backscatter Diffraction (EBSD) analysis was made to get quantitative microstructural information about the crystallographic nature of samples. The equipment used was Zeiss Merlin VP compact (Figure 35), which was equipped with EDS and EBSD detectors. The Zeiss Merlin VP Compact is a field-emitter scanning electron microscope with a resolution down to 1nm (scanning transmission electron microscopy, STEM). The instrument is equipped with Zeiss in-lens, SE, AsB and STEM detectors as well as a Bruker Quantax X-ray detector. These allow for high-resolution imaging in SEM and STEM mode. Owing to the attached Leica cryo load-lock and a cryo-stage SEM measurements can also be conducted at cryogenic temperatures. The Quantax X-ray detector allows for energy-dispersive X-ray spectroscopy and imaging. The Merlin is equipped with a nitrogen charge-compensator. The electron energies range from 500V to 30kV. [51]

Figure 35: Zeiss Merlin VP Compact device scanning electron microscope

3.4.5 **Temperature Analysis**

The FLIR SC 660 infrared camera (Figure 36) was used in temperature analysis of F2T. This is a highly sensible and most advanced featured IR camera which supplies a combination of infrared and visible spectrum images of superior quality and temperature measurement accuracy [52].

Figure 36: FLIR SC 660 IR camera [51]

4 APPLICATION AND DEVELOPMENT OF F2T

4.1 Introduction

The chapter was focused into an application and development of friction flash to tube.

In Section 4.2, the development of experimental condition was described. The proper clamping system of test pieces and the anvil design where the test piece plunges to produce tubes has been described here. More details on cooling system used in F2T facility and information on various tools were presented.

In Section 4.3, the application of Taguchi method was presented. The factor which has effect on outcome of the tests such as forging load, rpm of machine, plunging distance etc. were described here. The selection of the parameters to perform design of experiment by Taguchi method is also presented here.

In Section 4.4, Optimization of parameters was done. The computation of average performances, analysis of variance, prediction of optimum performances, confirmation test etc. were presented in this section.

In section 4.5, the thermal and mechanical characterization was done. The analysis of temperature in consumable from infra-red images, analysis of temperature of tungsten carbide from thermocouple and analysis of log file were presented here.

4.2 Development of Experimental Condition

4.2.1 Consumable Rod

The Consumable rod means a test piece of structural steel which is plunged to the tungsten carbide anvil to produce tube. One of the critical part in producing tube is to create a good initial flash. The characteristics of flash is also depended upon the geometry of consumable rod; (a) the length of the consumable rod and (b) tip geometry of consumable as shown in Figure 37.

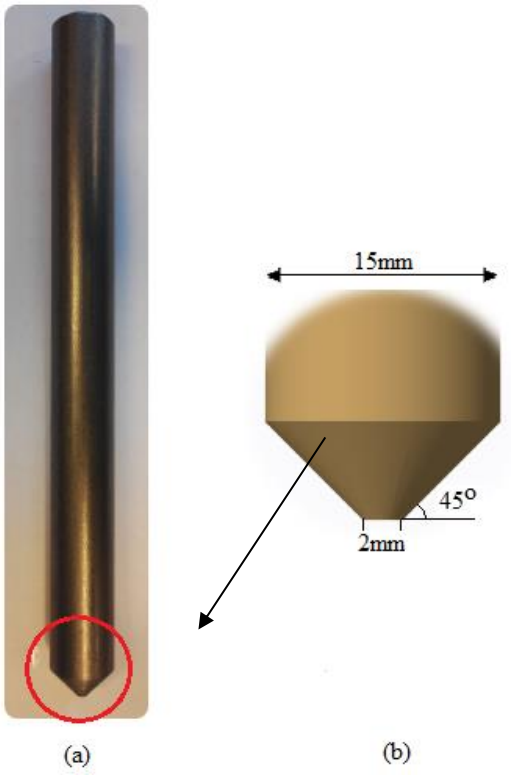

Figure 37: Consumable rod (a) Structural steel test piece. (b) Tip geometry of test piece

The diameter of the consumable rods used in test are 15 mm and length are 120 mm and 200 mm. Initially design of experiments using Taguchi method was performed in a consumable rod of length 120 mm. Test piece has tip tapered in 45 degree with tip diameter 2mm. The tip has point of 2 mm to create a high pressure even with small forces at the beginning. The pressure developed by a tip mechanically creates a heat which changes the state of rod´s tip to the viscoplastic and changes into flash and eventually into the tube. The tip also helps to make process stable by preventing unwanted vibration in its initial condition when flash is created. With similar tip geometry design of experiments using Taguchi method was also performed in 200 mm long consumable rod. Buckling was a main problem that complicate the longer tube which was overcome by introducing mechanical supporting guide. Section 4.2.3 describe in details about supporting guide used in production of longer tube.

4.2.2 **Anvil System**

The concept of F2T arise while doing friction surfacing which has been described in section 2.2.2. The very first task to perform F2T test in organized way is to develop the experimental facility which should be fully dedicated for F2T purpose. The anvil system in this chapter means the development of base system with tungsten carbide on it where consumable rod plunges and a cooling system provided into a base. The emphases in experimental design were given to achieve following features:

- The base design should have place/pocket to keep hard material: tungsten carbide (WC) where consumable rod plunges.
- The base should have proper cooling system that passes near to the tungsten carbide which helps to prevent to deform and increase the life of tungsten carbide.
- The system should withstand forces and temperature during the test.
- The system should have feature of repeatability.

Considering the above-mentioned features, the clamping system for test was made.

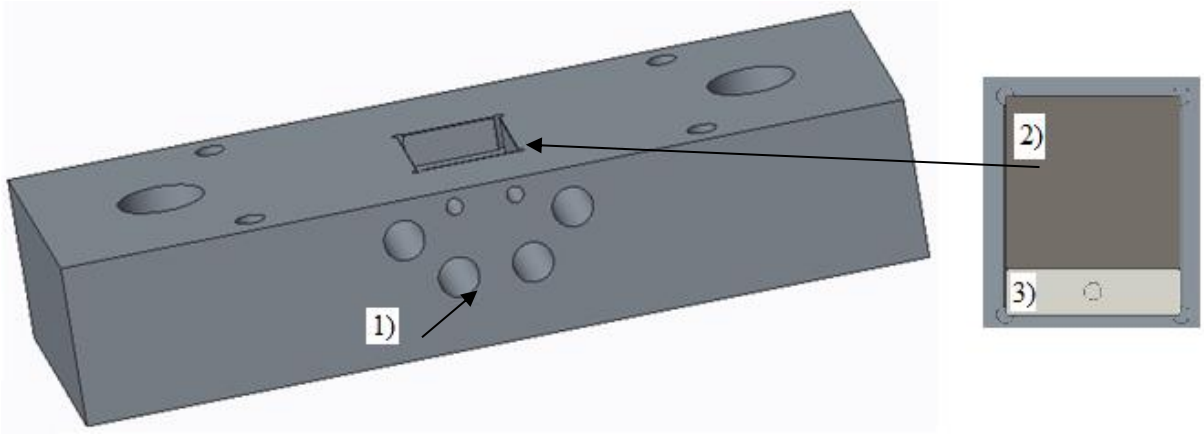

Figure 38: 3D model of a base for clamping system; 1) Four holes for cooling channel 2) square WC in pocket of a base 3) Steel plate placed along with WC

As shown in Figure 38, the base design for clamping system was made. The very first important requirement in this design is to have a pocket for tungsten carbide. Since the tungsten carbide is very expensive and very difficult to machine, the design was made up of steel having a small pocket where tungsten carbide was placed. The size of pocket was (30*38*10) mm because of tungsten carbide design which has dimension of (30*30*10) mm. The tungsten carbide was kept in the pocket along with small steel plate of (30*8*10) mm as shown in Figure 38 and tighten with the screw from the two small holes of M5 as shown in front side of same figure. This makes easy to replace tungsten carbide. The two big holes of M16 in top surface of figure was made to clamp the system in table of FSW machine. Similarly, four other holes were made to attach guiding system which will be described in section 4.2.3.

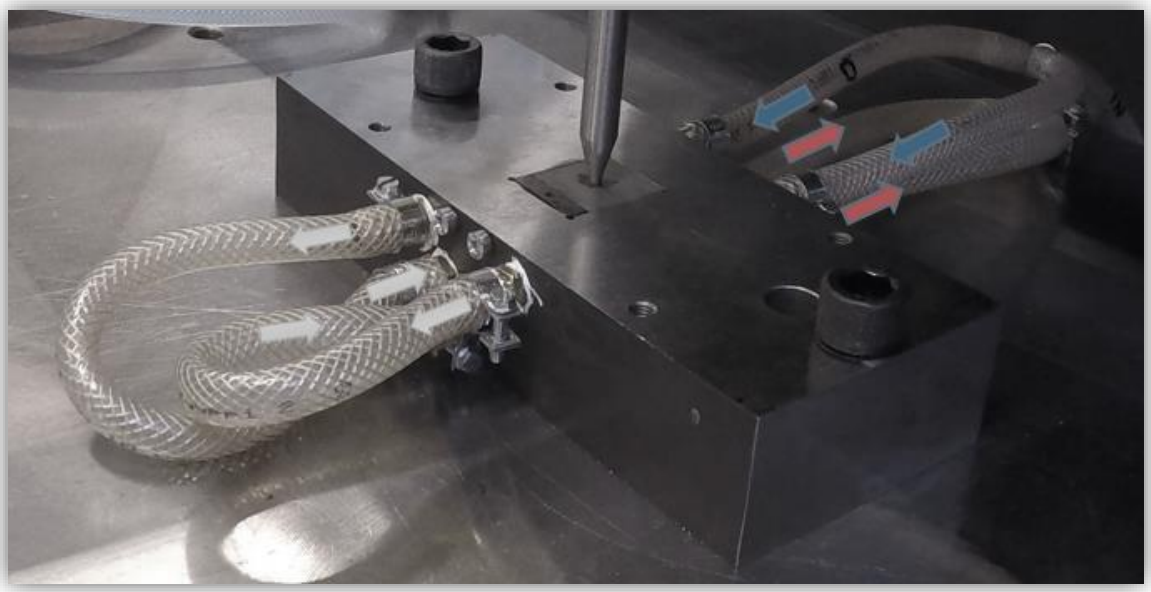

Figure 39: The water cooling channel in the system

The cooling channel was made near to pocket where WC was kept to protect it from deformation. The Figure 39 shows the path of water circulation which was kept in cooling channel designed for the system for cooling purpose. The water used in system is tap cold water. The cold water enters from the two port at the top part of system shown by blue coloured arrows in Figure 39 providing cooling system mostly to the side of the anvil. The water comes to other side of system and re-enter from the lower ports. This provide cooling system to the beneath of the anvil and the warm water goes back to the drainage and shown in red arrows in figure. The BOM of system can be find from appendix A.

- **Anvil (Tungsten Carbide)**

The consumable rod plunges into the hard material located at a base to create the flash initially and produces tube. The hard material used in a base is called anvil. The material which is harder than the consumable rod can be used as an Anvil. The square shape tungsten carbide was used as anvil during the test. The technical specification on tungsten carbide (ISO-range: K30) is presented in Table 5.

Table 5: Technical specification on Tungsten Carbide [53]

Grade	Wolfram Carbide (WC) [%]	Binder (Cobalt) [%]	Grain size	Density ±0.1g/cm3	Hardness		Transverse Rupture Strength (T.R.S.) [N/mm^2]	Remarks
					±0.3 HRA	±50 HV30		
K 30	92	8	Coarse	14,70	89	1250	>2450	As Sintered

The sintered tungsten strip with coarse grain size of 10 x 30 x 310 mm as shown in Figure 40 was cut using electrical discharge machine (EDM) into a square shape of 10 x 30 x 30 mm which was placed in anvil design as discussed in section 4.2.2 . Typically, tungsten carbide has a high wear resistance and can be used at high temperature application which is the reason of using it in F2T. The mechanical properties of tungsten carbide mainly include hardness, transverse rupture strength (TRS) and fracture toughness [54]. The tungsten carbide used in test have 92% of carbide content and 8% of cobalt binder.

Figure 40: K 30 grade tungsten carbide bar at left and square shape WC with dent on it at right

The dent was made in EDM cut square shaped WC which was used as anvil as shown in Figure 40. The dent helps to hold the tip of the consumable rod and reduce the vibration at initial stage. The dent was made in lab by milling on it where diamond ball was used as tool.

4.2.3 **Supporting Guide**

One of the main objective of thesis work is to increase the length of tube by introducing supporting guide in a system. Typically, the maximum length of tube produced without any guiding system is 40 mm in 15mm diameter´s and 120m length´s consumable rod. The problem of vibration and buckling is a big issue in case of longer consumable rod. The vibration was too big that consumable rod jumps from the center axis and eventually broke itself. To overcome the problem, supporting guide was designed and tested. This results an increment of tube length up to 85mm as shown in Figure 41 when consumable rod of 15mm diameter and 200mm length was used. The vertical stroke of FSW machine is 300mm which resist to use a consumable rod not more than 230 mm in this experimental design.

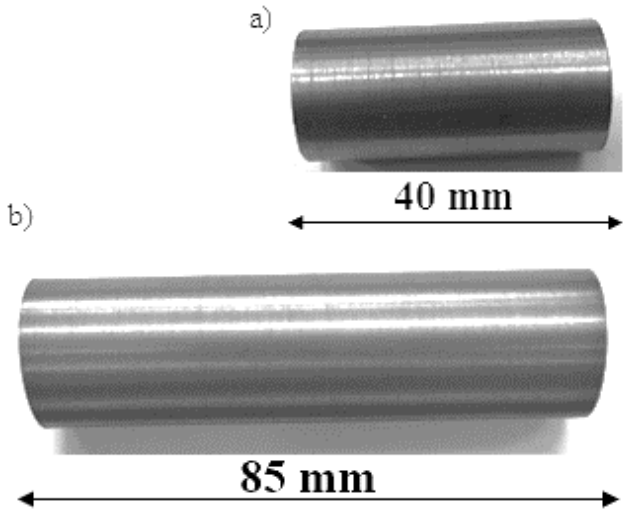

Figure 41: Comparison of produced tube´s maximum length a) Without using guiding system and b) Using guiding system

While designing the supporting guide, main consideration was given to hold consumable up to a point where good flash is created. Once flash is created, the consumable rod changes it states to viscoplasticity which makes process easy to forge by making it softer and make a tube.

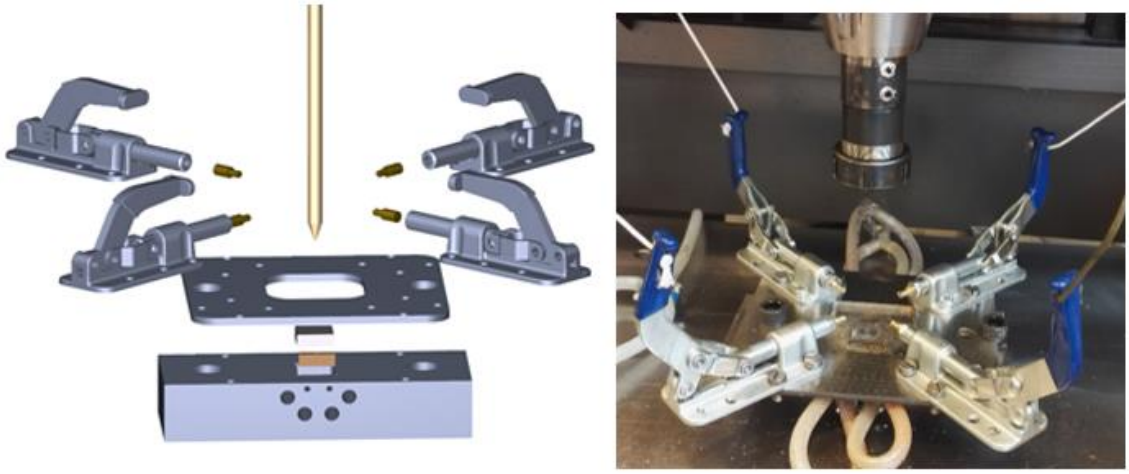

Figure 42: Supporting Guide to produce longer tube (200mm consumable rod). 3D CAD model exploded view in left side and picture from test in right side

As seen in Figure 42 the design was improvised by adding a guide to a consumable rod. In the top of the base of clamping system, four push-pull toggle clamps were used to hold consumable rod via brass ring. As the tube reaches to the level of brass ring, push-pull toggle clamps were pulled out manually so that the tube can be produced. The supporting guide system was integrated in the anvil design (previous design) which was mentioned in section 4.2.2. The main components brass ring and push-pull toggle clamps are described below in details.

❖ **Brass Ring**

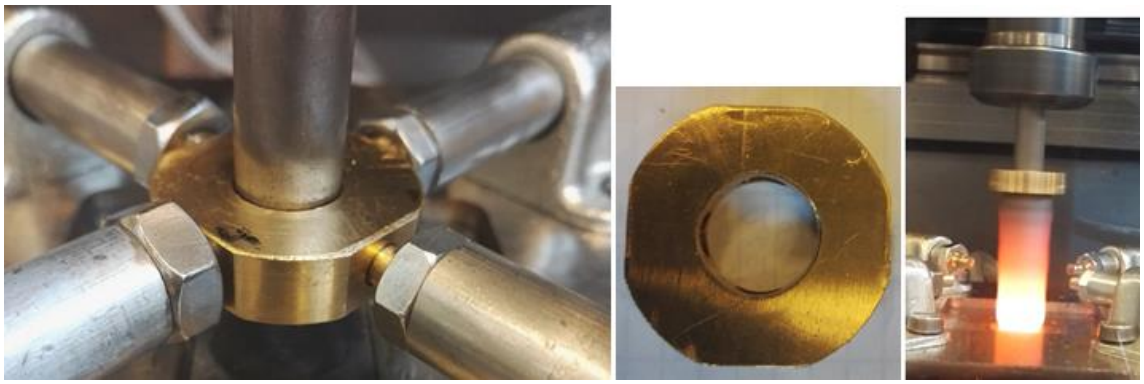

Figure 43: Brass ring used in supporting guide, brass ring and tube forming after releasing brass ring in F2T process (from left to right)

To prevent buckling in a consumable rod, the support is needed at as many points as possible. This led to concept of making brass ring that provide support along the circumference of consumable rod. The desired material for this purpose is bronze because of its self-lubricating property [55] but brass is used because of its availability at lab and properties similar to bronze to some extent. Brass is also widely used as an industrial material because of its high strength, high corrosion resistance, high electrical conductivity and thermal conductivity [56]. It is also easy to machined and change to the required shape which was the reason of using brass ring as a supporting guide. The ring was circular with diameter of 36mm and chamfered at four corner having four holes of diameter 6.3mm on four sides. Ring has 10 mm thickness and diameter of hold in center is equal to the diameter of consumable rod i.e. 15mm in this case. The pin from push-pull toggle clamp was kept in the hole at beginning of the process as shown in Figure 43 . System holds consumable rod until the proper flash was created and tube produce up to the level of ring then, was released by pulling toggle clamp. The release ring travel vertically along with the produced tube/flash which was removed later from another end of rod after plunging of a full length of rod as shown in Figure 43.

❖ **Push-Pull Toggle Clamp**

The releasing of a brass ring at right time is important to prevent the crash of a system. The Clamp-Rite push-pull toggle clamp was used for that purpose. The 13300CR model clamp was manual, have 1100kgf holding capacity and stroke of 50.8 mm [57].

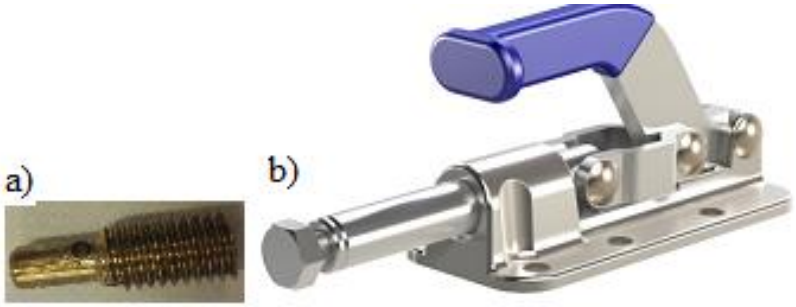

Figure 44: Push-pull toggle clamp set a) Brass pin b) 13300CR push-pull toggle clamp

The stroke of clamp was customized by using brass pin. The only reason of using brass pin is it´s good machinability in this case. Figure 44 shows the used toggle clamp set. The pin was tightened by the nut to the thread hole of toggle clamp and connected to the brass ring at another end. As shown in Figure 43, the clamps were connected by rope and pulled at the right time. The system is fully manual and has risk of human error. However, it is easy and faster process to conduct tests in beginning stage of F2T technology.

4.3 **Application of Taguchi method**

The design of experiments, Taguchi method was used to find the optimal performance parameters. The first task was to identify the main function followed by development of parameters and selection of level. The thickness stability, diameter stability and hardness factor were chosen as main functions which was further described in section4.3.1. The effect of parameters such as spindle rotation, forging force, plunging depth and speed etc. were studied and three important parameters in 3-level were selected to create L9 orthogonal matrix.

4.3.1 **Performance Assessment Parameters**

To assess the overall performance of the tubular shape produced by F2T method, geometrical analysis and hardness were taken into consideration, they are: thickness stability (T.S.), diameter stability (D.S.) and hardness factor (H). The higher the value is better in these assessment parameters. In this stage, the tubes with stable diameter, thickness and stable hardness thru the length were considered as a good tube. According to the Vilaça, equations 8, 9 and 10 respectively were developed.

$$t.s. = \frac{t_{max} - t_{max}}{t_{av}} \qquad \text{Equation 7}$$

Where,

t.s. =Thickness stability.

t_{max} = Maximum thickness measured in tubular shape [mm].

t_{min} = Minimum thickness measured in tubular shape [mm].

t_{av} = Average of measured thickness in tubular shape [mm].

$$d.s. = \frac{2 * t_{av}}{d_{max} - d_{min}} \qquad \text{Equation 8}$$

Where,

d.s. =Diameter stability.

d_{max} = Maximum outer diameter measured in tubular shape [mm].

d_{min} = Minimum outer diameter measured in tubular shape [mm].

t_{av} = Average of measured thickness in tubular shape [mm].

$$H = \frac{HV_{av} - 3 * HV_{\sigma}}{HV_{bm}}$$ Equation 9,

Where,

H = Hardness factor

HV_{av} = Average of measured Vickers hardness in tubular shape.

$HV\sigma$ = Standard deviation of measured Vickers hardness in tubular shape.

HV_{bm} = Vickers hardness measured in base material.

As per the above equations, the assessment parameters scale between 0 and 1. The quality of tubular products will be higher if the value of assessment parameters is near to 1.

4.3.2 **Development of Parameters and Selection of Level**

To perform performance assessment, it is important to conduct test in good parameters. The initial task was focused into finding out a minimum and maximum level of parameters where production of good tubular shape is possible. Number of tests as shown in Figure 45were done before confirming the right level of parameters.

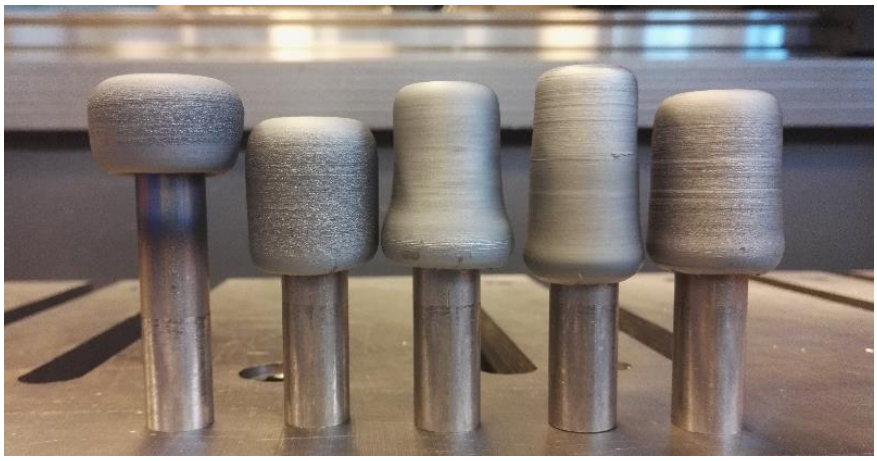

Figure 45: Samples to check feasibility of F2T in different parameters

The major parameters which has effect on the properties of tubular shape were of main interest. It was found that spindle tool rotation, forging load in stationary plunging period and plunging depth in initial transient plunging period has effect on output of F2T. It was decided to select these 3 parameters as a main factor in Taguchi method. The Taguchi test was performed initially in consumable of length 120 mm which was shorter compare to tube produce by supporting system where consumable of 200 mm was used. The shorter consumable produce shorter tube (tube A) which was approximately 30-40 mm length and in another method, approximate length of tube (tube B) was 70-85 mm.

❖ **Tube A**

Here the terms A represents the tube produced by the F2T method where consumable of length 120 mm was used. Initially tubes were produced without using guiding support which results the length of tube from 30-40 mm. After various test, the level of parameters for the initial test which was done to achieve shorter tube were assigned as in Table 6.

The variable parameters have three level to perform Taguchi design of experiment. There are other parameters which were kept constant during all test. They are plunging speed in initial transient plunging period, clockwise direction of spindle tool rotation, room temperature, anvil cooling system etc.

Table 6: Parameters and levels to perform Taguchi process in tube A

Parameters	**Symbol**	**Level 1**	**Level 1**	**Level 3**
Variable Parameters				
Forging Force [kN]	A	20	32,5	45
Spindle: Tool rotation [Ω,rpm]	B	2000	2500	3000
Initial transient plunging period: Plunge depth [mm]	C	3,4	4,7	6
Constant Parameters				
Initial transient Plunging Speed [mm/min]	1,5			
Stationary plunging period: Control Method	Force control method			
Tool Rotation direction	CW			
Cooling System	Water Cooling system in Anvil			
Machine´s angle of inclination [degree]	0^o			
Room temperature [^oC]	20-21			

❖ **Tube B**

The tubes were also produced in longer consumable of 200 mm length using the supporting guide to perform Taguchi method DOE. The tube produced for this purpose was termed as tube B. After analyzing the results from tube A which can be find in section 4.4, level of parameters was assigned for tube B. Based on the results, Table 7 shows the level of parameters for Taguchi method of produced tube using supporting guide. The variable parameters in tube were same to the tube A but different in their levels and constant parameters were kept without any changes.

Table 7: Parameters and levels to perform Taguchi process in tube B

Parameters	**Symbol**	**Level 1**	**Level 1**	**Level 3**
Variable Parameters				
Forging Force [kN]	A	25	30	35
Spindle: Tool rotation [Ω,rpm]	B	2600	2800	3000
Initial transient plunging period: Plunge depth [mm]	C	3,7	4,7	5,7
Constant Parameters				
Initial transient Plunging Speed [mm/min]	1,5			
Stationary plunging period: Control Method	Force control method			
Tool Rotation direction	CW			
Cooling System	Water Cooling system in Anvil			
Machine´s angle of inclination [degree]	0^o			
Room temperature [^oC]	20-21			

4.3.3 **Selection of Test Matrix**

There are many standard orthogonal arrays available and each array meant a specific number of independent design and variables. The L9 orthogonal array is meant for understanding the 4 different independent factors and 3 levels. The total degree of freedom need to be computed to determine the proper orthogonal array. The degrees of freedom are defined as the number of comparisons between process parameters that need to be made to determine which level is better and specifically how much better it is. The degree of freedom is associated with the interaction between two processes parameters are given by the product of the degrees of freedom for the two process parameters. There are total 6 degree of freedom owing to three parameters in this study. [58] A total of 27 parameters combinations are available in this sort of array because of availability of 26 degree of freedom here. However, only 9 combinations (L9 orthogonal array) were selected as shown in Table 8. The nine combination is minimum number to perform Taguchi analysis for 3 factors and 3 level test.

Table 8: Layout of L_9 (3^4) orthogonal array [40]

Test no.	Parameters			
	A	**B**	**C**	**D**
1	1	1	1	1
2	1	2	2	2
3	1	3	3	3
4	2	1	2	3
5	2	2	3	1
6	2	3	1	2
7	3	1	3	2
8	3	2	1	3
9	3	3	2	1

Since there were 3 major parameters: tool rotation, forging force and plunging depth, they were selected for the Taguchi experiment. In this case, the fourth column was eliminated. The use of only 3 columns result the matrix as shown in Table 9. The effect of parameters is increase as moved from right to left which is the reason of placing tool rotation and force in beginning columns and plunging depth was kept at last.

Table 9: Matrix for orthogonal vector L9 and matrix for 3-factor, 3- level test in tubes A

Test no.	Parameters		
	Ω [rpm]	**Force [kN]**	**Plunging depth (-z-axis) [mm]**
1	2000	20	3,4
2	2000	32,5	4,7
3	2000	45	6
4	2500	20	4,7
5	2500	32,5	6
6	2500	45	3,4
7	3000	20	6
8	3000	32,5	3,4
9	3000	45	4,7

Similarly, the matrix for Taguchi test for tube B is presented in Table 10. The results encountered in initial test helps to decide addition and elimination of few combination. For example, combination of 2-2-1 was felt important because it has parameters which are closer to the optimum parameter of the tube A. The more changes in this combination was made by placing a column of forging force in the first column and tool rotation in second. The effect of forging force is more critical in the characteristics of produced tube which is the reason of prioritizing force than any other factors.

Table 10: Matrix for orthogonal vector L9 and matrix for 3-factor, 3- level test in tubes B

Test no.	Parameters		
	Force [kN]	**Ω [rpm]**	**Plunging depth (-z-axis) [mm]**
1	25	2600	3,7
2	25	2800	4,7
3	25	3000	5,7
4	30	2600	4,7
5	30	2800	5,7
6	30	3000	3,7
7	35	2600	5,7
8	35	2800	3,7
9	35	3000	4,7

4.4 Optimization of Parameters

4.4.1 Computation of Average Performance

The first task after the tests were performed is to collect, analyze the data and to identify the optimal levels for all the control factors.

❖ **Tube A:**

The experimental results for thickness stability (t.s), diameter stability (d.s), and hardness (H) for tube A are presented in Table 11. As mentioned in section 4.3.2 the parameters shown used are spindle tool rotation, forging force in stationary plunging period and plunging depth in negative z-axis in initial transient plunging period.

Table 11: Experimental results for tube A

Test no.	Parameters			Thickness stability	Diameter stability	Hardness
	Ω [rpm]	**Force [kN]**	**Plunging depth [mm]**			
1	2000	20	3,4	0,946	0,964	0,817
2	2000	32,5	4,7	0,964	0,912	0,845
3	2000	45	6	0,930	0,886	0,825
4	2500	20	4,7	0,953	0,952	0,701
5	2500	32,5	6	0,883	0,756	0,817
6	2500	45	3,7	0,954	0,811	0,825
7	3000	20	6	0,974	0,826	0,833
8	3000	32,5	3,7	0,954	0,841	0,843
9	3000	45	4,7	0,981	0,903	0,871

Among the three categories of performance characteristics which are the higher- the better, the lower-the better and the nominal-the better, in this case the higher- the better was selected. As the value of t.s. and d.s. is higher (closer to 1), the geometrical performance of tube is good. Similarly, the mechanical behavior of tube will be better when value of hardness is higher.

In above nine tests, all three levels of every factor were equally represented. It is possible to separate out the effect of each factor at each level because the experimental design is orthogonal [59]. The mean average can be found by averaging the quality characteristic for each parameter at different level. For example, the mean percentage of t.s. at first level can be calculated by taking average value of tests 1.

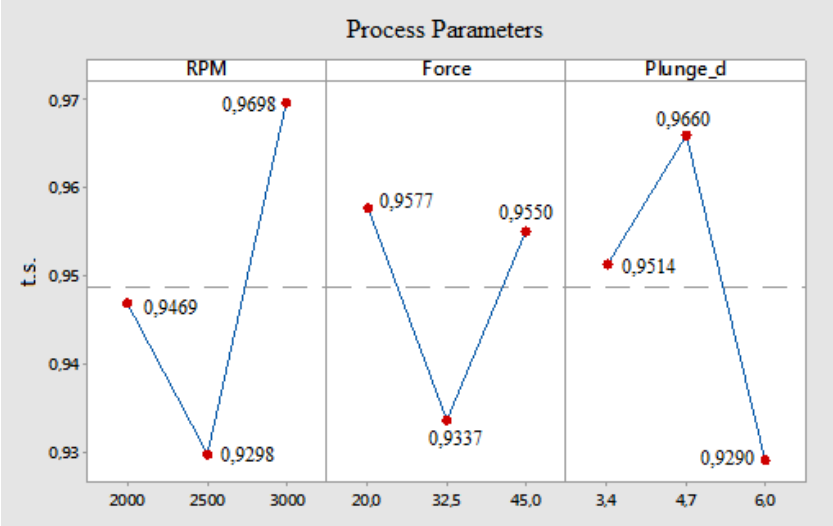

Figure 46: Effect of process parameters of thickness stability.

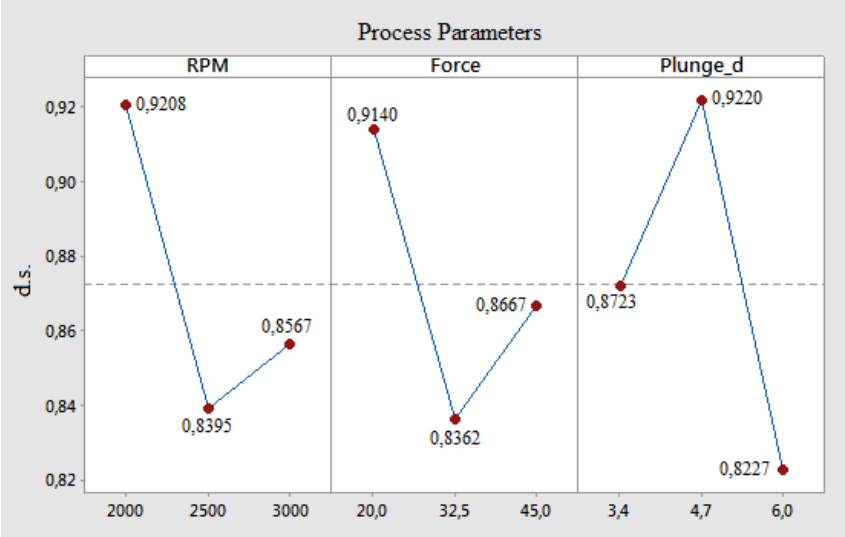

Figure 47: Effect of process parameters of diameter stability.

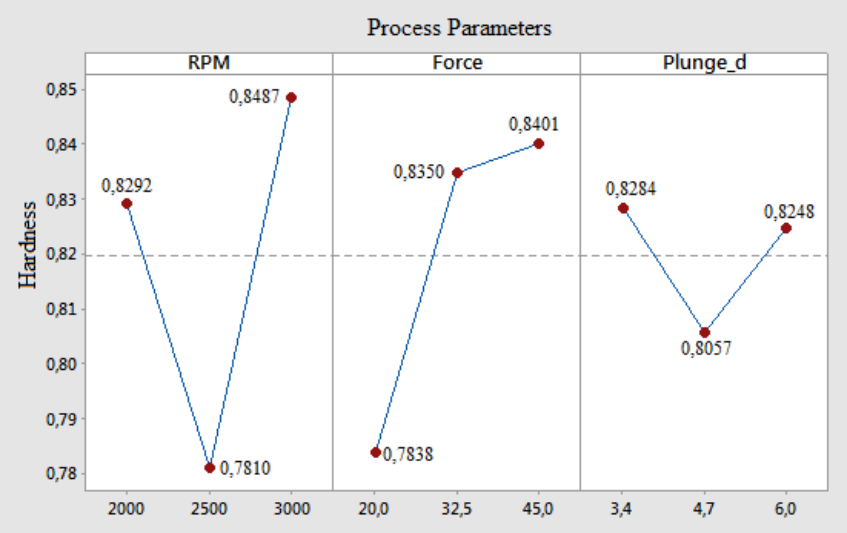

Figure 48: Effect of process parameters of hardness

The observation in Figure 46 shows that, the thickness stability factor is higher at the level 3 of the rpm of machine, level 1 of the forging force and level 2 of the plunging depth. The average value of rpm (i.e. level 2) has the lowest ever value of t.s. whereas increasing or decreasing gives the higher values. Similar type of characteristics of different level was also seen in case of forging force. The lowest t.s. 0,9337 was recorded in level 2. The highest value at lower force is reasonable because the F2T process produces wider tube with low speed when lower force is applied and the produced tubes are more stable. Contrariwise the t.s. at level 2 of plunge depth factor was higher. The characteristic of plunge depth´s chart seems decent than other factors here because the value of t.s. is higher at the middle (level 2) and lower at both level 1 and 3.

In Figure 47, effect of process parameters for diameter stability was shown. The characteristic of graphs in Figure 46and Figure 47 has some similarity because the thickness and diameter stability of tubes are related to each other. Here, the d.s. factor is higher at the level 1 of the rpm of machine, level 1 of the forging force and level 2 of the plunging depth. Both tool rotation and force has similar nature having highest d.s. value at level 1 and lowest at level 3. As for t.s., d.s. has also highest value at level 2 of plunge distance.

From Figure 48, it is observed that the hardness factor has highest value at level 3 of tool rotation and forging forces and level 1 of plunge depth. The highest rpm and force rapidly increases to the higher temperature and increases the rate of tube production resulting the highest hardness factor.

❖ Tube B

The experimental results for thickness stability (t.s), diameter stability (d.s), and hardness (H) for tube B are presented in Table 12. As in tube A, the parameters shown used are spindle tool rotation, forging force in stationary plunging period and plunging depth in negative z-axis in initial transient plunging period.

Table 12: Experimental results for tube B

Test no.	Parameters			Thickness stability	Hardness stability	Hardness
	Force [kN]	Ω [rpm]	Plunging depth [mm]			
1	25	2600	3,7	0,920	0,920	0,880
2	25	2800	4,7	0,878	0,815	0,845
3	25	3000	5,7	0,888	0,828	0,850
4	30	2600	4,7	0,821	0,742	0,860
5	30	2800	5,7	0,857	0,747	0,858
6	30	3000	3,7	0,930	0,831	0,871
7	35	2600	5,7	0,794	0,910	0,762
8	35	2800	3,7	0,834	0,804	0,784
9	35	3000	4,7	0,822	0,617	0,875

As in first case, the higher- the better performance characteristics was selected in this case too. This means the geometrical performance of tube will be good if the value of t.s and d.s is higher (closer to 1). Similarly, the mechanical behavior of tube will be better when value of hardness is higher.

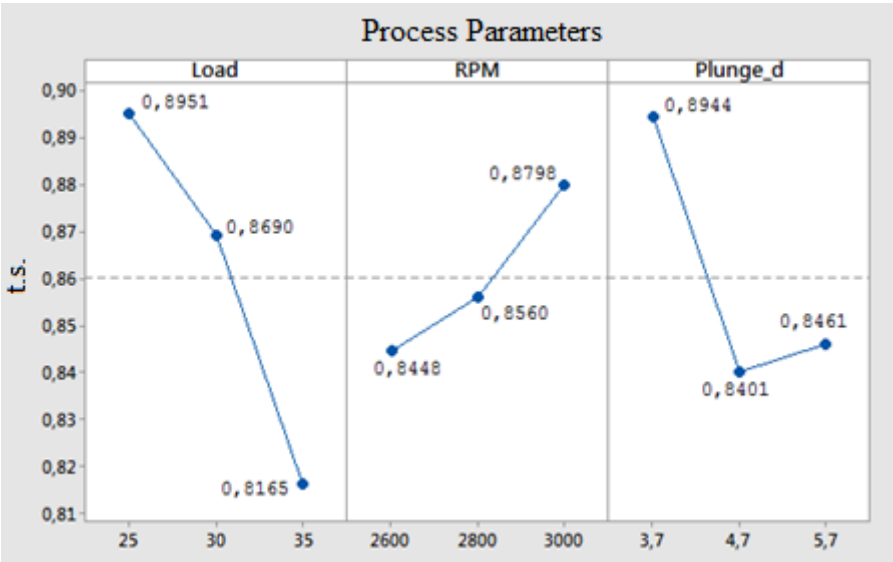

Figure 49: Effect of process parameters of thickness stability.

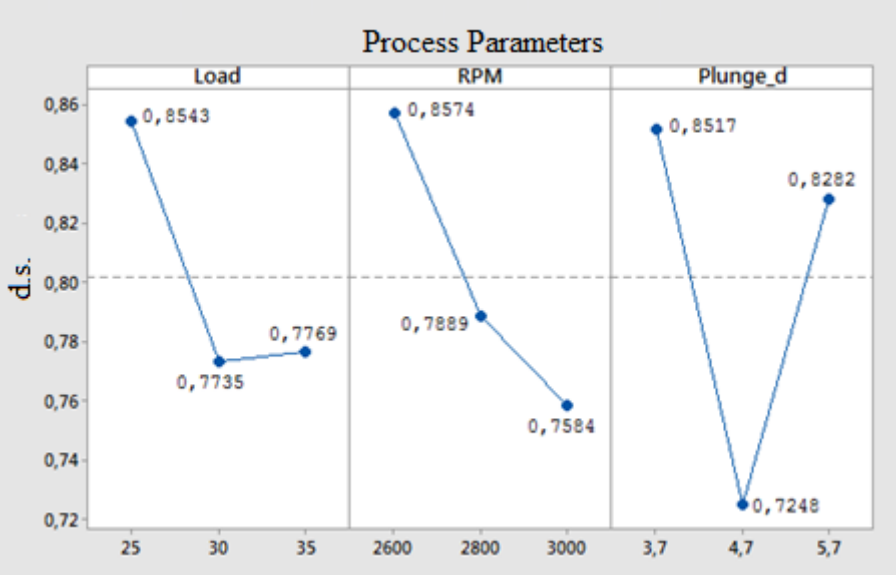

Figure 50: Effect of process parameters of diameter stability.

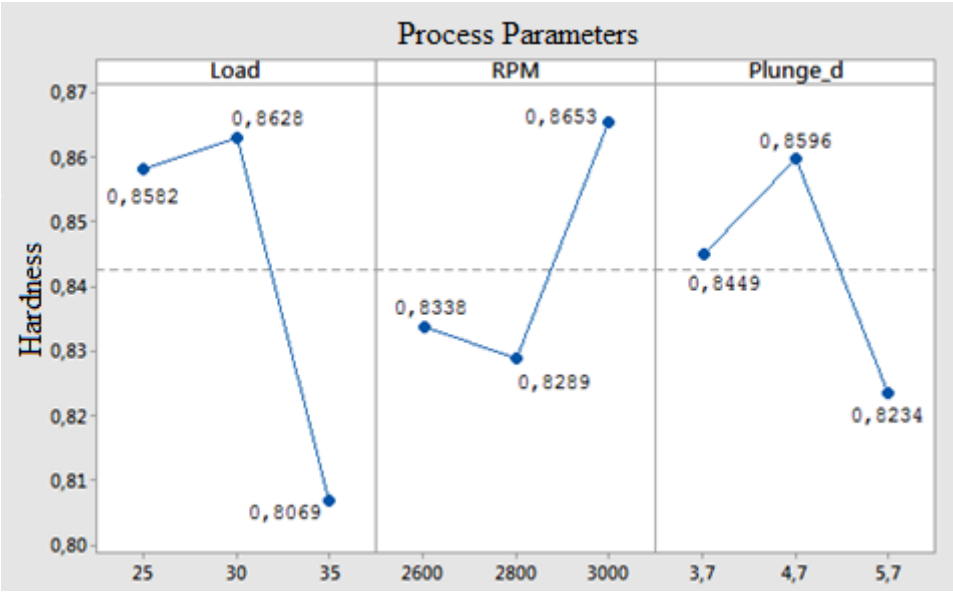

Figure 51: Effect of process parameters of hardness.

The Figure 49 shows that, the thickness stability factor is higher at the level 1 of the forging force, level 3 of the tool rotation and level 1 of the plunging depth. As in analysis for the tube A, in this figure also it has proved that, lower the force more stable is the condition that results higher value of t.s. The shaft changes to viscoplastic zone as it plunges initially before force is released. More initial plunge brings the bigger diameter in the tip of the tube which is the results of getting higher t.s. at level 1 of plunge depth.

The observation in Figure 50 shows that the effect of process parameters for diameter stability is higher at level 1 of all parameters i.e. forging force, tool rotation and plunge depth. For tubes, which are produced using support system (tube B) seems more stable value of parameters are minimum.

From Figure 51, it is observed that the hardness factor has highest value at level 2 of forging force, level 3 of tool rotation and level 2 of plunge depth. As in figure 3, the highest rpm results the highest value of rpm. Similarly, there is no big differences in level 1 and level 2 of forging forces.

4.4.2 **Analysis of Variance (ANOVA)**

ANOVA is the one-way analysis of variance which is used to determine the significant differences among the process parameters. Here the analysis of variance was done to investigate which parameters significantly affect the quality of characteristics. The percentage contribution of all parameters to the selected performance characteristic can be estimated by ANOVA. ANOVA can be accomplished by separating the total variability of the S/N ratios, which is measured by the sum of the squared deviations from the total mean S/N ratio, into contributions by each of the design parameters and the error. First, the total sum of squared deviations SST can be calculated as equation 11. [60]:

$$SS_T = \sum_{i=1}^{n} (Y_i - Y_m)^2 \qquad \text{Equation 10}$$

Where, n is the number of experiments in the orthogonal array i.e. 9, Y_i is the experimental results for the test I and Y_m is expressed in equation 12.

$$Y_m = \frac{1}{n} \sum_{i=1}^{n} Y_i \qquad \text{Equation 11}$$

The total sum of the squared deviations SS_T is decomposed into two sources: the sum of the squared deviations SS_P due to each process parameter and the sum of the squared error SS_e. The equation 13 shows the equation to calculate SS_P.

$$SS_p = \sum_{j=1}^{r} \frac{(SY_j)^2}{r} - \frac{1}{n} [\sum_{i=1}^{n} Y_i]^2 \qquad \text{Equation 12}$$

Where p represents one of the parameters, j is the level of parameters P, r is the number of repetition which is 1 in this case and SY_j is the sum of the experimental results tha includes parameters P and level j. The sum of squares from error parameters is SS_e and it is shown in equation 14.

$$SS_e = SS_T - SS_A - SS_B - SS_c \qquad \text{Equation 13}$$

Where SS_A, SS_B and SS_C are sum of square deviations for parameters A, B and C respectively.

The next step is to determine the total number of degrees of freedom (DoF). The DoF is given by subtracting 1 from total number of test i.e. n-1and the DoF for each tested parameter is subtracting 1 from total number of factor i.e. t-1. The F-value for each design parameter is simply the ratio of the mean of squares deviations (V_p) to the mean of the squared error (V_e) as shown in equation 15 and the percentage contribution of each parameters ρ_p is calculated in equation 16.

$$F_p = \frac{V_p}{V_e} \qquad \text{Equation 14}$$

$$\rho_p = \frac{SS_p}{SS_T}$$ Equation 15

Using the equations 11-16, the results of the analysis of variance for all three factors: t.s., d.s., and H were made for both tube A and B which were presented in subheading below.

❖ **Tube A**

Table 13 to Table 15 shows the analysis of variance in tube A for thickness stability, diameter stability and hardness factors respectively

Table 13: Results of the analysis of variance for factor t.s.

Factors	DOF	Sum of Squares	Mean Square	F ratio	Contribution [%]
A	2	0,00242	0,00121	2,05085	36,02
B	2	0,00104	0,00052	0,88136	15,44
C	2	0,00208	0,00104	1,76271	31,02
Error	2	0,00118	0,00059		17,52
Total	8	0,00672			100

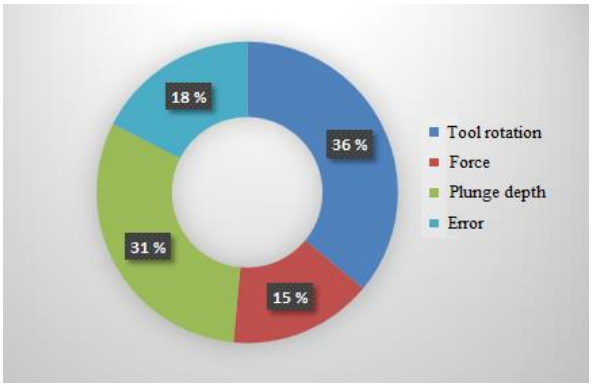

Figure 52: Percentage contribution of each parameters for factor t.s.

Table 14: Results of the analysis of variance for factor d.s.

Factors	DOF	Sum of Squares	Mean Square	F ratio	Contribution [%]
A	2	0,01102	0,00551	3,8536	29,07
B	2	0,00922	0,00461	3,2229	24,32
C	2	0,01481	0,00104	5,1780	39,07
Error	2	0,00286	0,00143		7,54
Total	8	0,03791			100

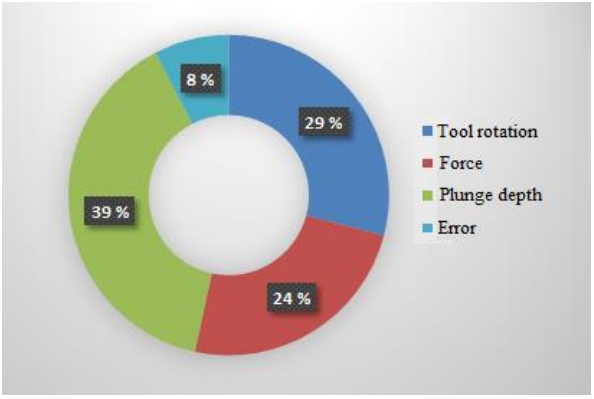

Figure 53: Percentage contribution of each parameters for factor d.s.

Table 15: Results of the analysis of variance for factor hardness

Factors	DOF	Sum of Squares	Mean Square	F ratio	Contribution [%]
A	2	0,00727	0,00363	1,8016	40,37
B	2	0,00291	0,00291	1,4407	32,28
C	2	0,00089	0,00044	0,2206	4,94
Error	2	0,00403	0,00202		22,41
Total	8	0,01800			100

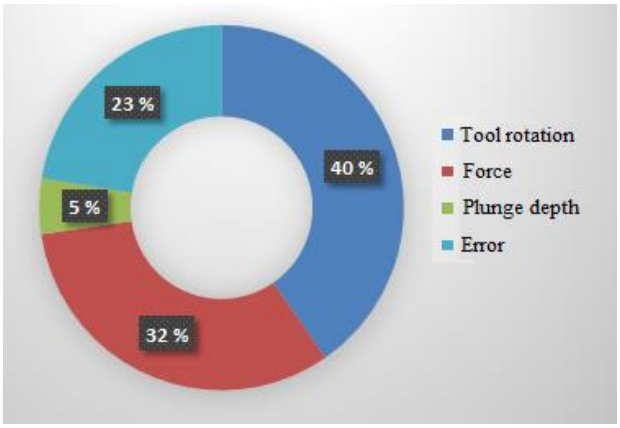

Figure 54: Percentage contribution of each parameters for factor hardness

Percentage contribution of each parameters in tube A for factors t.s., d.s., and hardness were presented in Figure 52, Figure 53 and Figure 54 respectively. It was known that, the tool rotation and plunge depth are the most significant parameters that has affect in thickness stability whereas tool rotation and force has similar affect in both d.s. and hardness. The exception in d.s. is that, plunge depth has the highest effect than other parameters. The least error percentage of 5% was found in hardness as shown in Figure 54.

❖ **Tube B**

Table 16, Table 17 and Table 18 shows the analysis of variance in tube B for thickness stability, diameter stability and hardness factors respectively.

Table 16: Results of the analysis of variance for factor t.s.

Factors	DoF	Sum of Squares	Mean Square	F ratio	Contribution [%]
A	2	0,00963	0,00481	13,1601	54,76
B	2	0,00192	0,00096	2,62212	10,91
C	2	0,0053	0,00265	7,2508	30,17
Error	2	0,00073	0,00037		4,16
Total	8	0,01758	0,00879		100

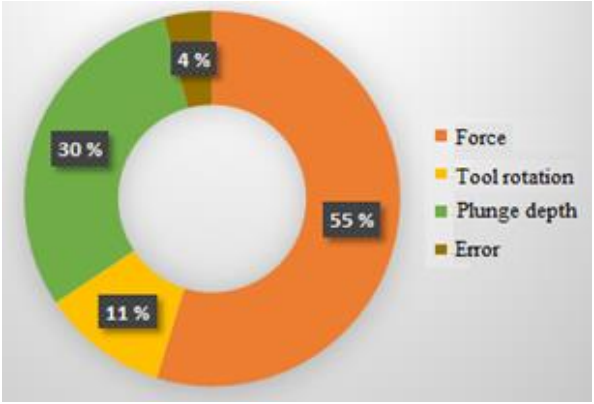

Figure 55: Percentage contribution of each parameters for factor t.s.

Table 17: Results of the analysis of variance for factor d.s.

Factors	DoF	Sum of Squares	Mean Square	F ratio	Contribution [%]
A	2	0,01252	0,00626	0,97945	18,39
B	2	0,01543	0,00771	1,20687	22,66
C	2	0,02734	0,01367	2,13911	40,17
Error	2	0,01278	0,00639		18,78
Total	8	0,01758	0,03403		100

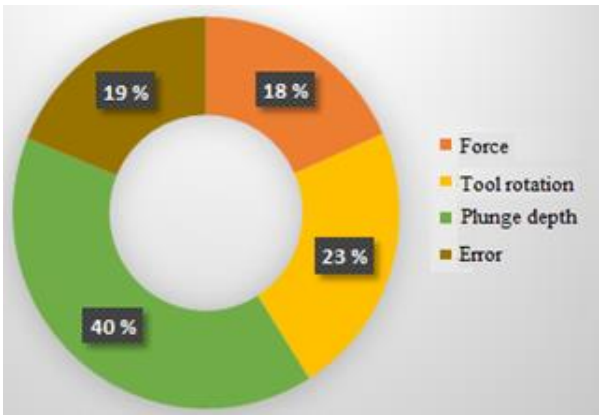

Figure 56: Percentage contribution of each parameters for factor d.s.

Table 18: Results of the analysis of variance for factor hardness

Factors	DoF	Sum of Squares	Mean Square	F ratio	Contribution [%]
A	2	0,00577	0,00289	1,61571	42,21
B	2	0,00234	0,00117	0,65464	17,10
C	2	0,00199	0,001	0,55751	14,56
Error	2	0,00357	0,00179		26,12
Total	8	0,01758	0,00684		100

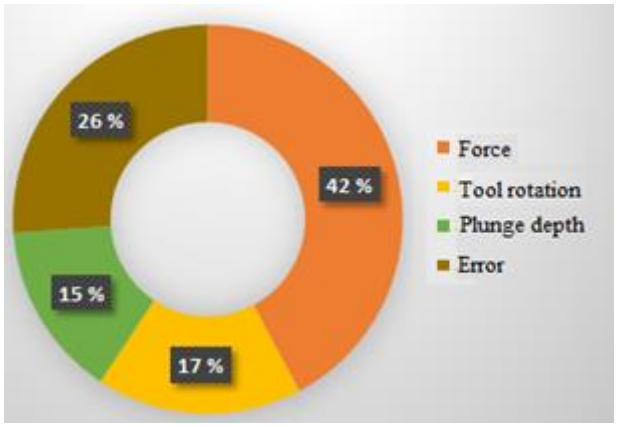

Figure 57: Percentage contribution of each parameters for factor hardness

Percentage contribution of each parameters in tube B for factors t.s., d.s., and hardness were presented in Figure 54, Figure 55 and Figure 56 respectively. From the figures, it was known that, the forging force is the most significant parameters in case of t.s. and hardness whereas, the plunge depth is bigger affect in case of d.s. The least error percentage of 4% was found in t.s. as shown in Figure 54.

4.4.3 **Prediction of the Optimum Performances**

The analysis of variance assist to predict the optimum performance. It is important to perform confirmation test in optimum parameters which were derived from Taguchi

methods. The response achieved from tests performed in optimum parameters should be near to the predicted optimum performance. As the quality characteristic of "higher the better" was chose already, the predictions were made based on predetermined characteristics. For example, the highest value in t.s. for tube A is third level of tool rotation, first level of force and second level of plunge depth i.e. A3-B1-C2. It can be seen in Figure 46. Another example is A1-B3-C1 has a higher value in t.s. in case of tube B and can be seen in Figure 49. Knowing the highest value in every performance, the optimum performance Y_{opt} (optimum value of the response characteristic) can be estimated as equation 17 [39].

$$Y_{opt} = \bar{x} + (A_1 - \bar{x}) + (B_2 - \bar{x}) + (C_3 - \bar{x}) \qquad \text{Equation 16}$$

Where, $\bar{x}$ is the mean of the results and A_1, B_2 and C_3 are the highest values of the responses.

Finally, according to the equation 17, the optimum performance values for the shorter and tube B were presented in Table 19.

Table 19: Results for the optimum performances

	Thickness stability	**Diameter stability**	**Hardness**
Tube A	0,97	0,98	0,88
Tube B	0,95	0,96	0,90

4.4.4 **Algebraic Model**

To achieve more robust parametric combination which would improve the entire properties of F2T, algebraic models were presented [60]. The considerations were made on three different combinations predicted by Taguchi method and the percentage contribution of each parameters obtained by ANOVA. The algebraic model for tube A and tube B were presented in subheading a. and b.

❖ **Tube A**

In Table 20, highest performance parameters for tube A were presented which form matrix P.

Table 20: Optimum values

	Thickness stability		Diameter stability		Hardness	
Tool rotation [Ω]	A3	3000	A1	2000	A3	3000
Forging Force [KN]	B1	20	B1	20	B3	45
Plunge depth [mm]	C2	4,7	C2	4,7	C1	3,4
Optimum performance [%]	97		98		88	

$$P = \begin{bmatrix} A3 & A1 & A3 \\ B1 & B1 & B3 \\ C2 & C2 & C1 \end{bmatrix} = \begin{bmatrix} 3000 & 2000 & 3000 \\ 20 & 20 & 45 \\ 4{,}7 & 4{,}7 & 3{,}4 \end{bmatrix}$$

Similarly, in Table 21, the percentage contributions used in algebraic model were presented and that form matrix Q.

Table 21: Percentage contribution

	Tool rotation		Forging force		Plunge depth	
Thickness stability	$\rho_{A.t.s}$	36,02	$\rho_{B.t.s}$	29,07	$\rho_{C.t.s}$	40,37
Diameter stability	$\rho_{A.d.s}$	15,44	$\rho_{B.d.s}$	24,32	$\rho_{C.d.s}$	32,28
Hardness	$\rho_{A.hard}$	31,02	$\rho_{B.hard}$	39,07	$\rho_{C.hard}$	4,94
Total	$\rho_{A.T}$	**82,48**	$\rho_{B.T}$	**92,46**	$\rho_{C.T}$	**77,59**

$$Q = \begin{bmatrix} \frac{\rho_{A.t.s}}{\rho_{A.T}} & \frac{\rho_{B.t.s}}{\rho_{B.T}} & \frac{\rho_{C.t.s}}{\rho_{C.T}} \\ \frac{\rho_{A.d.s}}{\rho_{A.T}} & \frac{\rho_{B.d.s}}{\rho_{B.T}} & \frac{\rho_{C.d.s}}{\rho_{C.T}} \\ \frac{\rho_{A.hard}}{\rho_{A.T}} & \frac{\rho_{B.hard}}{\rho_{B.T}} & \frac{\rho_{C.hard}}{\rho_{C.T}} \end{bmatrix} = \begin{bmatrix} 0{,}44 & 0{,}31 & 0{,}52 \\ 0{,}19 & 0{,}26 & 0{,}42 \\ 0{,}38 & 0{,}42 & 0{,}06 \end{bmatrix}$$

The optimum parameters can be calculated by multiplying matrix P and Q as in equation 18.

$$[Optimum\ Parameters] = [P]\ x\ [Q]$$ Equation 17

$$\begin{bmatrix} Rotation & x & x \\ x & Force & x \\ x & x & Plung \end{bmatrix} = \begin{bmatrix} A3 & A1 & A3 \\ B1 & B1 & B3 \\ C2 & C2 & C1 \end{bmatrix} \begin{bmatrix} \frac{\rho_{A.t.s}}{\rho_{A.T}} & \frac{\rho_{B.t.s}}{\rho_{B.T}} & \frac{\rho_{C.t.s}}{\rho_{C.T}} \\ \frac{\rho_{A.d.s}}{\rho_{A.T}} & \frac{\rho_{B.d.s}}{\rho_{B.T}} & \frac{\rho_{C.d.s}}{\rho_{C.T}} \\ \frac{\rho_{A.hard}}{\rho_{A.T}} & \frac{\rho_{B.hard}}{\rho_{B.T}} & \frac{\rho_{C.hard}}{\rho_{C.T}} \end{bmatrix}$$

The calculated optimum parameters of F2T conducted in tube A were presented in Table 22. The next step in Taguchi method is to perform the confirmation test.

Table 22: Optimum Parameters

Optimum Parameters	
Tool rotation [Ω]	2813
Forging Force [KN]	30,4
Plunge depth [mm]	4,62

❖ **Tube B**

Here the processes done in tube A are repeated. Since the factor, forging force was kept in first column of orthogonal array which is the most important factor in F2T, the tables and matrices were presented by interchanging force and tool rotation than the tube A´s algebraic model process. In Table 23, highest performance parameters for tube B were presented which form matrix P.

Table 23: Optimum values

	Thickness stability		Diameter stability		Hardness	
Forging Force [KN]	A1	25	A1	25	A2	30
Tool rotation [Ω]	B3	3000	B1	2600	B3	3000
Plunge depth [mm]	C1	3,7	C1	3,7	C2	4,7
Optimum performance [%]	95		96		90	

$$P = \begin{bmatrix} A1 & A1 & A3 \\ B3 & B1 & B3 \\ C1 & C1 & C2 \end{bmatrix} = \begin{bmatrix} 25 & 25 & 30 \\ 3000 & 2600 & 3000 \\ 3,7 & 3,7 & 4,7 \end{bmatrix}$$

Similarly, in Table 24, the percentage contributions used in algebraic model were presented and that form matrix Q.

Table 24: Percentage contribution

	Forging Force		Tool rotation		Plunge depth	
Thickness stability	$\rho_{B.t.s}$	54,76	$\rho_{A.t.s}$	18,39	$\rho_{C.t.s}$	42,21
Diameter stability	$\rho_{B.d.s}$	10,91	$\rho_{A.d.s}$	22,66	$\rho_{C.d.s}$	17,10
Hardness	$\rho_{B.hard}$	30,17	$\rho_{A.hard}$	40,17	$\rho_{C.hard}$	14,56
Total	$\rho_{B.T}$	**95,84**	$\rho_{A.T}$	**81,22**	$\rho_{C.T}$	**73,87**

$$Q = \begin{bmatrix} \frac{\rho_{A.t.s}}{\rho_{A.T}} & \frac{\rho_{B.t.s}}{\rho_{B.T}} & \frac{\rho_{C.t.s}}{\rho_{C.T}} \\ \frac{\rho_{A.d.s}}{\rho_{A.T}} & \frac{\rho_{B.d.s}}{\rho_{B.T}} & \frac{\rho_{C.d.s}}{\rho_{C.T}} \\ \frac{\rho_{A.hard}}{\rho_{A.T}} & \frac{\rho_{B.hard}}{\rho_{B.T}} & \frac{\rho_{C.hard}}{\rho_{C.T}} \end{bmatrix} = \begin{bmatrix} 0,57 & 0,23 & 0,57 \\ 0,11 & 0,28 & 0,23 \\ 0,32 & 0,49 & 0,20 \end{bmatrix}$$

As in the process of tube A, the optimum parameters can be calculated by multiplying matric P and Q as in equation 18. And the calculated optimum parameters of F2T conducted in tube B were presented in Table 25. The next step in Taguchi method is to perform the confirmation test.

Table 25: Optimum Parameters

Optimum Parameters	
Forging Force [KN]	26,60
Tool rotation [Ω]	2888
Plunge depth [mm]	3,90

4.4.5 **Confirmation test**

As the optimum parameters were found, the next task is to perform confirmation test to verify the improvement of the performance characteristics.

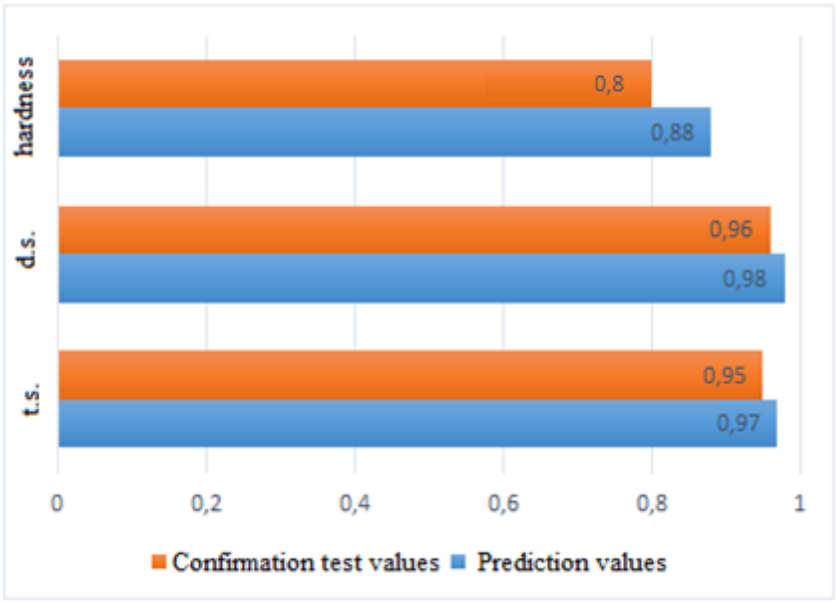

Figure 58: Comparison of test values and predicted values for tube A

Figure 58 shows the comparison of the values obtained from the confirmation test which was carried out in optimal F2T parameters and previously predicted values of tube A. It can be seen that, values of the confirmation test were close enough to the predicted one except the hardness factor. Based on the confirmation test, the percentage change in t.s. and d.s. are 2% only whereas in hardness factor, it is 9%.

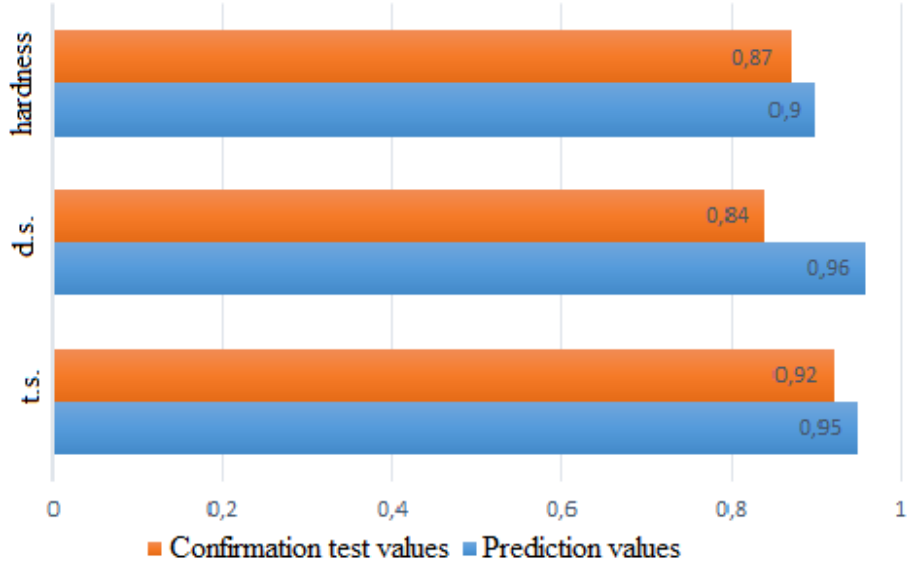

Figure 59: Comparison of test values and predicted values for tube B

Similarly, in Figure 59, the comparison of confirmation test values and predicted values for tube B was presented. In this figure, values of the confirmation test were close to the predicted one for t.s. and hardness factors. In a contrast, the percentage change in d.s. is 13% than the predicted one while the changes in t.s. and d.s. is only 3%.

4.5 Thermal and Mechanical Analysis

4.5.1 Log File Analysis

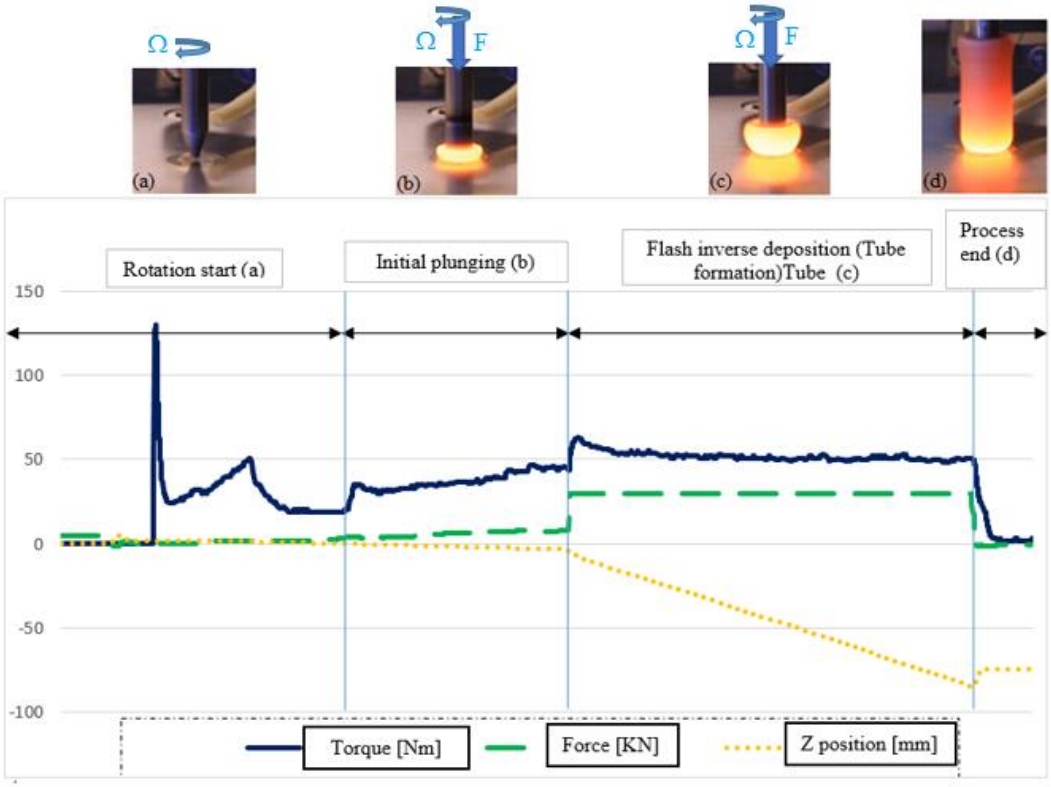

Figure 60: Behaviour of torque, axial force and displacement

Based on the development of torque, axial forging force and displacement, F2T process can be divided into two main periods: i) initial transient plunging period and ii) stationary plunging period. Figure 60 shows the typical behaviour of torque, axial forging force and displacement in F2T process along with the consumable rod representation. At the beginning the spindle of machine started to rotate where maximum torque can be seen. As machine reached to the maximum adjusted rpm, the consumable rod smoothly touches to the anvil. From that instant, initial transient plunging period starts and continue for short length towards the negative z-axis. In this period, speed control method was applied. For example in Figure 61, which shows the evolution of different parameters of F2T process where optimal parameters were used to produce F2T using supporting guide. The maximum rpm of 2888 was reached and initial transient plunging period was last up to -3,9 mm in z-axis and the speed of 1,5 mm/min was used. The force and torque gradually increases in this period because the feeding of consumable rod to the anvil so generate frictional heat at the tip of the consumable rod that makes tip soft. This frictional heat generates a viscoplastic boundary layer at the rod tip. The second period: stationary plunging period was force controlled and as seen in Figure 61 the force of maximum 26,60 kN was used. The period last up to 73 mm in negative z-axis. The value of torque and force was risen as it started a stationary plunging period and goes smoothly till the end of the period. The analysis of forging force, torque, speed, displacement etc. helps to understand the F2T process. The stability in these parameters is very important in the stability of tube shape.

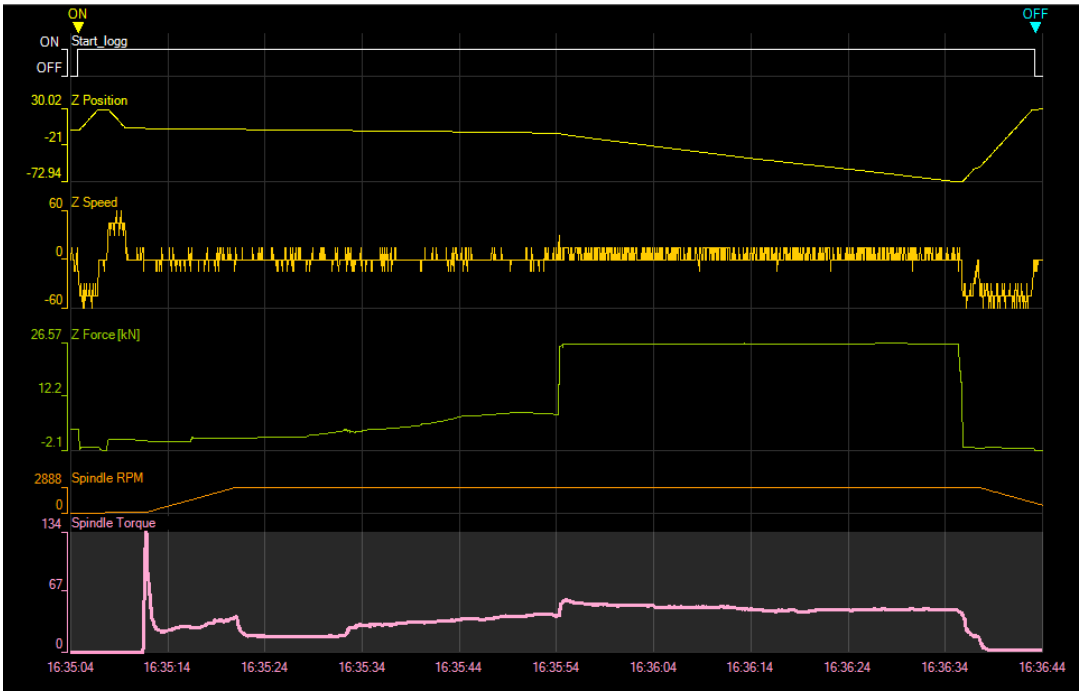

Figure 61: Log file of F2T using supporting guide in optimal parameters

Figure 61 shows the log file of F2T (directly obtained from FSW machine) which was made using supporting guide in optimal parameters. Besides forging force, torque, speed etc. there was also forces developed in x- and y- direction. The amount of forces were negligible which was the reason, it was not shown in the figure. The method was speed controlled in initial transient plunging period and force controlled stationary plunging

period however the speed in stationary plunging period has same value to the speed at initial transient plunging period as seen in Figure 61.

4.5.2 **Infra-red Measured Temperature Analysis**

The thermal camera used in infra-red temperature analysis was FLIR SC660 which was explained in section 3.4.5. The camera has 40mm lens, the distance between the camera and the target was about 500mm and the emissivity was set to 0,65. The temperature range of minimum 300 degree Celsius and maximum of 1500 degree Celsius was set. To cover the whole F2T process sequence of 180 was used.

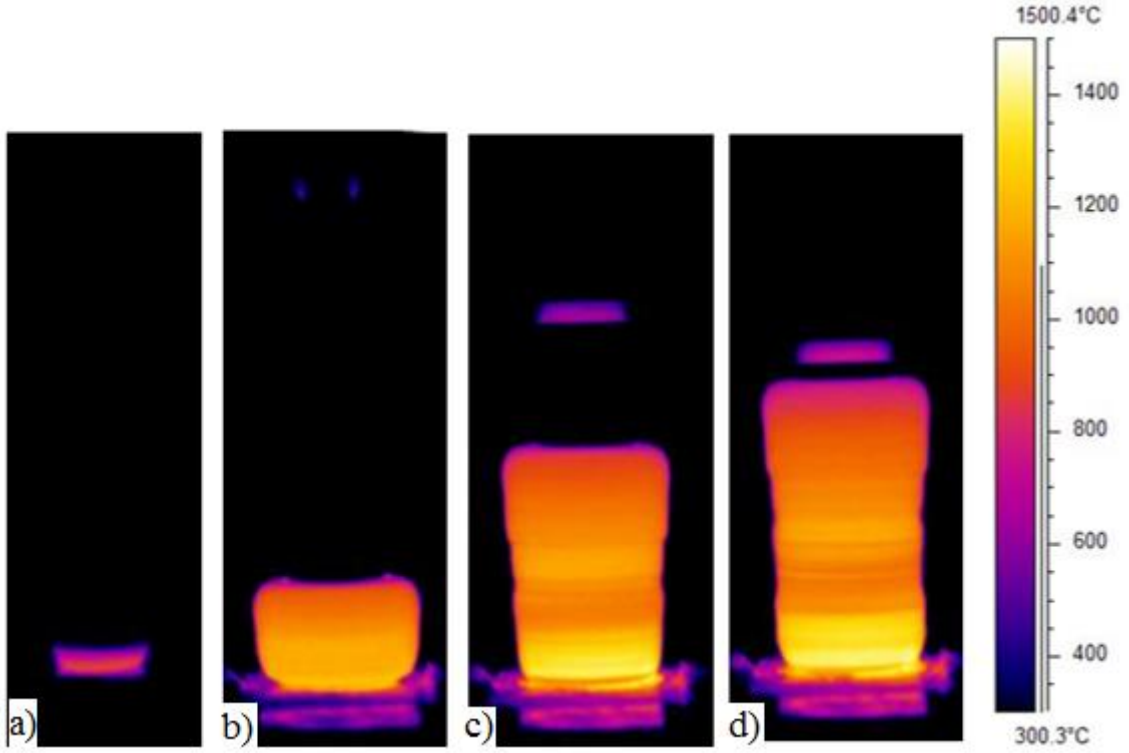

Figure 62: Infra-red images at a) Initial transient plunging period start b) Stationary transient plunging period end c) In middle of stationary plunging period d) Process end

Figure 62 shows the IR images at different time period of F2T: a) starting of initial transient plunging period b) starting of stationary plunging period c) during the stationary plunging period and d) end of the process. The point at the viscoplastic zone where anvil and consumable rod get contacted is a place, maximum temperature was recorded. Figure 63 depicts the temperature recorded at spot 1 (contact point between anvil and consumable) throughout the process.

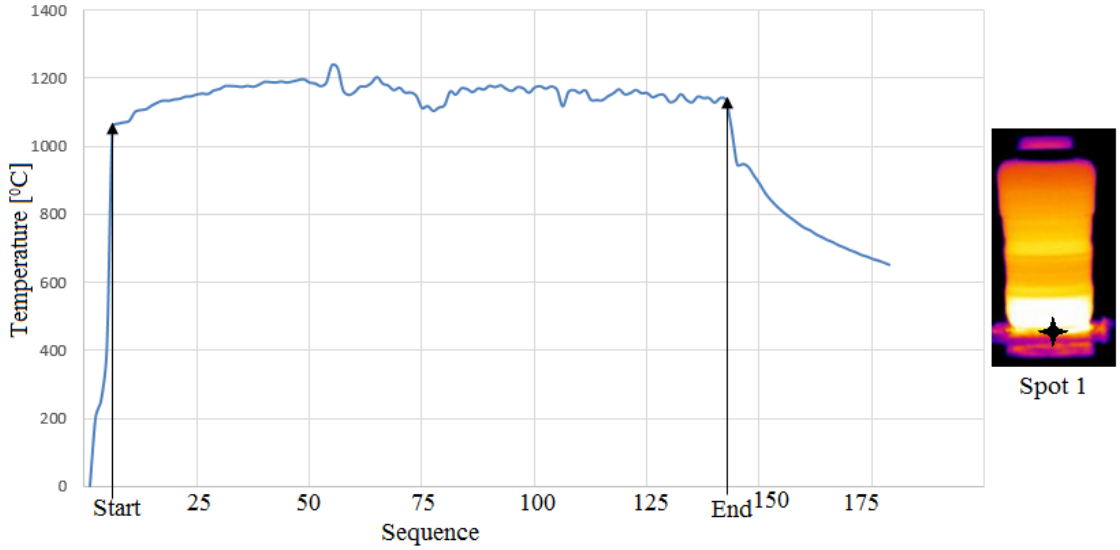

Figure 63: Temperature measurement at spot 1 (in right side) throughout the process

The spot 1 was shown in the right side of Figure 63 which was the contact point between anvil and consumable. The temperature measurement covered both initial transient plunging period and stationary plunging period. The sudden rise of the temperature can be seen during the initial transient plunging period and gradual increase till the stationary plunging period. Since the F2T is a thermomechanical process and as expected the average temperature during the stationary plunging period was recorded 1115^0C and the maximum temperature recorded was 1238^0C. Another way to validate maximum temperature and emissivity was measuring temperature by thermocouple. Because of rotary movement in tool and test piece, it was not possible to used thermocouple in this condition. However, measurement of temperature in anvil surrounding was done and presented in section 4.5.3.

4.5.3 **Thermocouple Measured Temperature in Anvil**

The section 4.2.2 has described about the anvil system and cooling method apply on it. The cooling is necessary to prevent or minimize the deformation of tungsten. The study of temperature on it is also necessary to understand the F2T process. Temperature study on consumable rod (F2T) using thermocouple is tricky because of its rotation during the process therefore, the analysis were made using infra-red images in section 4.5.24.5.3. Thermocouple temperature analysis was done in two side and beneath of tungsten carbide as shown in Figure 64. The tungsten carbide goes into the pocket of anvil design in figure and thermocouple B, A and C were remained in the beneath, left and right side respectively.

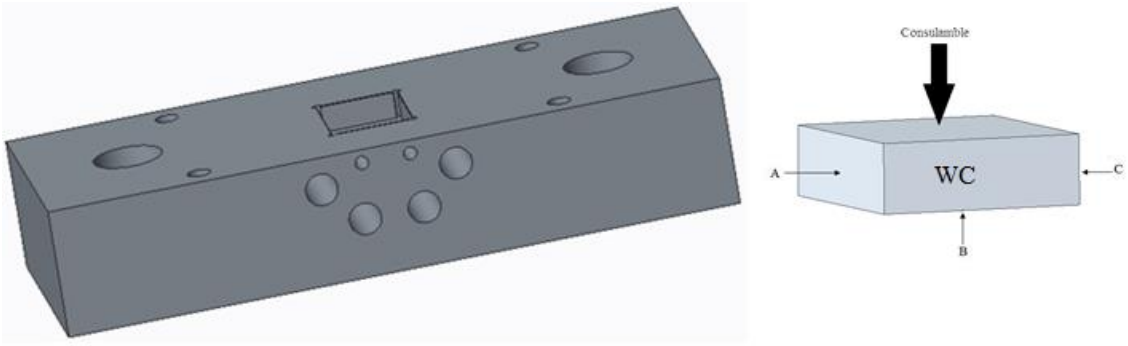

Figure 64: Position of thermocouple wire (A, B and C) in tungsten carbide

The temperature obtained in three difference position was presented in Figure 65. Initially because of the cold water cooling system temperature around tungsten carbide is less than a room temperature. As the process starts, the temperature started to increase gradually and stay constant during the F2T process. The maximum temperature reached in three position A, B, C are 273 ºC, 275 ºC and 273ºC respectively. The rise in temperature around anvil has deformation effect on tungsten carbide which decrease the life of tungsten carbide and has direct effect on F2T process.

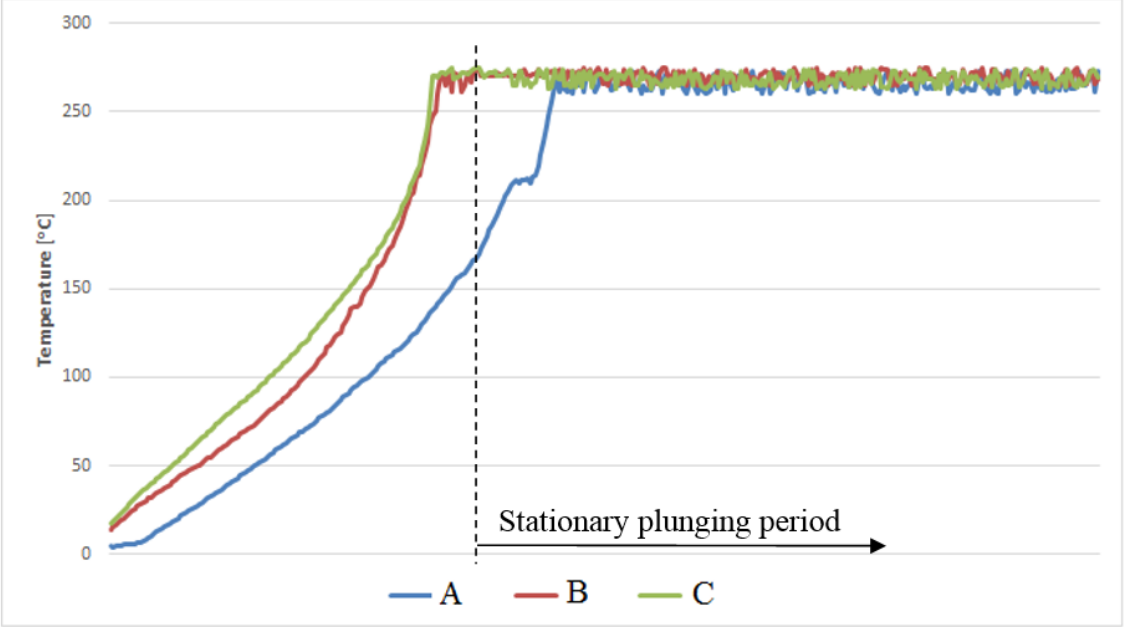

Figure 65: Temperature recorded in Anvil

Measuring temperature in contact point between test piece and anvil would be interesting but because of rotary movement at the surface of anvil, it was not easy. The temperature around the surface of anvil which are measured by thermocouple were not significantly high however, it could be reduce with improvise cooling system.

5 MATERIALS ENGINEERING ANALYSIS

5.1 Introduction

In this chapter, material engineering analysis is presented. Since the research was done in structural steel S355, it is important to analysis mechanical properties and metallurgical properties of tube produce by F2T and compare it with tube produce by different technique.

In Section 5.2, result and analysis of mechanical tests are performed. Tensile test, flattening test, flare test and micro-hardness test are the standard test performed in tube which are presented in different sub heading in this section.

In Section 5.3, metallurgical analysis is presented. The optical microscopy test and EBSD were performed in metallurgical analysis. Metallurgical analysis is important in terms of revealing microstructure, processes performed on the material during manufacture etc.

5.2 Mechanical Test

5.2.1 Tensile Test

The tensile test was conducted in two tubes. One was produced by F2T method using supporting guide for a longer tube´s (tube B) using optimal parameters. Another tube was produced by machining in a similar base material. The objective of test is not only to know the mechanical properties of produced F2T tube but also to compare it with similar kind of commercial tubes. To be a precise with material, base material was machined to produce a tube with similar tube geometry. The machining process includes turning of a round shaft followed by drilling in lathe machine.

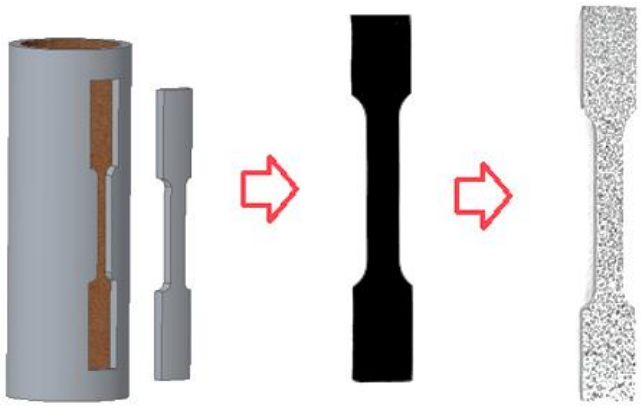

Figure 66: Preparation of Tensile test specimen

The tensile test specimen was extracted from F2T tube and machined tube as shown in Figure 66. The engineering drawing of specimen is available in appendix C. The thickness of the specimen was 2 mm, gage width was 4 mm and gage length was 20 mm. The

specimen was first cut by EDM followed by polishing using sand paper. The specimen was not flat since it was extracted from tube. The full length of specimen along with grip section was kept as it is. The specimens were then painted with white colour and sprayed with black colour as shown in Figure 66. Since the total length of specimen is shorter which makes difficult to have potentiometer to measure strain, Digital Image Correlation (DIC) method was used. The method of tracking and comparing images in certain action to measure the changes in those images is called DIC method and more about DIC equipment was presented in section 3.4.2.

The MTS Landmark machine (presented in section 3.4.2) was used in laboratory of Aalto University to perform tensile test. For DIC measurement, Lavision Imager Pro X camera system was used. The pictures were taken at the frequency of 2 Hz during the test. The pattern of black spot on the specimen changes while increasing the strain and based on those patterns, the behavior of the strain and its localization was estimated. The estimation was done in DaVis software.

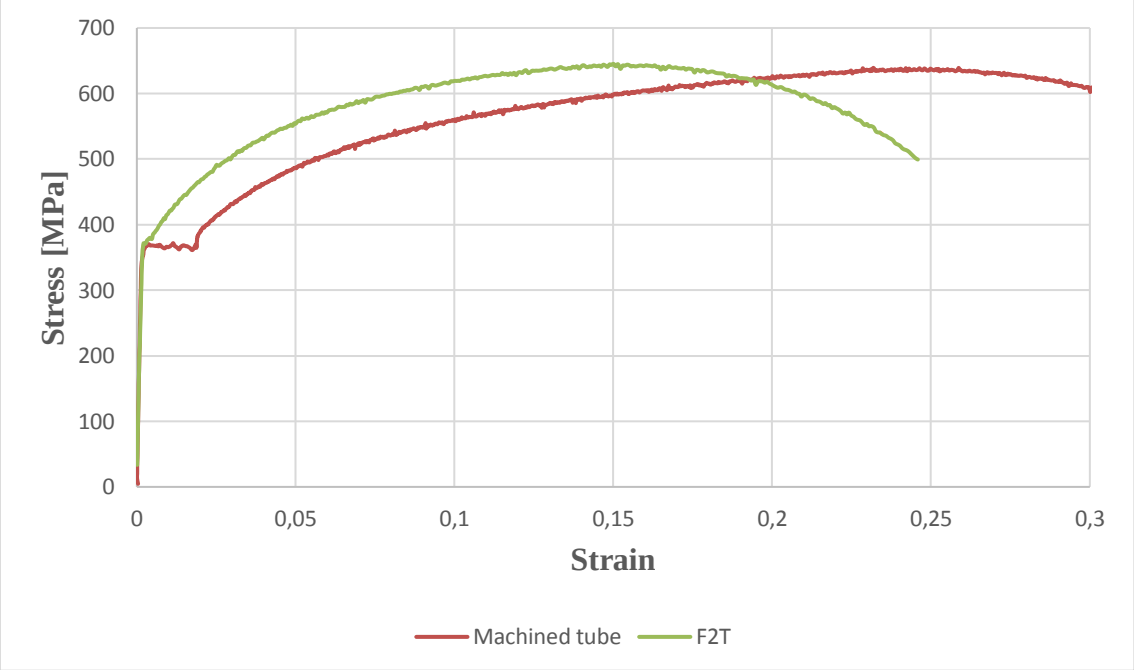

Figure 67: Stress-Strain curve of F2 tube and machined tube

The Figure 67 shows the stress-strain curve for F2T and machined tube. The data for F2T and machined tube were extracted from DIC method using Davis software. The nature of the curve for both machined tube and F2T tube was found similar however, the elongation of machined tube was found more. Similarly, in Figure 68, the mechanical properties of F2T and machined tube are presented which were derived from the stress-strain curve in Figure 67.

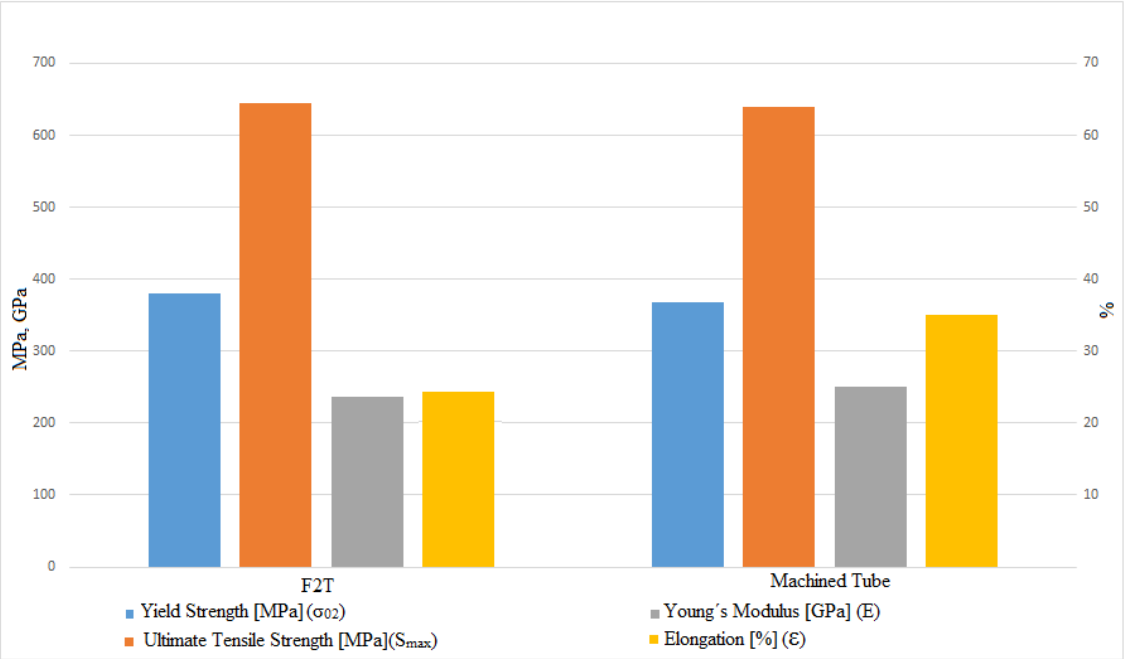

Figure 68: Comparison of yield strength, ultimate tensile strength young´s modulus and elongation

Table 26: Comparison of mechanical properties

	F2T	Machined
Yield Strength [Mpa] (0,2% offset yeild)	380	368
Ultimate Tensile Strength [Mpa]	644	639
Young`s Modulus [Gpa] E	236	250
Elongation (%)	24	36

As in stress-strain curve, the values obtained for F2T and machined tube are close to each other. For example, the yield strength (at offset of 0,02%) of F2T and machined tube has value of 380 and 368 MPa respectively. Comparison of other mechanical properties can be find in Table 26. In a contrast, the elongation percent value in F2T was noticeably less than machin3ed tube. The values are 24% in F2T and 36% in machined tube. The analysis of tensile test concludes that, there was no huge changes in the mechanical properties of F2T tube compare to machined tube

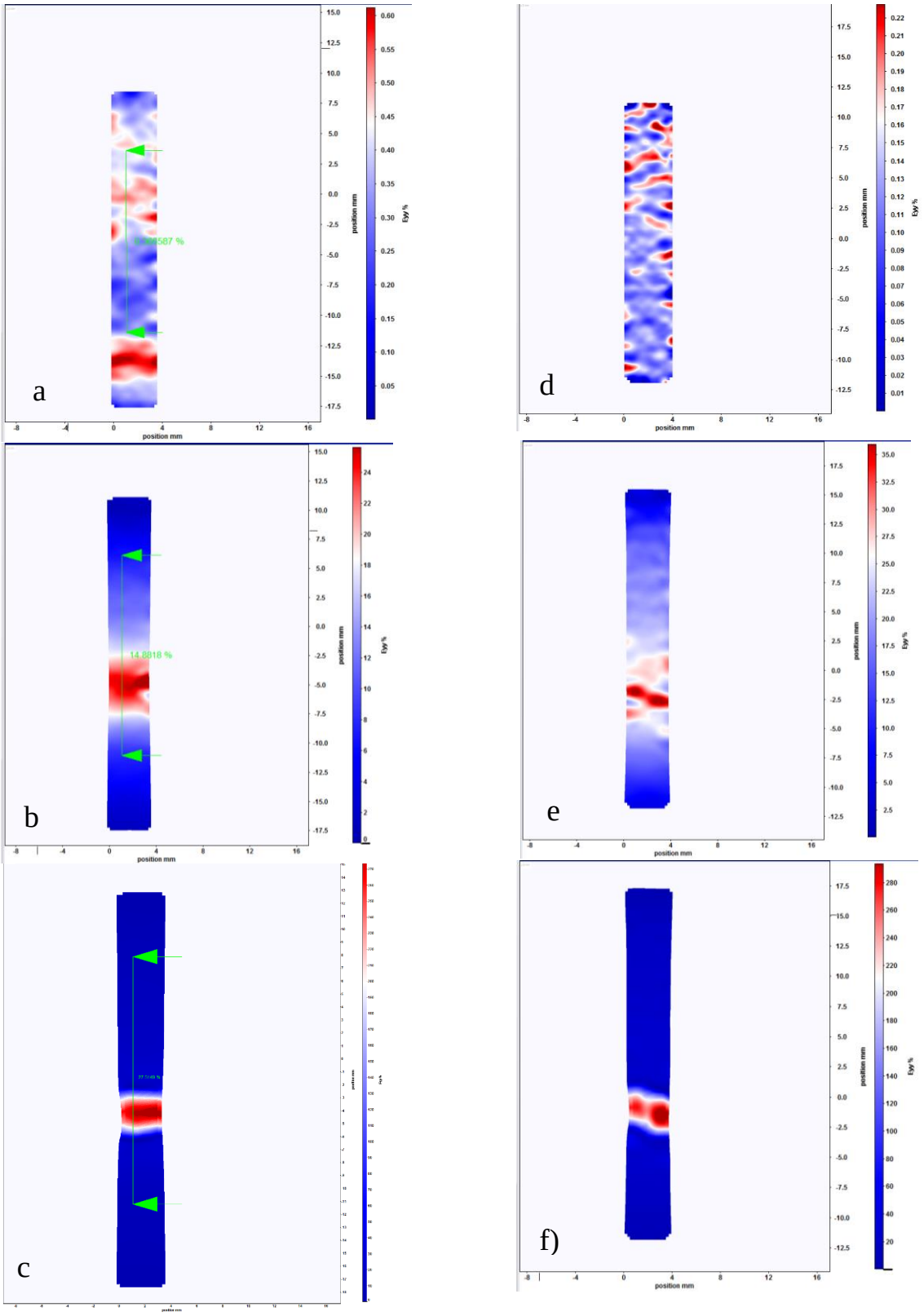

Figure 69: Results of DIC-measurement: a) Yield point b) UTS c) Specimen as it fracture point of F2T and d) Yield point e) UTS f) Specimen as it fracture of machined tube.

The localization of strain for F2T and machined tube was analyzed using DIC method and presented in Figure 69. The images were taken at 3 different point: yield point, ultimate tensile strength point and at the point just before crack.

5.2.2 **Flattening Test**

Flattening test of F2T was performed according to the ASTM standard [28]. The objective of flattening test was to evaluate the ability of tubes to undergo plastic deformation and may be the defect on it. The compression strength of the tube will be known from the test which also aid to know about the ductility. To perform the test, the tube was produced by F2T method using supporting guide using optimal parameters and by machining as in tensile test. The dimension of both tubes were identical.

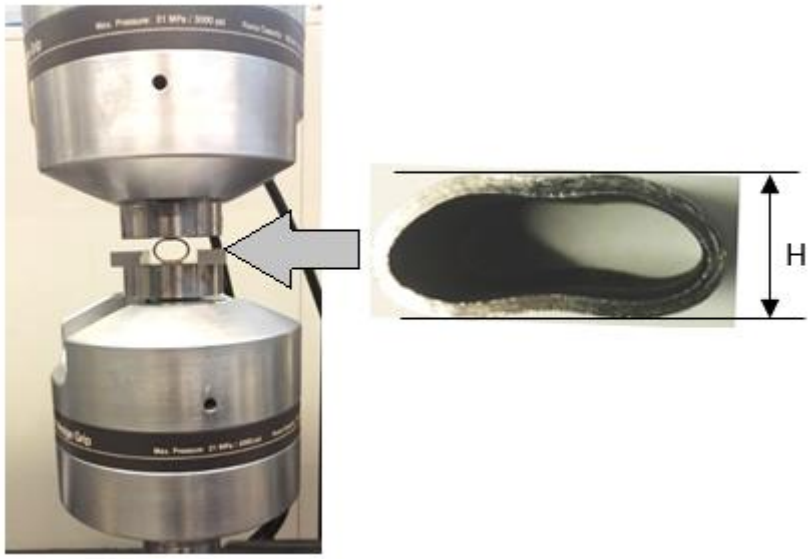

Figure 70: Experimental setup of Flattening test

The Figure 70 shows the experimental setup of flattening test, where MTS Landmark machine was used to compress the specimen. Same machine was used in tensile test too. The displacement and force data were collected during the test however, objective of test is to see whether the specimen develop the crack as it flattened to the depth of H as shown in Figure 70. Since the diameter of specimen was 24,4mm and thickness was 1,65 therefore according to the equation 5, the value of H was calculated 12,2 mm. The speed of applied load was 5 mm/minute for both test.

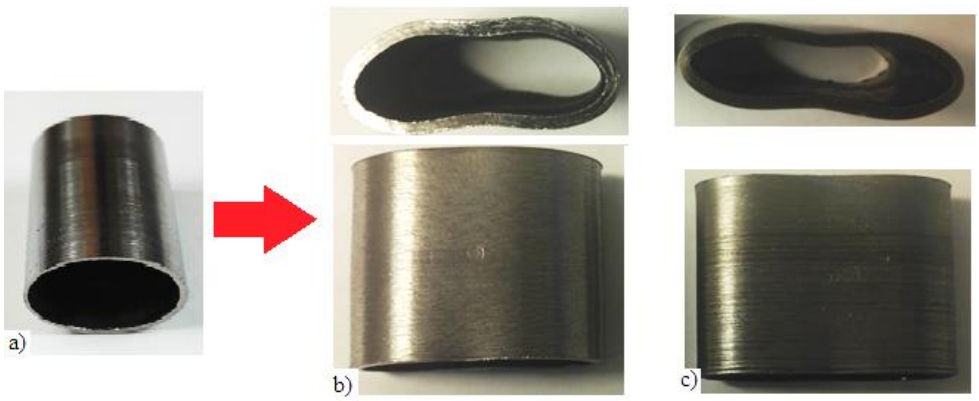

Figure 71: Flattening test a) Specimen before test b) F2T tube and c) Machined tube after test

The surface and all edges were checked carefully (Figure 71) and no defect was found which means both tubes are good according to the ASTM standard [28]. This assure that tubes are able to undergo plastic deformation. Moreover the force-displacement data of both test were collected to calculate the energy absorbed. Figure 72 depicts the force-displacement curve of F2T and machined tube during the flattening test. The arrowhead in the figure represent that, displacement in flattening test was done to obtain final dimension of H as shown in Figure 70. The value is difference of outer diameter (O.D) of tube and H.

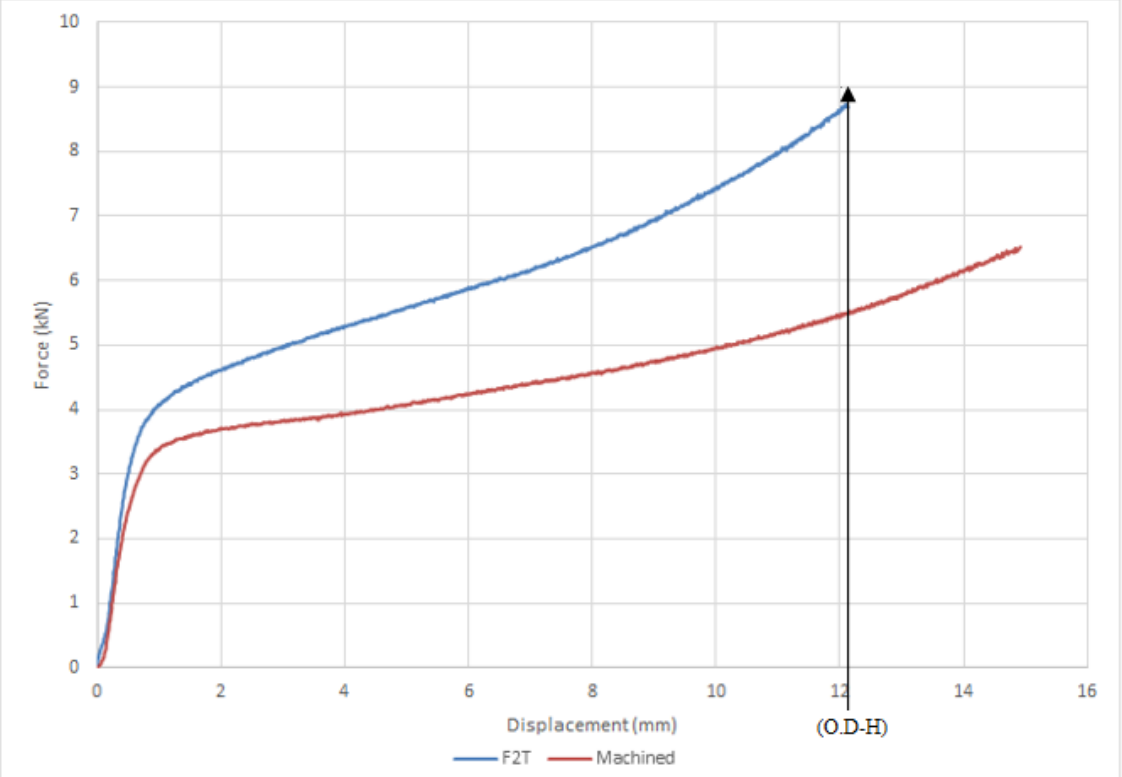

Figure 72: Force-Displacement curve

To achieve H dimension in flattening test, the force was reached up to 5,5 kN in machined tube whereas in F2T, it was 8,7 kN. The energy absorbed in the test is the area inside the force-displacement curve which was presented in Table 27. The difference in energy level is easily distinguishable in Figure 72.

Table 27: Energy absorption in F2T and machined tube

Tube	**Energy Absorption [J]**
F2T	72,67
Machined	50,8

5.2.3 **Flare Test**

Flare test also known as tube-drift expansion test was performed to determine the ability of tube to undergo plastic deformation in drift expansion. Though flare and flattening test are different in procedure, both test have same objective. As in other mechanical test, two specimen were used in this test too. They are F2T tube and machined tube. The test was performed according to the British standard [29]. The preparation of machined tube was described in section 5.2.1. Both tubes were prepared identical in dimension. The outer diameter of 25mm with thickness 2,5 mm and length of the specimen was 50 mm. The experimental setup of the test was presented in Figure 73.

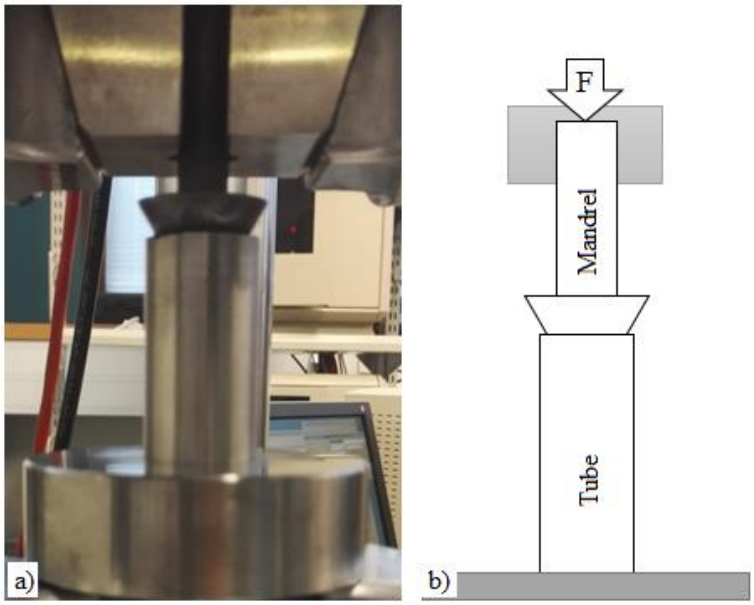

Figure 73: Flare test a) Experimental setup b) Experimental setup layout

As in Flattening, the test was done in MTS Landmark machine. The speed used was 5mm/min. Moreover, the specimen was compressed by using mandrel as shown in Figure 73. The mandrel was made up of AISI H13 tool steel which was tempered to achieve high strength and hardness. The AISI H13 tool steel was used because of its availability in workshop. Moreover, the material has easy machinability, good elevated-temperature strength, fatigue resistance and wear resistance. The mandrel tip was designed 60 degree. The engineering drawing of mandrel can be find in appendix D. During the test, mandrel was clamped in the upper jaw of MTS Landmark machine and on the tip of the mandrel, some lubricant was applied for smoothness in the test.

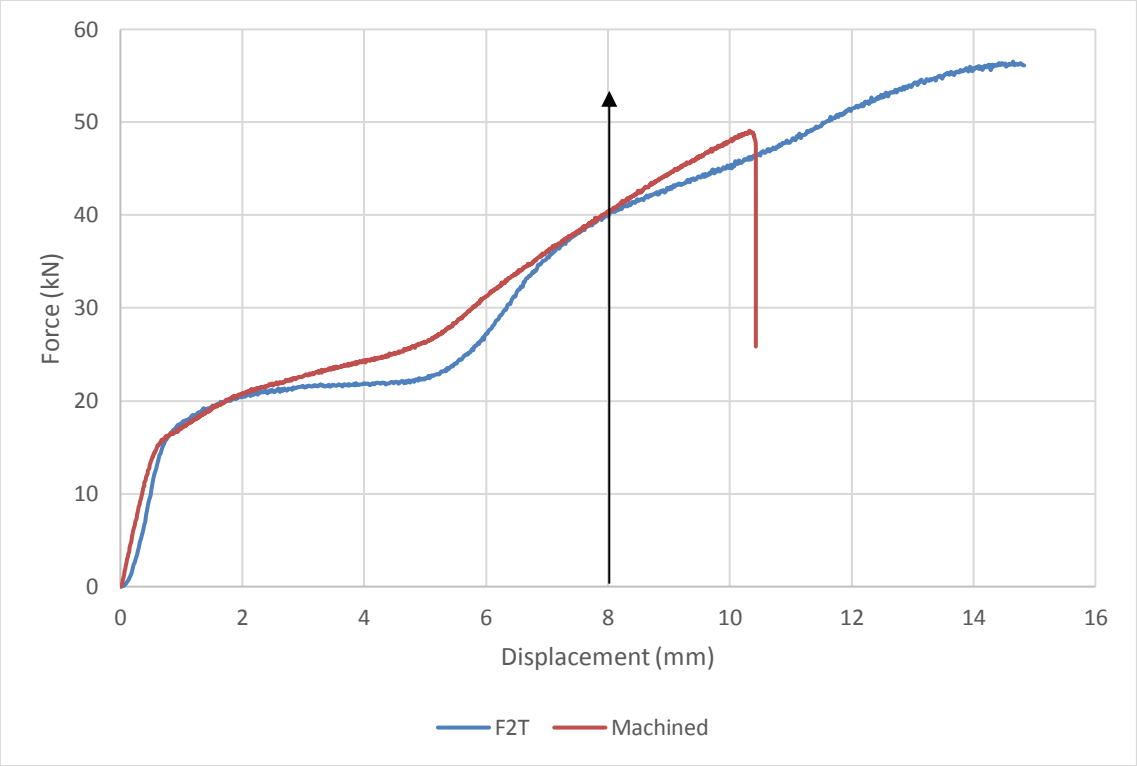

Figure 74: Force-Displacement curve

According to the standard, the specimen should expand up to the 30% -35% of the outer diameter of tube followed by visual inspection to see if the cracks were developed. Since the diameter of specimen was 25 mm, the test has to stop as the diameter of specimen reach maximum 33,75 mm which is 35% of expansion. It is very hard to find out the expanded diameter during the test which is the reason test was carried out more expansion than required. The Figure 74 shows the force-displacement graph for F2T and machined tube. The nature of the graph in both cases seems similar and there was no crack developed up to the expansion of 35% of O.D which was estimated in displacement of 8,1 mm. The energy absorptions to that point for F2T and machined tube are presented in Table 28.

Table 28: Energy absorption in F2T and machined tube

Tube	**Energy Absorption [J]**
F2T	187,60
Machined	201,9

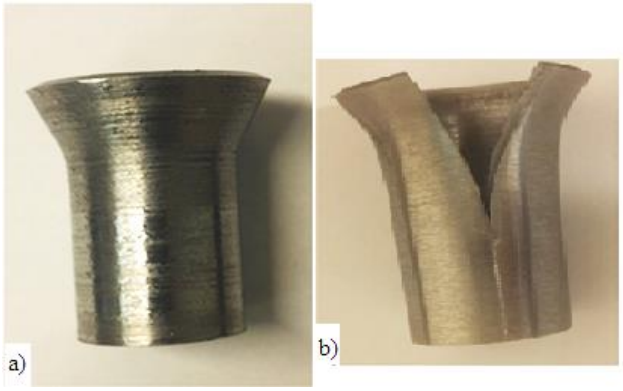

Figure 75: Test Specimen after Flare test: a) F2T tube b) Machined tube

The test up to expansion of 35% of O.D. was enough as per the standard however, the test was continued above 35%. The visual inspection in the F2T tube which was presented in Figure 75 was done. There was no crack developed which conclude that the tube is ductile to withstand the load up to 55kN. However in case of machined tube the specimen cracked when the load of 48kN was reached.

5.2.4 **Microhardness**

Hardness has a direct relation to the mechanical properties of material because a hardness increase so does yield strength and ultimate tensile strength. The F2T tube made in optimal parameters was used for microhardness test. Four specimens were extracted from F2T tube. One was taken from the longitudinal section of the tube and remaining three were taken from the cross section in different three parts: top, middle and bottom as shown in Figure 76. The longitudinal section specimen (sample 1) helps to measure hardness throughout the length whereas three different cross section gives result on starting position, near to the end position and in mid position (sample 2.c, 2.b and 2.a) respectively. All three positions were in stationary plunge period.

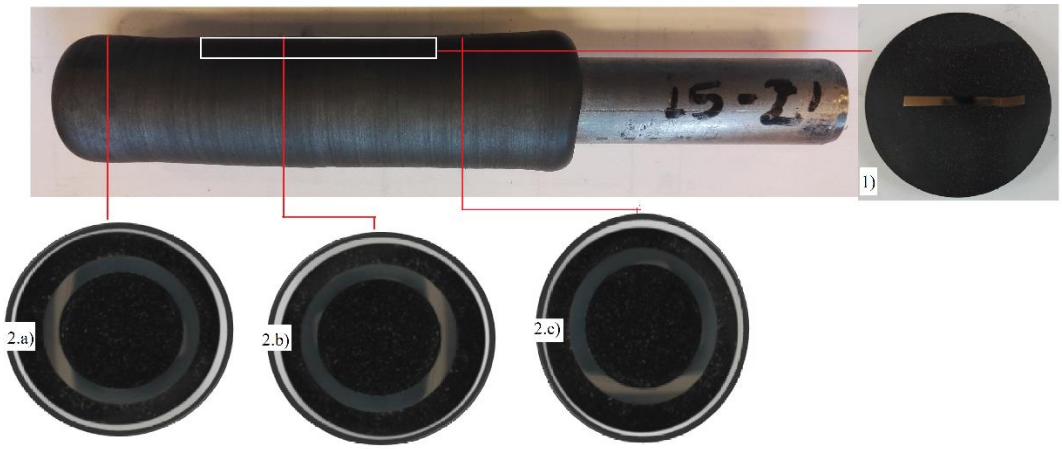

Figure 76: Specimen preparation for microhardness

The specimens were prepared by cutting in a disc cutter in a lab followed by moulding of it and polishing. As per the best practice, specimens were grinded in grit sand paper in following order: 800 – 1200 – 2000. Then the polishing was done with 5 micron, and 1

micron diamond paste. The specimens were cleaned with ethanol and dried to prevent oxide layer on it. The CMS instrumented platform that was equipped with Vickers indentation head was used in microhardness test. The matrix form in sample 1 was 3x50 having distance between two indentation 0,3 mm along to the thickness and 0,5 mm along to the length. Similarly, in sample 2.a, b and c, matrices were made in one quarter only. The total number of indentation was 51 in three columns. The distance between each column was 0,5 mm along the thickness. The matrix in sample 1 can be seen in Figure 77 and for sample 2 can be seen in Figure 79.d. In all samples, the load of 1 kg was applied and loading time was 10s. Instead of using length of the indentation diagonals, this equipment uses the depth of indentation with Oliver-Pharr method to calculate hardness value. This means that these results are not Vickers hardness by definition but this fact does not impact the results.

Figure 77: Images of microhardness test a) Matrix in longitudinal sample b) Closeup view of indentation

Figure 78 depicts the hardness distribution in the longitudinal section (sample 1) of F2T. The highest Vickers hardness value recorded was 243 HV1 in the outer edge of the tube and the lowest value was 184 HV1. The average value was 206 HV1. The result shows that the hardness distribution in the middle of the sample has no big alterations. The top part in the sample which is outer side of tube has higher hardness value compare to the inner side of tube. This could be because of high cooling rate in outer circumference of tube. While compare to the hardness value of base material in longitudinal section which is 244 HV1, the value of F2T is way lower. The thermomechanical process do form fine microstructure and improve mechanical properties but not in case of F2T of structural steel.

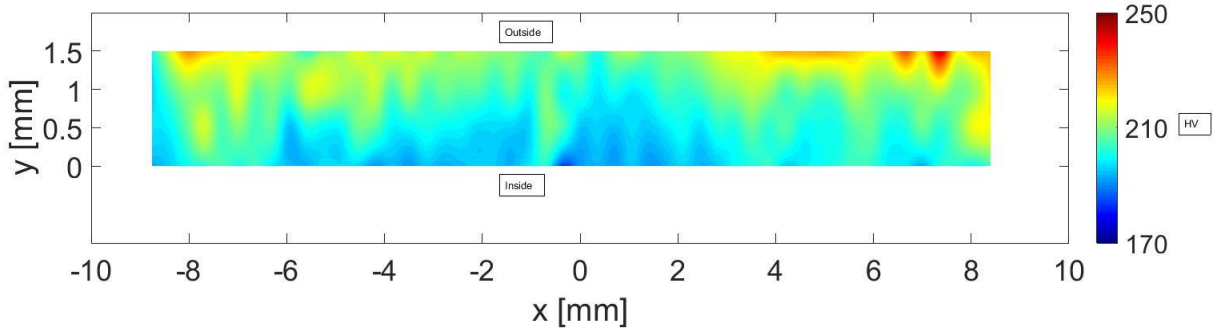

Figure 78: Hardness Map in longitudinal section of F2T

Similarly, Figure 79 shows the Vickers hardness value measure in the radial section of F2T tube in three different section i.e. sample 2.a, 2.b and 2.c.. The hardness maps were made in one-quarter of each radial section. Indentations were made in matrix of 17x3; 3

indentation in the thickness and 17 in circular section as shown in Figure 79.d. The maximum, minimum and average Vickers hardness value recorded in those three samples were presented in Table 29.

Table 29: Vickers hardness values in circular section

Hardness value [HV1]	**Specimens**		
	2.a	**2.b**	**2.c**
Max	225	238	267
Min	190	204	218
Average	210	218	233

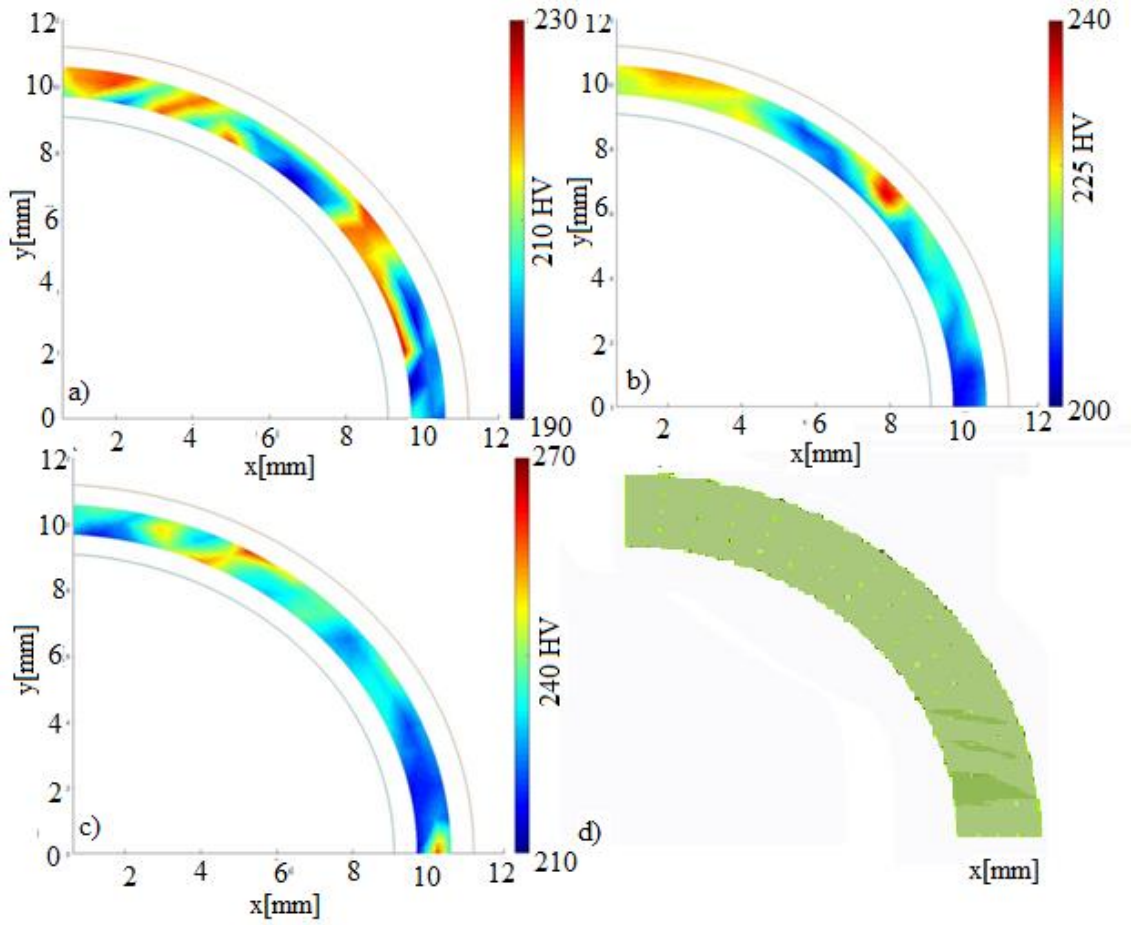

Figure 79: Hardness map in radial section of F2T a) bottom position (specimen 2.a), b) middle position (specimen 2.b), c) Top position (specimen 2.c) and d) Indentation´s matrix in circular section

In all samples the hardness value seems increasing as it moves far from inner circumference to the outer. The average value of hardness values in F2T tube was 190 HV1 to 218 HV1. In other hands, the hardness value of base material was 244 HV1 in longitudinal section and 235 HV1 in radial section which was measure in same micro-indentation equipment. Analyzing hardness map of both longitudinal section and circular section, it can be conclude that the hardness value in structural steel S355 decreases as F2T process was done. However, thermomechanical process increases the hardness and strength in other materials such as carbon steel, tool steel and so on [61]. The cooling process of

outer layer of F2T tube become faster because of direct contact of air which could be the reason of lower hardness in that area compare to the inner part.

❖ **Microhardness in longitudinal section and flash:**

This section explain about the hardness measured in longitudinal section of F2T from starting point to the end of F2T specimen. The specimen was shown in Figure 80. The hardness measurement was taken in the middle of the longitudinal section throughout the length of F2T. The Vickers hardness was measured using different equipment than microhardness in this section. Figure 32 shows the Vickers hardness instrument in lab of Aalto University. In this method, the indentations were made by a diamond pyramid and diagonal of indentations were measured and interpreted via the Vickers equation. More description can be find in section 2.5.2.

The measurement was done manually and presented in Figure 80.The initial plunging period process in F2T which was speed controlled method was shown in left side of the figure as section A. The right section (B) was the result of stationary plunging period controlled my force. The objective of this test is to show the differences in the hardness in these two section. The average value in section A was 190HV and in section B was 186HV. Overall average value of both section was 188HV whereas value of base materials was202 HV. It shows that there is no big changes in hardness value in section A and section B however, the fluctuation can be seen at the meeting point of both section. That was the point where speed controlled initial plunging period finished and force controlled stationary plunging period started. The maximum value of 220HV was recorded in the measurement.

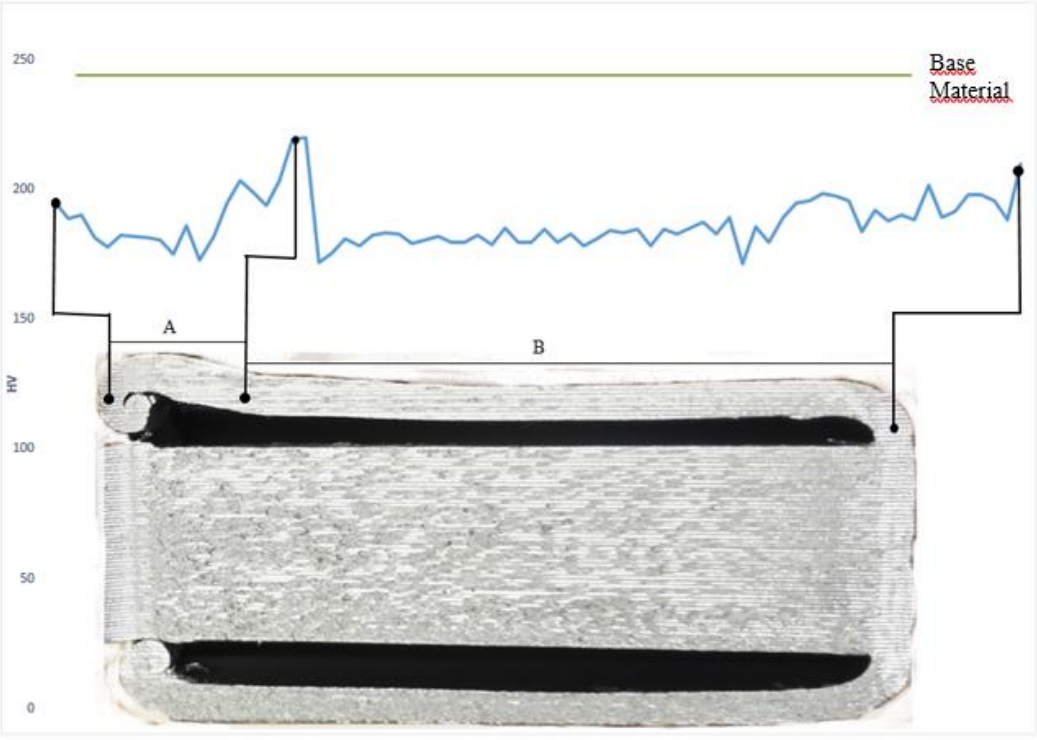

Figure 80: Vickers hardness measurement through the longitudinal section of F2T.

5.3 **Metallographic Analysis**

5.3.1 **Optical Microscopy**

Optical microscopy was used in analysis and characterization of materials in F2T tube produced in optimal parameters. Understanding the microstructural quantities furthermore, helps to understand material properties. The specimen for optical microscopy was taken from F2T and base material. The sample from base material was prepared in first step. And then specimens from F2T were extracted. Sample 1 and 2.b was taken (Figure 76) for optical microscopy analysis.

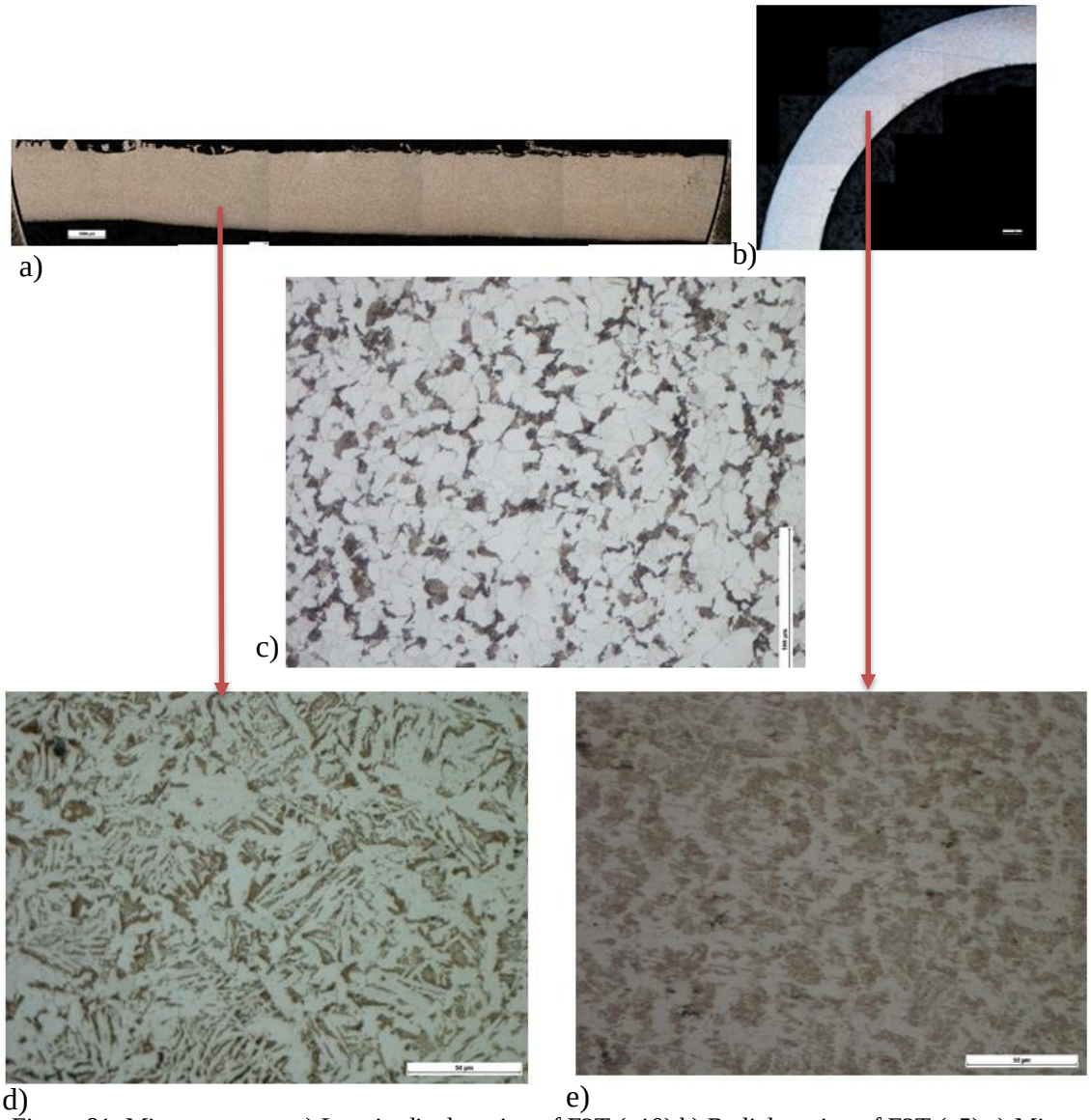

Figure 81: Microstructures a) Longitudinal section of F2T (x10) b) Radial section of F2T (x5) c) Microstructure of base material (x50) d) Microstructure of longitudinal section (x50) e) Microstructure of radial section (x50)

The preparation of the samples was done as in sample preparation for microhardness test which was described in 5.2.4. Few more step needed in optical microscopy was cleaning of the samples in ethanol and etching of samples in nital 2% for 15 to 30 seconds. Normally, treatment in etchant for 15 seconds is sufficient to see the macroscopic features in

sample such as voids, deformation etc. Analysis of microstructure was also done by EBSD which is presented in 5.3.2.

5.3.2 **EBSD**

Electron backscatter Diffraction (EBSD) is a microstructural-crystallographic characterization technique that provides quantitative microstructural information about the crystallographic nature of metals, minerals, semiconductors, and ceramics-in fact most inorganic crystalline materials [62]. Zeiss Ultra FEG.SEM equipped with Nordlys detector equipment and Channel 5 software were used for EBSD analysis. The EBSD was performed in longitudinal and radial section of F2T produced in optimal parameters. As shown in Figure 76, sample 1 and 2.b were examined and compared with the base material. Those sections were selected to understand the metallographic phenomena to support the changes in mechanical properties in those section and base material as well. The specimens including sample prepared from base material were first cut, grinded in grit paper and polished by diamond polisher as described in section 5.2.4. The specimens were then put into silica for 6 hours and followed by ultrasonic cleaning by dipping it into ethanol for 1 minute. Cleaning in silica removed the residual deformation from the surface and ultrasonic cleaning removed silica from the specimen.

Metallurgical features of base materials (S355 cold rolled structural steel) showing the body-centered cubic (BCC) before F2T are presented in Figure 82 that shows the map of grain boundaries, inverse pole figure and map of twin boundaries. Different colours in the figure indicate different crystallographic orientation of grain. The average grain size is 7,6 µm which was calculated by equivalent circle diameter (ECD) method.

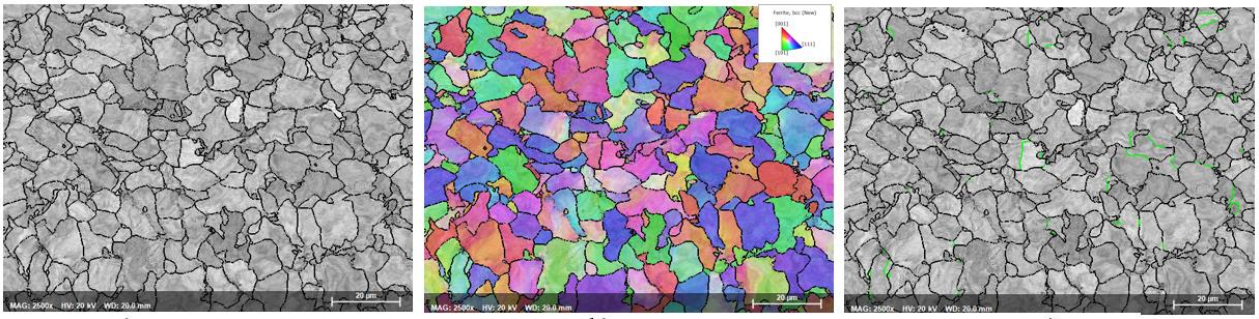

a) b) c)

Figure 82: Base Material in as-received condition (x2,500). a) Map of grain boundaries b) Inverse pole figure (IPF) map c) Map of grain and twin boundaries

Similarly, the metallurgical features of F2T in longitudinal section (specimen 1 in Figure 76) are presented in Figure 83 that shows the map of grain boundaries, inverse pole figure and map of twin boundaries. The average grain size is 8,3 µm.

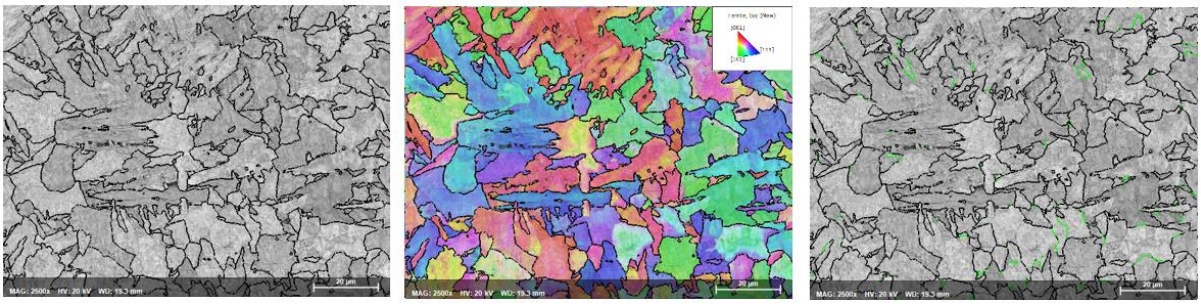

a) b) c)

Figure 83: Longitudinal section of F2T (x2,500). a) Map of grain boundaries b) Inverse pole figure (IPF) map c) Map of grain and twin boundarie

The metallurgical features of F2T in radial section (specimen 2.b in Figure 76) are presented in Figure 84 that shows the map of grain boundaries, inverse pole figure and map of twin boundaries. The average grain size is 9,3 µm.

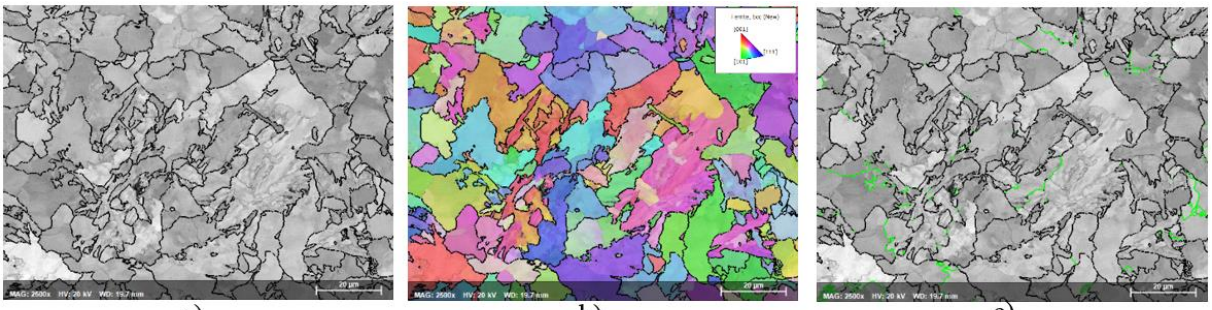

a) b) c)

Figure 84: Radial section of F2T (x2,500). a) Map of grain boundaries b) Inverse pole figure (IPF) map c) Map of grain and twin boundaries

The average grain size of the base material was found less than the longitudinal and radial section of F2T however, the difference is only 0,7 µm than longitudinal section and 1,7 than radial section. The hardness value obtained in the base material (in section 5.2.4) has higher value than the F2T which was supported by the smaller grain size in a base material obtained from EBSD analysis. The grains in base material (Figure 82) was found equally distributed and have similar grain structure whereas as in F2T because of thermos-mechanically processed (Figure 83 and Figure 84), grains are stretched and uneven and also there is variation in the grain sizes.

6 FINAL REMARKS

6.1 Conclusions

The F2T was performed successfully in cold rolled structural steel S355. The other significant conclusions of this thesis work are presented as follows:

1. The developed experimental condition without supporting guide is able to produce tube shorter than 40 mm in length. The experimental condition to produce shorter tube is simple in design and convenient to produce F2T tube.

2. The developed experimental condition with supporting guide is able to produce tube about 80 mm in length. There is challenge to produce longer than 80 mm tube because of vertical stroke limitation in ESAB FSW machine.

3. The cooling system provided in hard material tungsten carbide which act as anvil in F2T helps to prevent wear, that results smoothness in the process and longer anvil life. However, it is recommended to replace anvil after 4 to 5 tests in each side.

4. Taguchi method (Design of Experiments) was performed initially to produce shorter tube (tube A) without use of supporting guide system. From the data analysis of Taguchi method, following optimal parameters were identified:

Optimal Parameters	
Tool rotation [Ω]	2813
Forging Force [kN]	30,4
Plunge depth [mm]	4,62

   These parameters were used as a base to estimate the level of parameters in next step of Taguchi method for longer tube (tube B).

5. Taguchi method: Optimization of F2T tubes using supporting guide:

   - From the data analysis using Taguchi method, following optimal parameters were obtained:

Optimal Parameters	
Tool rotation [Ω]	2888
Forging Force [kN]	26,60
Plunge depth [mm]	3,90

     For mechanical and metallurgical analysis, specimens were made by producing F2T tube in these optimal parameters.

   - From the analysis of variance (ANOVA), it is concluded that the forging force is the parameter that has most influences in thickness stability and hardness values, which is 55% and 42% respectively. Similarly, the influence of initial plunge depth was highest in diameter stability with value of 40%.

6. The mechanical properties of F2T tubes obtained from tensile test was compared with machined tubes. There was about 5% differences in the value of yield strength, ultimate tensile strength and young´s modulus. In a contrast, percentage elongation of F2T tube was 24% and of machined tube was 36%.

7. Flattening test on both F2T tube and machined tube was successful. The energy absorption in F2T was 187,60 J and in machined tube was 201,9 J.

8. Flare test on both F2T tube and machined tube was successful. The energy absorption in F2T was 72,67 J and in machined tube was 50,8

9. The inner side of the F2T has comparatively lower hardness value than the outer side. The thermomechanical process in F2T of structural steel S355 rather decreases the hardness value.

10. The temperature reached up to 1238ºC in F2T which was acquired from the IR image analysis.

6.2 Future Developments

The feasibility of application of the F2T technique has been shown in this thesis work. This fact opens the door to explore high value applications via the application to high performance materials. The experimental work performed in this thesis work developed a solid foundation for future work, the following points are noted for further researches:

1. Development of buckling control mechanism is important to produce longer F2T tubes.

2. Development of F2T dedicated system is essential because existing manufacturing system does not fulfill the demands of specific components and control of F2T.

3. The current design of consumable need to be revised to prevent unnecessary waste of materials.

4. Tungsten carbide was used as anvil and it has wearing problem after every 4 to 5 test. More study can be done for proper selection of anvil materials and design to increase the anvil life.

5. The thesis work was performed in structural steel S355 to verify the feasibility of technique. The research can be performed in various other materials. Emphasis can be given to high value material such as nickel based alloy, titanium etc.

REFERENCES

[1] "Seamless Pipes and Tubes – A Global Strategic Business Report," Global Industry Analysts, Inc., San Jose, CA, MCP-8146, 2016.

[2] P. Vilaça, "Aalto-TUTL Friction Flash to Tube – F2T,"February, 2016.

[3] R. A. Serway & C. Vuille, "Sound," in *Essential of College Physics*, 1st ed. Cram101 textbook reviews, 2007, ch 14.

[4] Perzyna, P. (1966), "Fundamental problems in viscoplasticity," *Advances in applied mechanics*, vol. 9, pp. 243-377, 1966.

[5] J. Betten, "Viscoplastic Materials," in *Creep Mechanics*, 2nd ed. Aachen, Germany. Springer, 2005, ch. 12, pp. 237-244.

[6] J. Lubliner, "Constitutive Theory," in *Plasticity Theory*, 3rd ed., Dover Publication INC, 2008, ch. 3, pp. 111-122.

[7] L. Prandtl, "Spannungsverteilung in plastischen Koerpern". In *Proceedings of the 1st International Congress on Applied Mechanics*. Delft, 1924. pp. 43.

[8] P. Vilaça, J. Gandra, J. Vidal, "Linear Friction Based Processing Technolo-gies for Aluminum Alloys: Surfacing, Stir Welding and Stir Channeling", in *Aluminium Alloys - New Trends in Fabrication and Applications, InTech*, 2012, 159-172.

[9] J. Gandra, R.M. Miranda, P. Vilaça, "Performance analysis of friction surfac-ing". In: *Journal of Materials Processing Technology*, 212, 2012, 1676–1686.

[10] Aalto University, "Friction Flash to Tube (F2T)," Finnish Patent and Registration Office. Feb 22, 2016.

[11] S. Kyriakides and E. Corona, "Pipe and Tube Manufacturing Processes," in *Mechanics of Offshore Pipelines Volume 1: Buckling and Collapse*, 1st ed., Oxford: Elsevier, 2007, ch. 3, pp. 60-87.

[12] B. Kozak & J. Dzierzawski. *Continuous Casting of Steel: Basic Principle* (2016 Aug 12). [Online] Available at http://www.steel.org/making-steel/how-its-made/processes/processes-info/continuous-casting-of-steel---basic-principles.aspx

[13] D. Koshal, "Metal Forming," in *Manufacturing Engineer´s Reference Book*,1st ed., Oxford, England: Butterworth-Heinemann, 1993, ch. 4, pp 73-80.

[14] "Welded Stainless Steel Tubes & Pipes vs. Seamless," in *A corrosion management and applications engineering magazine from Outokumpu*, Outokumpu, Finland, 2011-2, pp. 1-11.

[15] Dr. –Ing. K. H. Breinsing et al., "*Steel Tube and Pipe Manufacturing Processes*," Salzgitter Mannesmann Röhrenwerke, Mülheim, Germany. pp. 34.

[16] H. B. Cary and S. C. Helzer, "Arc welding with a consumable electrode & Resistance, electron beam and laser beam welding and cutting," in *Modern Welding Technology*, 6th ed., Columbus, NJ: Pearson, 2005, ch. 6 & 8, pp. 90-163 &192-213.

[17] B. Morrett, "How to improve your welds: helpful hints for GMAW," Practical Welding Today, Feb, 2002.

[18] PIR, Petroleum Industry Review (2015). [Online] Available at http://www.petroleumindustryreview.com/2015/05/your-oil-gas-news-technology-from-honey-wells-uop-to-run-largest-refinery-in-africa/

[19] H. Regutit. Eurofer-The European Steel Association (2016). [Online] Available at http://www.eurofer.org/Eurofer%20Stainless/About%20Stainless%20Steel.fhtml

[20] J. Charles and B. Vincent, "Duplex stainless steels for chemical tankers," in *Duplex Stainless Steel-5th World Conf.*, St.-Chamond, France, 1997, pp. 727-737.

[21] K. Bujis, "Characterstics and uses of titanium" in *Stainless Steel World*, Netherlands, 2008.

[22] E. Lundin, "TPJ-The Tube & Pipe Journal," *Quality control for tube, pipe producers*, vol. 26, no. 6, pp. 12-15, Jul. 2012.

[23] *Standard Test Methods and Definitions for Mechanical Testing of Steel Products1*, ASTM A370-14.

[24] J.R. Davis, "*Introduction to Tensile Testing*," in Tensile Testing, 2nd ed. Materials Park, OH: ASM Int., 2004, ch. 1, pp. 1-8.

[25] Mechanical Engineering Department (2016). [Online] Available at http://me.aut.ac.ir/staff/solidmechanics/alizadeh/Tensile%20Testing.htm

[26] Independent Metallurgical and Consultant, Gordon, Eng-land, *Hardness test*, [Online]. Available: http://civil.eng.buffalo.edu/CIE616/2-LECTURES/Lecture%204a%20-%20Material%20Testing/HARDNESS%20TEST.pdf

[27] *Method for flattening test on metallic tubes*, IS 2328, 2005.

[28] *Standard Test Methods and Definitions for Mechanical Testing of Steel Products*, A370-14, 2014.

[29] *Metallic materials-Tube-Drift-expanding test*, BS EN ISO 8493:2004.

[30] Professional testing services, (2013). *Flattening test, Flaring/Flanging Test, Crush Test.* [Online]. Available: http://www.ptspl.com/Flattening_Test.html

[31] L. Cartz, "Quality Control and Nondestructive Testing," in *Non-destructive Testing*, 1st ed., Materials Park, OH. ASM International, 1995, ch. 1, pp 1-8.

[32] B. Roberts, *"Monitoring the quality of welded tube and pipe*," Sep. 2001. [Online]. Available: http://www.thefabricator.com/article/testingmeasuring/monitoring-the-quality-of-welded-tube-and-pipe. Accessed: Aug. 15, 2016.

[33] G. Mook, O. Hesses & V. Uchanin J et al., "Deep Penetrating Eddy Currents and Probes," in *Non-Destructive Testing*, ECNDT 2006-Tu.3-6-2, pp. 1.

[34] T. Hasiotis, E. Badogiannis and N. G. Tsouvalis et al., "Application of Ultrasonic C-Scan Techniques for Tracing Defects in Laminated Composite Materials". In: *Journal of Mechanical Engineering* 57, (2011), pp. 193-203.

[35] "Introduction to ultrasonic testing," in NDT Resource center. [Online]. Available: https://www.nde-ed.org/EducationResources/CommunityCollege/Ultrasonics/Introduction/description.htm

[36] Rufe and Philip D., "Non-destructive Testing," in *Fundamentals of Manufacturing*, 3rd ed., Society of Manufacturing Engineers (SME), Dearborn, MI. 2013, ch. 50 pp 517.

[37] Instruments and Oxford Instruments Industrial Analysis, "*Positive materials identification PMI – x-ray fluorescence and optical emission spectroscopy by Oxford instruments*," in Materials Article, AZoM, 2013. [Online]. Available: http://www.azom.com/article.aspx?ArticleID=4065. Accessed: Aug. 16, 2016

[38] Julie Z. Zhang, Joseph C. Chen, E. Daniel Kirby, "Surface roughness optimization in an end-milling operation using the Taguchi design method". In: *Journal of Materials Processing Technology* 184, (2007), pp. 233–239.

[39] R. Roy, "The Taguchi Approach to Quality and Cost Improvement," in *A Primer on the Taguchi Method*, Dearborn, MI, 1990, ch. 2, pp. 7-18.

[40] C.I.S. Vidal, "Análise da Melhoria do Comportamento à Fadiga em Juntas Soldadas por Fricção Linear de Ligas de Alumínio para a Indústria Aeronáutica," M-S. Thesis, Aerospace Eng., University of Lisbon, Lisbon, Portugal, 2009.

[41] P. R. Apte. (2000, Dec 14). Introduction to Taguchi Method (3rd ed.) [Online]. Available: https://www.ee.iitb.ac.in/~apte/CV_PRA_TAGUCHI_INTRO.htm

[42] *European structural steel standard*, EN 10025: 2004.

[43] Parker Steel Company (2016, Oct 3). S355 Grade Description [Online]. Available at http://www.metricmetal.com/products/Grade%20Descriptions/S355%20Grade%20Description.php

[44] S355J2C (2016, Oct. 3). European Steel and Alloy Grades / Numbers [Online]. Available at http://www.steelnumber.com/en/steel_composition_eu.php?name_id=146

[45] ESAB. (2014). LEGIO™ FSW 5U Friction Stir Welding Machine [Instruction manual and spare parts list]. Gothenberg, Sweden.

[46] Buehler Ltd. (1998). Buehler 1600-6400 microhardness tester [Manual]. Lake Bluff, IL.

[47] CMS instruments. (2009). SM Micro Combi Tester Platform (nano and micro indentation and scratch modules) [Manual]. Peseux, Switzerland.

[48] MTS Landmark. (2006). MTS 810 Material Testing System [Manual]. Eden Prairie, MN.

[49] Lavision. Imager proX. [Product guide]. Göttingen, Germany.

[50] Nikon (1997). Inverted Metallurgical Microscope Epiphot 200. [Manual]. Melville, NY.

[51] Carl Zeiss Microscopy GmbH (2015). Merlin VP Compact SEM. [Product Information version 2.0]. Jena, Germany.

[52] FLIR (2017). FLIR SC660. [Online]. Available: http://www.flir.co.uk/cs/display/?id=41413

[53] P. Heino. (2016, Feb 02). Tungsten carbide information [Online]. Available email: info@kovametalli-in.fi

[54] H. Zhang, "Study of the mechanical behavior of WC-Co composites using Hertzian indentation technique," Ph.D. dissertation, Metallurgical Lab., The Univ. of Utah, Salt lake city, UT, 2008.

[55] National Bronze MFG. (2016, Oct 5). Self-lubrication options for bronze bearings. Available at http://www.nationalbronze.com/News/self-lubrication-options-for-bronze-bearings/

[56] C. Meran, "The joint properties of brass plates by friction stir welding". In: *Journal of Materials and design* 27, (2006), pp. 719-726.

[57] Clamp-Rite (2016, Oct 5). Push-pull toggle clamp. Available at http://www.clamp-rite.com/clamps/push-pull-toggle-clamp/13300cr.html

[58] Nalbant, M.; Gökkaya,H.; Sur, G., Application of Taguchi Method in the optimization of cutting parameters for surface roughness in turning, Turkey, July 2005.

[59] J.L. Rosa et al., "Electrodeposition of copper on titanium wires: Taguchi experimental design approach". In: *Journal of Materials Processing Technology 209,* (2009), pp. 1181-1188.

[60] W.H. Yang, Y.S. Tarng, "Design optimization of cutting parameters for turning operations based on the Taguchi method". In: *Journal of Materials Processing Technology* 84, (1998), pp. 122-129.

[61] Y. M. Potak, Y.F. Orzhekhovskii, L.M. Pevzner, et al.(1961), "Thermomechanical treatment of steel for high strength" in *Metal Science Heat Treatment*, vol. 3, issues5. pp. 185-190.

[62] T. Maitland and S. Sitzman, "Electron Backscatter Diffraction (EBSD) Technique and Materials Characterization Examples," in *Scanning Microscopy for Nanotechnology Techniques and Application, 1*st ed. New York: Springler, 2007, ch. *2*, pp. *41-75.*

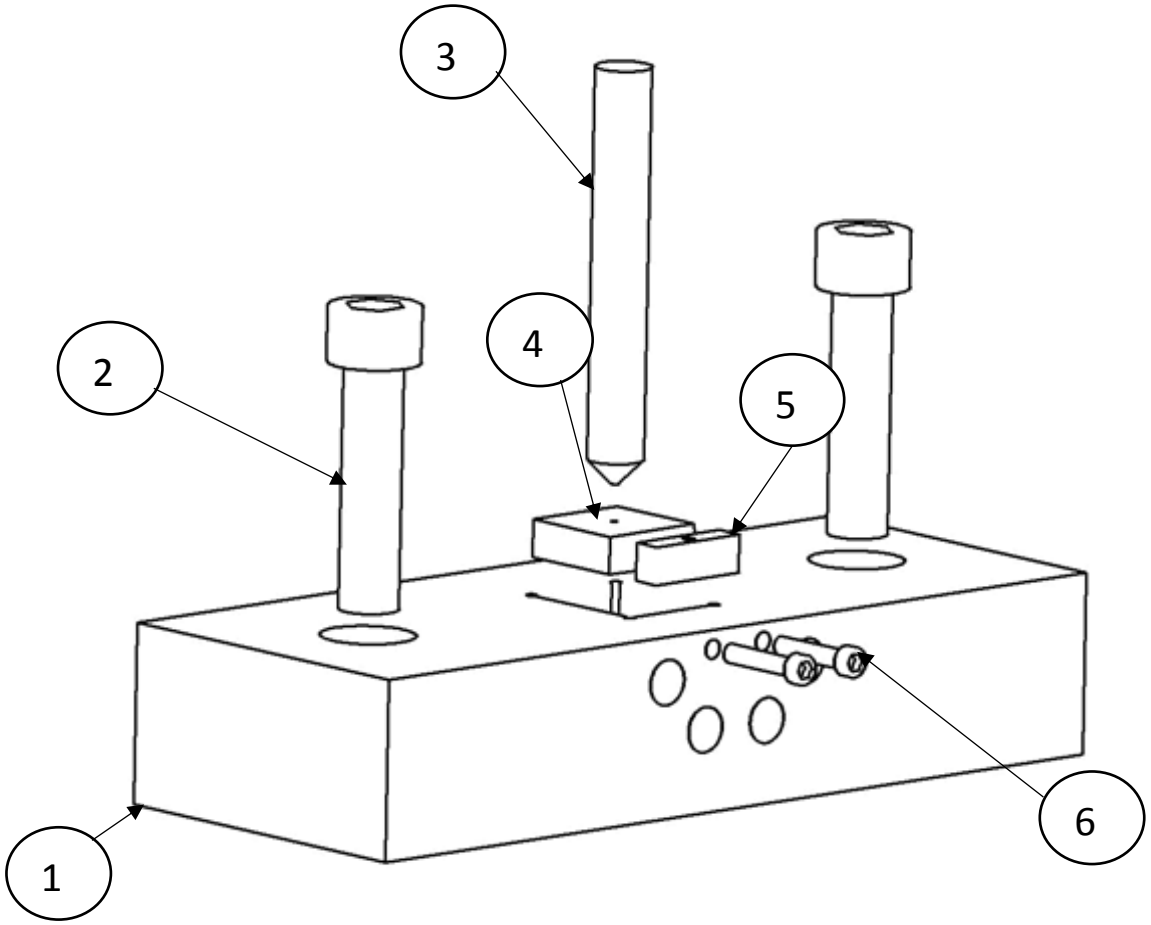

6		Bolt M5			2
5		Anvil lock			1
4		Hard material Anvil		WC	1
3		Consumable		S355	1
2		Bolt M16			2
1		Anvil holder			1
Part	ID-Code	Description		Materials	Pcs
Tolerance	Scale	Product	Customer		

Aalto University School of Science and Technology		Rev	Date	Model name
		Drawn		Anvil System
		Check		
	Mass	Acc		

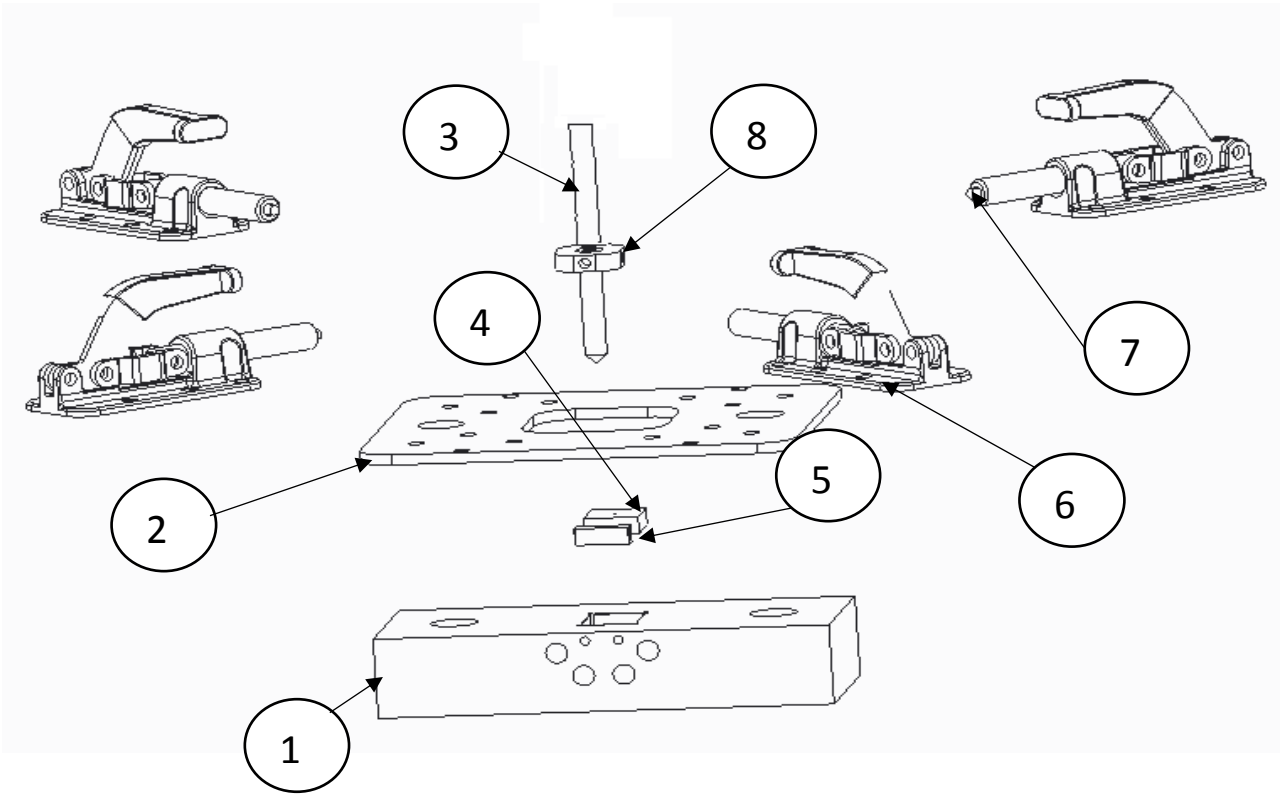

8		Brass ring		Brass	1
7		Pin		Brass	4
6		Clamprite push pull toggle clamp			4
5		Anvil lock			1
4		Hard material Anvil		WC	1
3		Consumable		S355	1
2		Clamprite clamp holder			1
1		Anvil holder			1
Part	ID-Code	Description		Materials	Pcs
Tolerance	Scale	Product	Customer		

Aalto University School of Science and Technology		Rev	Date	Model name
		Drawn		Anvil System
		Check		
	Mass	Acc		

Rev.	Change	Date	Changed	Appr.

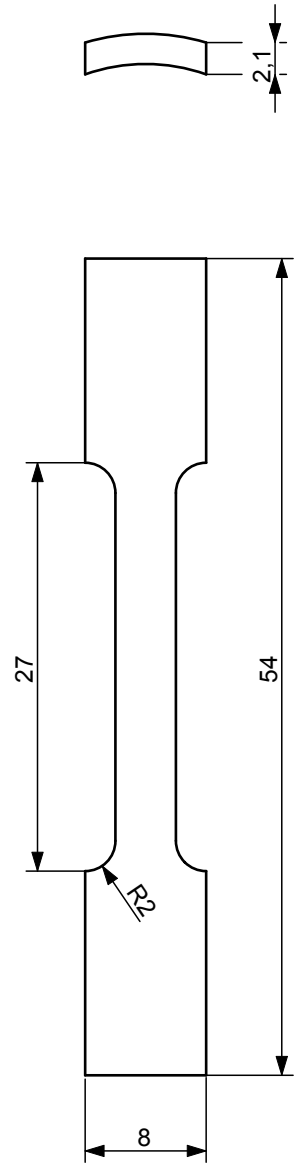

Osa Part	Nimike ID-Code	Nimitys Description	Standardi Standard	Kpl Pcs

General tol.	Scale 2,000	Product	Customer	
Aalto University School of Science and Technology	Mass kg	Rev. -	Date	Model name TENSILE_SPECIMEN
		Drawn -		TENSILE_SPECIMEN
		Check -		
		Acc. -		

Rev.	Change	Date	Changed	Appr.

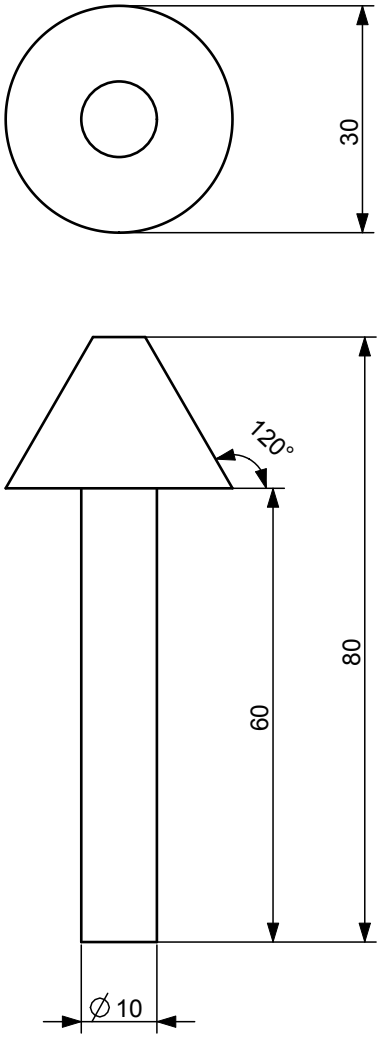

Osa Part	Nimike ID-Code	Nimitys Description	Standardi Standard	Kpl Pcs

General tol.	Scale 1,000	Product	Customer	
Aalto University School of Science and Technology		Rev. -	Date	Model name MANDREL
		Drawn -		MANDREL_FOR_FLARE_TEST
	Mass kg	Check -		
		Acc. -		